Microchimica Acta (2019) 186: 682
https://doi.org/10.1007/s00604-019-3770-5

REVIEW ARTICLE

Nanoparticle-based surface assisted laser desorption ionization mass spectrometry: a review

Hani Nasser Abdelhamid[1]

Received: 9 March 2019 / Accepted: 16 August 2019 / Published online: 13 September 2019

Abstract

Great endeavors are undertaken to find effective nanoparticles to replace organic matrices for the analysis of small molecules using laser desorption ionization mass spectrometry (LDI-MS). Nanoparticles offer high sensitivity and better selectivity compared to conventional organic matrices. **S**urface assisted LDI-MS (SALDI-MS), and **s**urface **e**nhanced LDI-MS (SELDI-MS) provide clear background spectra without observable interferences peaks, and cause no fragmentation (soft ionization) of thermal and acidity labile molecules. This review article (with 460 references) summarizes the recent applications of nanoparticles including metallic, metal oxides, silicon, quantum dots, metal-organic frameworks and covalent organic frameworks, for the analysis of small molecules. Nanoparticles serve not only as surface for LDI-MS, but they can be also used as probe or pseudo-stationary phase for separation, enrichment, and microextraction. Hopefully, the knowledge and learning points gained from this review will deepen the understanding of nanoparticles applications for LDI-MS.

Keywords MOF · Nanoparticles · Small molecules · Matrix assisted laser desorption ionization mass spectrometry · SALDI-MS · SELDI-MS · Metal-organic frameworks

Introduction

Soft ionization **m**ass spectrometry (MS), including **m**atrix **a**-ssisted **l**aser **d**esorption **i**onization (MALDI-MS) [1–4], and **e**lectro**s**pray **i**onization (ESI-MS) [5–9], have advanced the analysis of thermal labile and nonvolatile analytes. An organic compound, defined as matrices, is usually used to assist the process of LDI-MS [10–16]. The organic matrices undergo self-ionization using the laser energy and consequently cause a proton transfer with the investigated analyte. Most of the organic matrices offer soft ionization with low degree of fragmentation. MALDI-MS offers high tolerance to salts, detergents, and buffers. It offers high sensitivity, rapid analysis, and requires simple sample preparation. Thus, MALDI-MS was reported for biological analysis [17], proteomics [18, 19], glycan [20], lipid profiling of mammalian cells [21], environmental species [22], chemical and biomedical applications [23]. However, the analysis of small molecules (molecular weight< 1000 Da) is still a challenge [24]. Conventional organic matrices usually show interferences peaks in the low mass range (<1000 Da) [11]. They can also produce overlapped peaks with the investigated analytes, create cluster ions species, and cause fragmentation of thermal labile molecules. Thus, organic matrix salts, are defined also as ionic liquids matrices (ILMs), were applied as alternative to organic matrices [14, 25–28].

Nanoparticles (NPs) have advanced several applications [29–38] including drug delivery [39], mass spectrometry [12, 40]. They have been used as an alternative to organic matrices. Cobalt NPs (30 nm) was the first example of a nanoparticle for the analysis of lysozyme using LDI-MS [41]. A plethora of NPs [42–45] were used as surface to assist LDI-MS process [46]. Nanoparticles including 1) metallic nanoparticles: silver (Ag NPs) [47], gold (Au NPs) [48–52], palladium (Pd NPs) [53], and platinum nanoflowers [54]; 2) metal oxides: porous alumina [55], titanium dioxide (TiO_2) [56, 57], manganese oxides (MnO_2 and Mn_2O_3 cores) [58], ZnO nanowire [59], ZrO_2 NPs and ZrO_2-SiO_2 nanorods (NRs) [60], iron oxide NPs (Fe_3O_4) [61], and Fe_3O_4-TiO_2 core-shell NPs [62]; 3) silicon-based NPs: titanium silicon oxide-barium strontium titanium oxide [63], nanostructure silicon substrates [64–68], and silicon nitride NPs [69]; 4) quantum dots (QDs): germanium nanodots (Ge NDs) [70], HgTe nanostructure [71], zinc sulfide (ZnS QDs) [72], cadmium selenide (CdSe QDs),

✉ Hani Nasser Abdelhamid
hany.abdelhameed@science.au.edu.eg; chemist.hani@yahoo.com

[1] Advanced Multifunctional Materials Laboratory, Department of Chemistry, Assiut University, Assiut 71515, Egypt

FePtCu NPs [47], and GaP NPs [73]; 5) carbon-based nanomaterials: diamond [74, 75], carbon nanotube [76, 77], and 6) porous materials, were investigated as surface for MALDI-MS [78, 79].

MALDI-MS offers high throughput analysis, high sensitivity, high tolerance towards salts, fast analysis ability, small sample consumption, and simple sample preparation, and no or little fragmentations. Several techniques including **s**urface **a**ssisted **l**aser **d**esorption **i**onization **m**ass **s**pectrometry (SALDI-MS), **s**urface **e**nhanced LDI-MS (SELDI-MS), **g**raphite **a**ssisted LDI-MS [80], nanoparticle assisted LDI [81], nanostructure-assisted LDI [82], matrix-enhanced nanostructure initiator mass spectrometry [83], desorption ionization on silicon (DIOS) [84], nanostructure initiator mass spectrometry (NIMS) [85], material enhanced LDI [86], silicon nanoparticle assisted LDI [87], nanowire assisted LDI-MS [59], desorption ionization on mesoporous silicate [88], and cationic gold nanoparticle-enhanced target [89], were reported. These techniques offer clear background spectra with very few interference peaks.

This review article summarizes the applications of NPs and key parameters govern their efficiency for the analysis of small molecules using LDI-MS [90–92]. In this review, applications, mechanism, pros and cons for each NPs, are discussed. Finally, perspectives on the future applications of nanoparticles for LDI-MS are given. NPs show clear background and improve the limit of detection (LOD). NPs offer large surface area and can be used for separation, enrichment and microextraction.

Applications of nanoparticles for LDI-MS

Nanoparticles can be used as surface, probe, and substrate for the analysis of small molecules using LDI-MS. They can be used for qualitative and quantitative analysis of small therapeutic and diagnostic molecules [93]. They can also be used as extracting probes for the analysis of hydrophobic peptides, and proteins in aqueous solutions [94], microextraction and preconcentration [95–97], and for forensic applications [98].

NPs offered many advantages that make it suitable as surface for SALDI-MS. They have high molar absorption coefficients of laser radiation and can be used to promote analyte ionization [99]. Applications of nanoparticles require no homogeneous sample spots [100]. Nanoparticles can be used with or without internal calibration [100], and for imaging [101]. They have large surface area, and offers high analyte loading capacities (e.g., > 1000 small molecules per NP) [99]. They show high tolerance for salts that can suppress ionization. They can be used for preconcentration or separation of the analyte from the solutions through centrifugation or magnetic separation [102]. The sample spotting using nanoparticles is easy, and requires simple mixing of the target analyte with the nanoparticles before the spotting in the MALDI substrate. Nanoparticle can be used as a probe, and stationary phase for separation, enrichment, and extraction. Magnetic nanoparticles offer simple separation for target analyte using simple external magnet. The sample after separation, enrichment, or extraction can be directly spotted in MALDI plate. Most of nanoparticle can be served as surface for the desorption ionization process of small molecules. Compared to conventional organic matrices, LDI-MS using NPs produce highly reproducible spectra [103], with high sensitivity [104], and minimal sample preparation [105].

Several nanoparticles were used for the analysis of small molecules (Fig. 1). These nanoparticles can be classified to:- 1) metallic nanoparticles (Table 1); 2) metal oxide nanoparticles (Table 2); 3) silicon based nanostructure (Table 3); 4) carbon nanomaterials (Table 4); 5) quantum dots; 6) metal-organic frameworks (MOFs) [168], and 7) covalent organic frameworks (COFs, Table 5). Nanoparticles can be used as a dispersion, thin film, chips, or microarrays (Fig. 1). These nanostructures offer simple sample preparation (Fig. 2). Analyte from organs, tissues or animal can be analyzed using direct method or after separation using common separation methods (Fig. 2). Nanoparticles provide high sensitive detection, wide applications, clear background spectra, low fragmentation, and can be used for preconcentration or separation of analytes with low concentrations.

Metallic nanoparticles assisted LDI-MS

SALDI-MS using Au NPs was reported [181, 182]. Au NPs assisted LDI-MS has been used for wide range of small molecules (Table 1) [106, 109, 183–187]. Au NPs were used for the analysis of metals [167], monosaccharides, and disaccharides (glucose, sorbitol, and sucrose) [50], amino acids, synthetic polymers [188], aminothiols [99], polymer dots [189], over-the-counter (OTC) drugs, and Chinese herbal medicine granules [190], drugs (desipramine and enrofloxacin), alkanethiolates [191], peptides (valinomycin and gramicidin D), and phosphopeptides from casein proteins (α-, β-casein and nonfat milk) [192].

Au NPs offer low LOD. They show high selectivity glutathione (GSH) [193]. N-2-mercaptopropionyl glycine@Au NPs can be used as internal standard calibrant for quantitative analysis of GSH in the lysates of human red blood cells and MCF-7 cancer breast cells [194]. Au nanobowls was used quantitative detection of oligonucleotides and polypeptides [107]. Au NPs can be used in the presence and absence of the anti-inflammatory drug sulfasalazine [194]. Inkjet-printing of Au NPs was applied for the detection of amino acids such as arginine, and histidine at levels as low as 25 fmol [111]. Au NPs can be applied as dispersant in solvent, thin films, and chips. It was possible to amplify the mass spectral signals and analyze macromolecules with minimum errors via monitoring

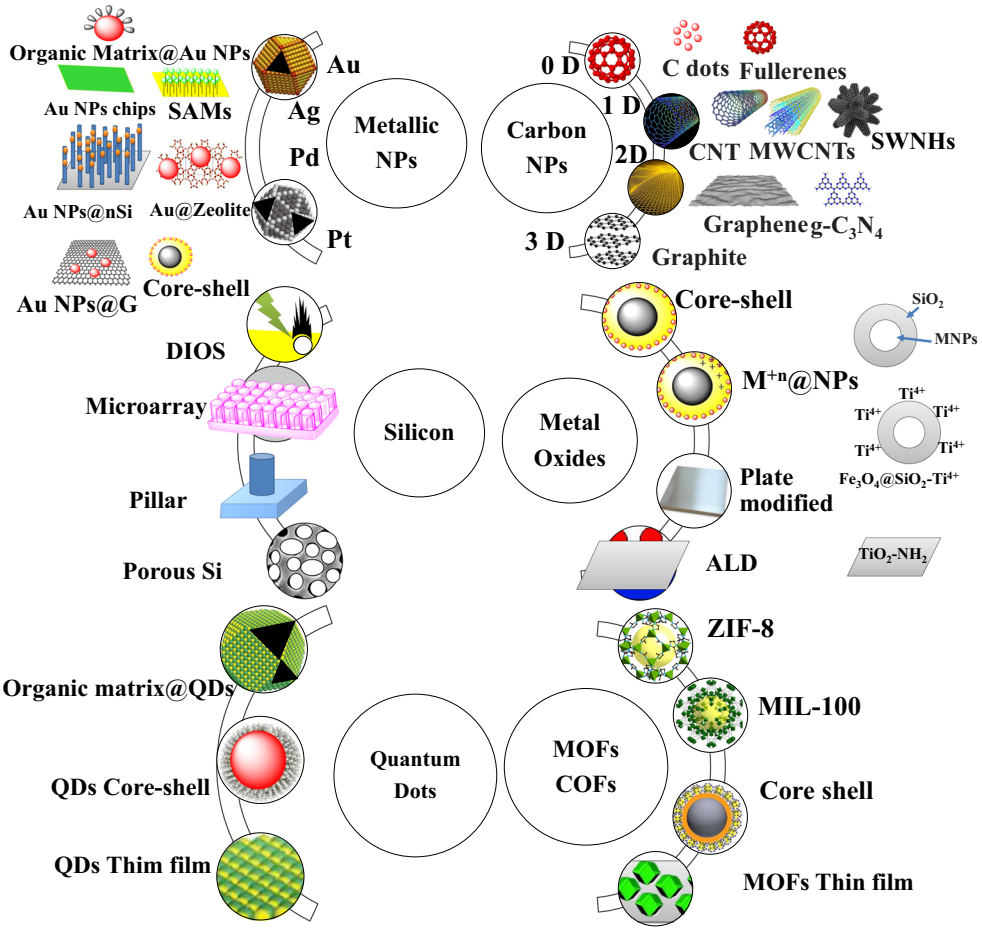

Fig. 1 Overview of nanoparticles and their technologies for LDI-MS

surface capping agents, and Au cluster ions [195]. Au NPs can be used as surface for the quantitative analysis of five targeted metabolites; glycine (Gly), alanine (Ala), phosphocholine (PCho), glucose (Glu), and GSH, in breast cancer cells (MCF7, MDA-MB-231) and the nontumoral counterpart (MCF10A) [196]. Thin film based on Au NPs is used for the analysis of bone biomarker, hydroxyproline (HYP) for osteoporosis with only 9.3% relative signal variation [108].

LDI-MS imaging using Au NPs was used for tumor markers on cell membrane [197], anti-counterfeiting applications [198], analysis of metabolites [199], metabolomics [200], and banknotes and checks [201]. Imaging using Au NPs offer minimum destructive and show high sensitivity [201]. Au NPs enhance the spatial resolution imaging up to the cellular level [126], offer solvent-free LDI-MS [201], require simple sample preparation, form homogenous coverage of the sample section or tissue, offer sensitive detection of low concentration, selective detection of species such as thiols, and require tiny sample amount [202].

Ag NPs were used for the analysis of wide range of different small molecules analytes (Table 1) [203]. Ag NPs assisted LDI-MS was applied for folic acid and amphotericin B [119], peptides [204, 205], cysteine containing peptides [206], small carbohydrates (sucrose and fructans) [63], estrogens, (E1, E2, and E3) [207], olefins [208], and aminoglycoside antibiotics [116]. Fluorosilane-coated silica (Ag NPs/SHC) loaded on a cover glass was used as SALDI-MS substrate for the analysis of dye, amino acid, peptides, fatty acid, and polymer [121].

Ag NPs assisted LDI-MS was used for imaging of lipids in rat brain tissue [209], galactoceramides, diacylglycerols, ceramides, phosphatidylcholines, cholesteryl ester, and cholesterol, in positive mode and phosphatidyl ethanolamides, sulfatides, phosphatidyl inositol, and sphingomyelins in negative ion mode [209]. Ag NPs were applied for both modes e.g. positive and negative modes. Thus, it can be used for imaging of lipids in heart tissue [118], normal rat kidney [210], brain tissue [209], and on the surface of *Arabidopsis thaliana* [211]. Imaging of fatty acids, including stearic, oleic, linoleic, arachidonic, and eicosapentaenoic acids, as well as palmitic acid, were reported in mouse liver sections [114]. They were also reported for visualization of ibuprofen, anticancer 5-fluorouracil on the finger [212], cholesterol, and other olefinic compounds [213]. Polyvinylpyrrolidone (PVP) capped Ag NPs offered imaging of 10 classes of lipids from the brain simultaneously (Fig. 3) [214]. PVP@Ag NPs enhanced ionization of poor ionized compounds such as unsaturated fatty acid (FAs) and sterols [214]. The method showed successful applications for the analysis of brain stroke using middle cerebral

Table 1 An overview on selected methods for LDI-MS using metallic nanoparticles

Probe	Size (nm)	Analyte	LOD	Linear Range	Ref.
Citrate- and DDAB-capped Au NPs, bare Au NPs	9-14	Ribose, glucose, cellobiose, and maltose	82-151 nM		[50]
Au NPs@graphene	13	Cys, Hcys, GSH	0.625 ng/μL		[106]
Au nanobowls array	300-600	Oligonucleotides and polypeptides	0.05 μM	0.3-6.6 μM	[107]
MTF-Au NPs	13.7	Hydroxyproline (HYP)	1 μM	1–100 μM	[108]
4-MPBA@Au NPs	50	Glycopeptides			[109]
Au NPs@Zeolite		Amino acids	6.5-13.3 nmol		[110]
$S(CH_2)_{11}(OCH_2)_4OH$@Au NPs	2		25 fmol		[111]
Diphenylalanine@Au NPs		Estrogens	0.38-0.58	1-100 ng L^{-1}	[112]
Au NPs-nSi	20-50 (Si) 350 × 50 nm (Au thin film)	Glucose	10 nM	10^{-1} - 10^{-8} M (R^2 = 0.93)	[113]
Ag NPs	3.84	Fatty acids in mouse liver sections	50 pmol		[114]
Ab–Au or Ag	30	Virus	1.0×10^3 PFU mL^{-1}	$1.0 \times 10^3 - 1.0 \times 10^5$ PFU mL^{-1}	[115]
Au@Ag NPs	39	Antibiotics	3-38 nM		[116]
Ag NPs	102	Saccharides, amino acids, nucleosides, glycosides, sulfonic acids, aldehydes, and nucleic bases	33 amol		[117]
	0.5–15	PCs, PEs, PIs, PGs, CLs, and TAGs	5 nmol		[118]
	20	Folic acid and amphotericin B	100pmol·mL^{-1}		[119]
Ag NPs thin film	~650	Angiotensin I-III triglyceride mixtureand phosphatidylcholines, phospholipids and sterols	6.19-10.7 pmol		[120]
Ag NPs-SHC	16.8	Amino acid, fatty acid, dye molecule, polypeptide, and polymer	1 pmol/μL	1-50 fmol/μL	[121]
TOAB@Ag NPs	< 50	Met- and Leu-enkephalins (Met-enk and Leu-enk) and gramicidin	160- 210 nM		[122]
$(Ag\ NPs\text{-}rGO)_9$ multilayer film	30	Carboxyl-containing small molecules	5-10 pmol		[123]
Pd NPs	60-180	Fattyacids (oleic acid, C18:1; linoleic acid, C18:2; linolenic acid, C18:3;and stearic acid, C18:0), amino acids (arginine, histidine and cysteine), small drugs (erythromycin, sulfamethazine and reserpine), carbohydrates(glucose, maltose and lactose) and peptides (bradykininand angiotensin I and II)	5 nmol		[124]
Te NS	>1 μm, ~ 40 nm	Nucleobases, fatty acids and amino acids	1 μg·$μL^{-1}$	0-25 nmol	[125]

Two-dimensional multilayered gold-nanoparticle thin film, MTF-Au NPs; PFU, plaque-forming units

Table 2 An overview on selected methods for LDI-MS using metal oxides

Probe	Size (nm)	Analyte	LOD	Linear Range	Ref.
GSH@Fe_3O_4 MNPs	10	Glycans			[126]
DHB@Fe_3O_4 MNPs		Dendrimers, and glycolipids	5 ppm		[127]
HA@Fe_3O_4 MNPs		Rhodamine B	0.02 $\mu g \cdot g^{-1}$		[128]
Chitosan@Fe_3O_4 MNPs	10	Hg^{2+}	0.05 nmol		[129]
SiO_2@Fe_3O_4 MNPs		Ferrofluid EMG 911, Raffinose, sucrose, and 2′-deoxycytidine, Berberine, jatrorrhizine, and palmatine,	5 fmol	0-1000 fmol\μl	[130]
Chitosan@$AgFeO_2$	1-40	Biothiols	1 pmol		[131]
Ti-PA-MNPs	10–30	Phosphopeptides in a β-casein tryptic digest	8×10^{-10} mol L^{-1}		[132]
TiO_2 NPs		Endogenous low molecular weight metabolites (LMWM) in mouse brain			[133]
PCs@(Ti-Zr)O_4	2.3	Phosphopeptides	0.1 fmol		[134]
PAA-Ti-TiO_2	100-200		2 fmol		[135]
Nylon nanoweb-TiO_2 particles	25-300	Amino acids	555.6-1668 $g \cdot mol^{-1}$		[136]
Ag NPs-ZnO NRs	50-255		1.0 fM	10-10000 nM	[137]
MoS_2 nanoflakes and polyallylamine	120	Amino acids, saccharides and fatty	10- 250 fmol		[138]

Table 3 An overview on selected methods for LDI-MS using silicon based nanoparticles

Probe	Size (nm)	Analyte	LOD	Linear Range	Ref.
Silicon nanopowder	5-50	Morphine and propaphenone in untreated urine and triazineherbicides in a soil extract, propafenone and verapamil drugs	fmol		[87]
C_{18}-SiO_2	200	hydrophobic antidepressant drugs desipramine and trimipramine in carbonated malt beverages	1 $ng \cdot mL^{-1}$		[139]
p^+ type-derived PS		MB^+Cl^- and Na^+MO^-	1 nmol		[140]
Ti^{4+} immobilized SiO_2 graphene-like multilayer		Phosphopeptides from a peptide mixture of bovine β-casein, and BSA	1.0 $pg \cdot \mu L^{-1}$ (4×10^{-17} $mol \cdot \mu L^{-1}$)		[141]
Fe_3O_4@SiO_2-PLP-Ti^{4+}	~250	Phosphopeptides	10 fmol		[142]
DIOS	70-120 in diameter with a depth of up to 200	Mixture of four peptides, BSA digest, amino acids, polyethylene glycol 1500	1-50 pmol	65 $fmol \cdot \mu L^{-1}$ to 2.5 $pmol \cdot \mu L^{-1}$	[143]
Si NPs	450 lengths, 450 diameters, an aspect ratio of 1.0	Methadone	32 $ng \cdot mL^{-1}$	20–2000 $ng \cdot mL^{-1}$	[144]
Si pillar	96700	Amino acids, dye molecules, polypeptides, and polymers	5 $fmol \cdot \mu L^{-1}$	5-1000 $fmol \cdot \mu L^{-1}$	[145]
Pd-PSi		Peptides	2.4 nmol L^{-1}		[146]

Table 4 An overview on selected methods for LDI-MS using carbon-based nanoparticles.

Probe	Size (nm)	Analyte	LOD	Linear Range	Ref.
Activated carbon		Estrone, β-estradiol, estriol, 17α-ethynylestradiol, progesterone, pregnenolone, 17α-hydroxy progesterone, corticosterone, cortisone and hydrocortisone	1.57-18.1 ng		[147]
Pencil lead		APG, PEG 2000, alpha-cyclodextrin, cocaine, substance P, uranium standard U005a	1 $mg{\cdot}mL^{-1}$ for analytes, 100 pg uranium		[148]
Graphite		Uranium and lanthanides	0.1-1 ng		[149]
	500	Citrulline	9.4 $\mu mol{\cdot}L^{-1}$	10–250 $\mu mol{\cdot}L^{-1}$	[150]
Graphene		NSAIDs	2 pmol		[151]
		Hg^{2+}	1 pmol		[152]
		Lipids			[153]
		Nitro-PAHs, namely 1-nitropyrene, 2-nitrofluorene, 6-nitrochrysene, and 9-nitroanthracene	2.31-9 $ng{\cdot}\ \mu L^{-1}$		[154]
N-doped graphene		Nilotinib	1 μM		[155]
C_{18}-CMK-8	5.49[a]	Doping agents (triamterene, trenbolone, testosterone, methyltestosterone, clenbuterol, and strychnine)	0.05–0.1 $ng{\cdot}mL^{-1}$		[156]
OMC	4.8[a]	Peptides in human serum	100 fmol		[157]
GO-Au NPs	13 nm (Au) 1 nm (GO)	Amino acid, carbohydrate, GSH	100 μM		[158]
g-C_3N_4 nanosheets		Amino acids, nucleobases, peptides, bisphenols, and nitropolycyclic aromatic hydrocarbons	1 pmol		[159]
SiO_2@Graphene		PEG 200, CPC, TMAOH, CTAB, gramicidin D, β-cyclodextrin, maltoheptose, gentobiose, palatinose, panose, tobramycin, spectinomycin and SDS	2 pmol		[78]
MoO_3@GO		Phosphopeptide	1 fmol		[160]
CuCoO–GO	10	7 different antibiotics and 3 additional chemical analogs, including sulfadiazine, sulfamethoxazole, norfloxacin, ampicillin, benzylpenicillin, streptomycin, tetracycline, sulfapyridine, sulfonamide and pyrimethanil	0.5 $\mu g{\cdot}L^{-1}$	10–1000 $\mu g{\cdot}L^{-1}$	[161]
CoC–NH_2 nanomagnets@Graphene	30	Pentachlorophenol, bisphenol A, and PFCs	0.1 $ng{\cdot}L^{-1}$		[162]
CeO_2-CB	23	Pharmaceutical drugs	100 $ng{\cdot}mL^{-1}$		[163]
Oxidized carbon nanotubes		Jatrorrhizine, and palmatine	3 fmol	1–100 $ng{\cdot}mL^{-1}$	[164]
C dots	2-5	Amino acids, peptides, fatty acids, as well as β-agonists and neutral oligosaccharides	0.2 fmol	0.1–9	[165]
N-doped C dots		Arginine	1 pmol	1 nmol–1 pmol	[166]
Au NPs-C dots		Fe^{2+}, Fe^{3+} and Cu^{2+} ions	5000 pmol		[167]

a, pore size

Table 5 An overview on selected methods for LDI-MS using MOFs, COFs and their composites

Probe	Size (nm)	Analyte	LOD	Linear Range	Ref.
MIL-101(Cr)	500	Quercetin, daidzein, genistein and naringenin	2.11 ng·mL^{-1}	0.25- 7.00 μg·mL^{-1} (R^2=0.996)	[169]
ZIF-7, ZIF-8 and ZIF-90	~50 for ZIF-7, ~50 for ZIF-8 and ~2 μm for ZIF-90	Bisphenols (BPA, BPB, BPS, BPF and BPAF)	1.17-2.98 ng·mL^{-1}	50-500 μM (R^2 = 0.9918- 0.9953)	[170]
Fe_3O_4@ZIF-8 MNCs	190	Amino acids, fatty acids, and peptides	0.5 μM (melatonin, MT)	0.5-500 μM (R^2 = 0.9965)	[171]
	200	Nitro-PAHs	5–8 pg	0.02–1.00 mg·mL^{-1}	[172]
Fe_3O_4@PDA@ZIF-8	500	BSA and HSA tryptic digest	0.001 μg		[173]
Fe_3O_4@MIL-100 (Fe))		Phosphopeptides	0.5 fmol		[174]
Fe_3O_4@SiO_2@UiO-66	10 (SiO_2)	Domoic acid	1.45 pg·mL^{-1}	2-1000 pg·mL^{-1}	[175]
NTU-9	5	Glucose	1.6 mM	0-4 mM	[176]
Nanoporous carbons derived from MIL-53 and cCYCU-3	2.2-17	Amino acids, carbohydrates, and pollutant	137 to 241 nM	1–200 ppm ((DEHP, R^2 0.994)	[177]
TpPa-2-Ti^{4+}		Phosphopeptide capturing from β-casein	4 fmol		[178]
Fe_3O_4@COFs	~25 nm	PAHs and their derivatives in PM2.5	0.08 ng (pyrene) and 0.01 ng (7-nitrobenz[a]anthracene)	0-100 ng	[179]
COFs		Amino acids, fatty acids, BPS and pyrene.	90 fmol		[180]

Bisphenol S, BPS; Bovine serum albumin, BSA; Diethylhexyl phthalate, DEHP; Human serum albumin, HSA; Polyfluorinated compounds, PFCs; Porous silicon, PS.

artery occlusion (MCAO) model (Fig. 3) [214]. Authors observed downregulation for unsaturated fatty acids (FAs), prostaglandins, cyclic lysophosphatidic acids (CPAs), vitamin A, neuraminic acid, 5-OH-tryptophan and the K^+ adducts of most phospholipids (phosphatidic acids (PAs), lysophosphatidylethanolamine (LPE) , phatidylethanolamines (PEs), phosphatidylcholines (PCs), phsopatidylserine (PS)) and sphingomyelins (SMs) in the ischemic region (Fig. 3) [214]. In other side, they observed highly expression for saturated FAs, ceramids (Cers), hexanoylcarnitine, stearaldehyde, the Na^+ adduct of phospholipids (lysophosphatidic acid (LPA), phosphatidic acids (PAs), LPE, PEs, lysophospatidylcholines (LPCs), patidylcholines (PCs)) and SMs in the damaged section (Fig. 3) [214].

Silicon nanowires (Si NWs) modified Ag nanoparticles (Ag NPs-Si NWs) was used for the analysis of unsaturated food components (e.g. squalene, oleic acid) oil extracts (e.g. extra virgin olive oil, peanut oil) [215]. Ag NPs@zeolite was used for the analysis of acetylsalicylic acid, L-histidine, glucose, urea, and cholesterol in human serum [216]. Zeolite improved the stability of Ag NPs, and prevent their destruction via photoexcitation [216]. Nanocomposites of Ag with reduced graphene oxide (rGO) [123], MoS_2 [217], Au [218], and polished steel target/acid etched targets [117], were also reported for the analysis of small molecules.

Metallic nanoparticles including Pt NPs was reported for analysis of amino acids, peptides, proteins, and microwave digested proteins (lysozyme and bovine serum albumin) [219]. Pt nanostructure showed high ionizability for high molecular weight protein 25 kDa [193], phosphatidylcholines and glycerolipids [220], and imaging [221]. Pt NPs can be applied for imaging inkjet ink on printed paper as well as for various other analytes (saccharides, pigments, and drugs) separated by thin-layer chromatography (TLC), without the need for extraction or concentration processes [221]. Pd NPs were reported for fatty acids, triglycerides, carbohydrates, and antibiotics [222]. Pd NPs was synthesized as thin film using galvanic electrochemical deposition. It offers simple sample preparation and provides background free spectra. Pd NPs can be used for the analysis of wide number of analytes [124]. Two-dimensional tellurium nanosheets were used to small molecules including nucleobases, fatty acids and amino acids [125]. The materials display good UV light absorption, minimal interference peaks in the low molecule-mass region, and high LDI in negative ion mode [125].

Advantages and disadvantages of metallic nanoparticles

Nobel metals Ag, Au, and Pt, showed higher LDI efficiency compared to transition metals and organic matrices (Fig. 4) [223]. Nobel metals offered clear imaging for most small metabolites including neutral lipids, such as triacylglycerols and diacylglycerols (Fig. 4) [223]. Ag NPs improved the

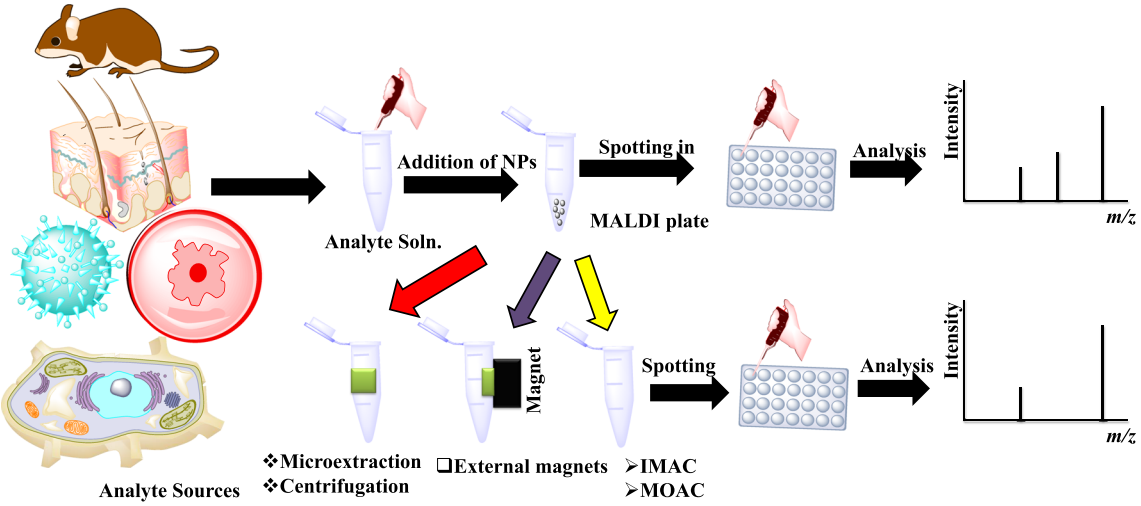

Fig. 2 Overview of the process for analysis using nanoparticles

ionization of long chain hydrocarbons [224]. Silver ions can form adducts species (Ag^{107}, or Ag^{109}) with the investigated analytes and thus improve the analyte ionization. The large surface area of nanoparticle offer high ionization efficiency and ensure the analysis of an analyte from a complex mixture [120]. Ag NPs offered also a solvent free method for small molecules analysis [225]. Au NPs offered excellent reproducibility with very low relative signal variation equal to 9.3% for HPY [108], and 15% for amino acids, carbohydrates, and peptides [158]. Metallic nanoparticles such as Ag and Au NPs can be modified with antibody for the analysis of viruses Enterovirus 71 (EV71), Japanese encephalitis virus (JEV), and Zika virus (ZIKV) in human serum samples [115].

Metallic nanoparticles including Ag NPs can be used for both negative and positive modes. This property offer selective analysis of galactoceramides, diacylglycerols, ceramides, phosphatidylcholines, cholesteryl ester, and cholesterol in positive mode, and the detection of phosphatidyl ethanolamides, sulfatides, phosphatidyl inositol, and sphingomyelins in negative ion mode [184].

Metallic nanoparticles can be used as probe and stationary phase. Ag NPs was used as a probe for single drop microextraction (SDME) of peptides [122]. The separation using metallic nanoparticles offer simple preconcentration method for low concentration before the analysis using LDI-MS [226]. Metallic nanoparticles offer matrix-free LDI-MS and provide low LOD (Table 1) [116]. They can be applied simultaneously for other analytical methods. For instance, Ag NPs functionalized glass fiber (Ag-GF) substrate can be used for the anlaysis of sulfur compounds using surface-enhanced Raman scattering spectroscopy (SERS) [227] and SALDI-MS [228]. The combination of different analytical methods offers quantitative and qualitative analysis [229, 230]. Analysis of structural isomers of pyridine compounds (*para*-, *meta*-, and *ortho*-pyridine carboxylic acid) using Au-decorated titania nanotube arrays (Au-TNA substrate) for SERS and SALDI-MS provide an useful methods for the discrimination of these isomers [231]. Au NPs can be used for solid-phase microextraction (SPME) for the analysis of estrogens [112].

Metallic nanoparticles are expensive. They tend to aggregate in the absence of stabilizing agents that sometime cause interference in the mass range < 500 Da. Ag NPs show toxicity and requires careful usage for biological sample applications. Metallic nanoparticles such as Au NPs produces peaks at *m/z* 197, 394, 591 representing Au_n^- ions ($n = 1–3$) [232]. However, these ions can react with CN^- and produce peak at *m/z* 249, indicating an abundant generation of gaseous $[Au(CN)_2]^-$ ions upon irradiation. Thus, it can be used to analysis CN^- ions species using LDI-MS [232]. Au NPs may cause also fragmentation of species such as diphenhydramine [233].

Oxides and chalcogenides nanoparticles assisted LDI-MS

Oxide and chalcogenides nanoparticles (Table 2) including mesoporous WO_3–TiO_2 [234], Fe_3O_4-TiO_2 core-shell nanoparticles [62], magnetic silica nanoparticles (MSNPs) [130], molecularly imprinted TiO_2 [235], TiO_2 nanowires [236], CeO_2 [237], mesoporous nanocrystalline titania sol–gel thin films [238], silver oxide (Ag_2O) [239], $AgFeO_2$ [131, 240, 241], $CuFeO_2$ [34, 242], ZnO NPs [243, 244], ZnO nanowire [59], Ag NPs-ZnO NRs [137], MoS_2 nanoflakes [138], ReO_3, and WO_3 in microparticle (μP) powder forms [245], MoS_2-Ag [217], indium tin oxide (ITO) [246], lithium-rich composite metal oxide (MnO_2, NiO and Co_3O_4) [247], and mesoporous silicate [88], were used as surface for SALDI-MS (Table 2).

Nylon nanoweb with TiO_2 particles enhances signal and offers low background spectra for amino acids [136].

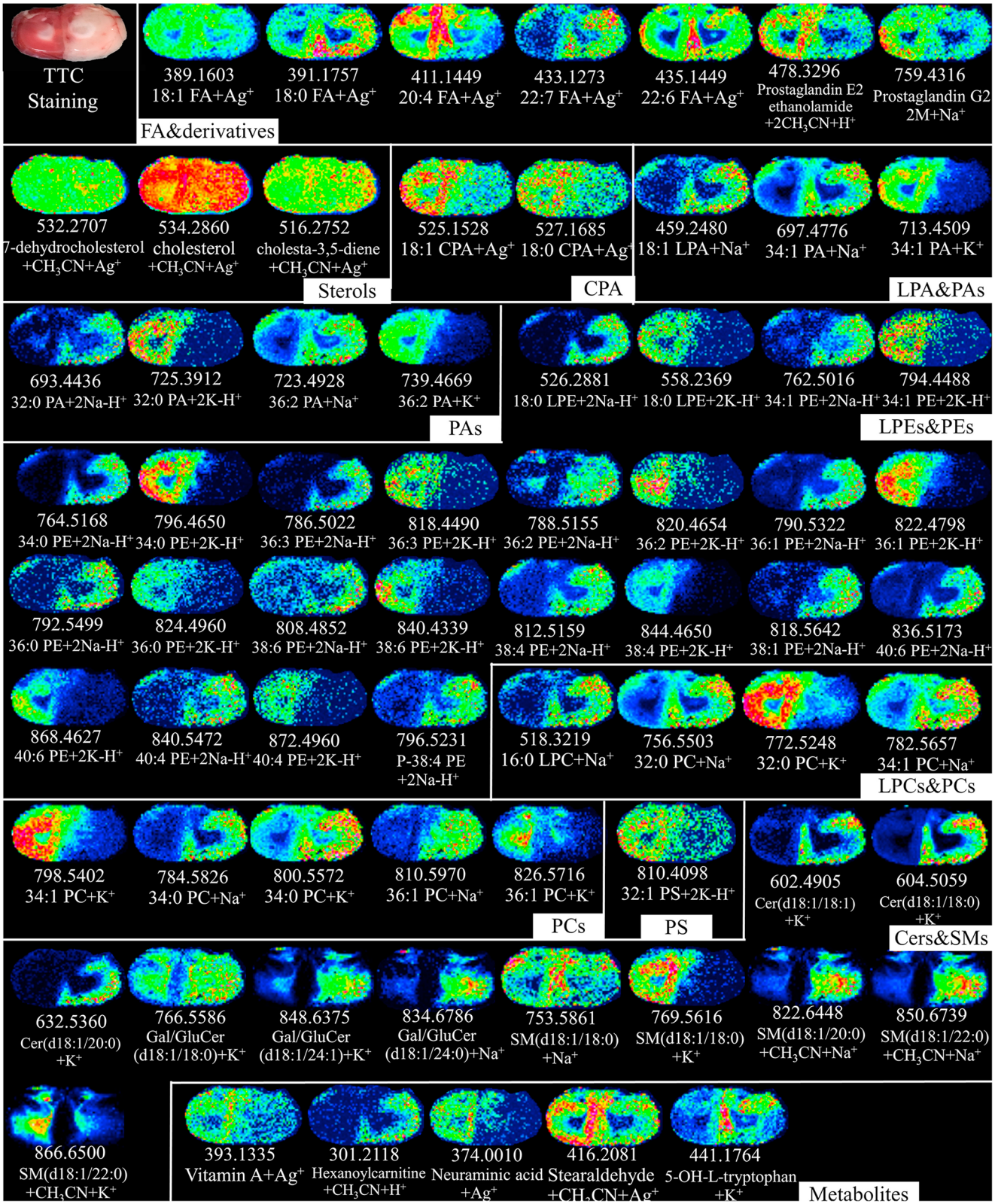

Fig. 3 In situ MALDI MS imaging of lipids and metabolites in the tissue section of rat brain using PVP@Ag NPs. Acronyms FA, CPAs, PAs, LPE, PEs, PCs, PS, SMs, Cers, LPA, PAs, LPCs, and PCs stand for fatty acids, cyclic lysophosphatidic acids, phosphatidic acids, lysophosphatidylethanolamine, phatidylethanolamines, phosphatidylcholines, phsopatidylserine, sphingomyelins, ceramids, lysophosphatidic acid, phosphatidic acids, lysophospatidylcholines, and patidylcholines, respectively. Figure reprinted with permission from Ref. [214]. Copyrights belong to Elsevier

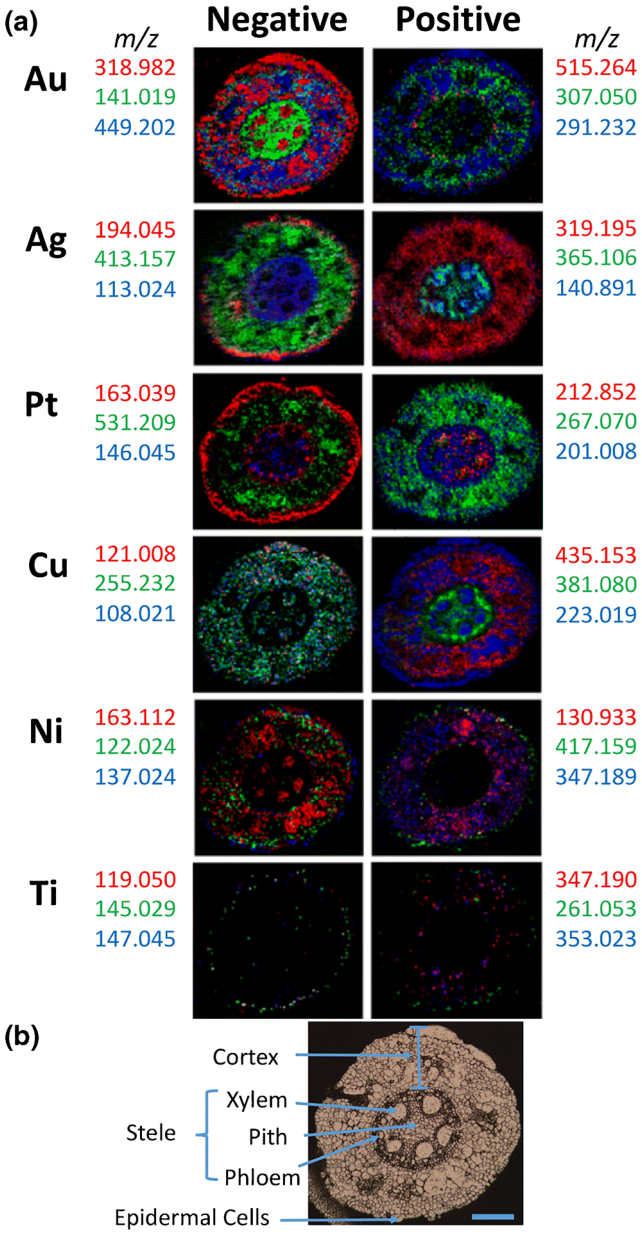

Fig. 4 **a** MALDI MSI of B73 maize root cross-sections showing localizations of various metabolites with each metal matrix, and (**b**) Morphology of maize root. Scale bar 200 μm. Figure reprinted from Ref. [223] with permission. Copyrights belong to Springer Nature.

Fe_3O_4@Au-B(OH)$_2$@mTiO_2 cores-shells microspheres was applied for the enrichment of phosphopeptides and glycopeptides after tryptic digestion [248]. TiO_2-based thin film was prepared on a MALDI plate by atomic layer deposition (ALD) technique and then modified with –NH_2 group [249]. The obtained TiO_2-NH_2 modified plate was applied for on-plate simultaneous enrichment of phosphopeptides and glycopeptides [249]. The surface of TiO_2 nanoparticles can be modified with pyridoxal 5′-phosphate (PLP) which can be used to immobilize Ti^{4+} (Fe_3O_4@SiO_2-PLP-Ti^{4+}) that can be applied for metal affinity chromatography (IMAC) for the enrichment of phosphopeptides. The core-shell Fe_3O_4@SiO_2-PLP-Ti^{4+} offered high efficiency for phosphopeptides enrichment with superior selectivity towards phosphopeptides with >1000-fold interferences of non-phosphopeptides [142]. Simple preparation of porous carbon (PCs)@(Ti-Zr)O_4 using calcination was reported [134]. PCs@(Ti-Zr)O_4 was applied for metal oxide affinity chromatography (MOAC) that offered effective and selective adsorption for β-casein [134]. The use of PCs@(Ti-Zr)O_4 offered selective analysis of BSA for mass ratio of 1:1500 (β-casein:bovine serum albumin (BSA)). The large surface area of the material offered low LOD (0.1 fmol), and can be applicable for enrichment of phosphopeptides from nonfat milk, human serum, and mice liver [134]. Nanoporous two-dimensional TiO_2 nanoflakes offered one-step enrichment and analysis of small molecules in real samples such as fish blood, fish-tissue extracts, and inks [250]. The materials showed high enrichment efficiency, and low background noise. The large surface area of the materials offered low LOD at ppt or even sub-ppt concentrations [250].

The surface of TiO_2 was intensively used for selective enrichment of phosphopeptides. TiO_2 modified with polyacrylate (PAA-Ti-TiO_2) was used for molar ratio of phosphopeptides:nonphosphopeptides (1:1000) [135]. PAA-Ti-TiO_2 showed high sensitivity and high recovery of phosphopeptides > 78% [135]. TiO_2-ZrO_2 was used for inverse opal film-based microfluidic devices for on-chip phosphopeptide enrichment using MALDI-MS [251]. Several modification of TiO_2 including DOTA (1,4,7,10-tetraazacyclododecane N, N′, N″, N‴-tetra-acetic acid) and Zr^{4+}(TiO_2@DOTA-Zr) [252], phytic acid (PA) [132], titanoniobate nanosheets embedded with Fe_3O_4 nanocrystals (Fe_3O_4–TiNb) [253], [Ti(IV)@poly(VPA-*co*-EDMA), poly (vinylphosphonic acid-*co*-ethylene dimethacrylate)] [254], MagSiO_2@SiO_2@PDA@Ti(IV) [255], magnetite-ceria-codecorated titanoniobate nanosheet (MC-TiNb) [256], polyethylene glycol (PEG)-Ce-CeO_2-Fe_3O_4, and nanosolid superacid (Ce-CeO_2-SO_4-Fe_2O_3) [257]. $CuFeMnO_4$ showed selective capture of phosphopeptides from A549 cells [258]. Other metal oxide nanoparticles including MoO_3 [160], $MnFe_2O_4$ [259], and zirconia incorporated ordered mesoporous carbon (OMC) composites [260] were also reported. These nanomaterials offered effective separation of phosphopeptides from non-phosphopeptides. They differentiate selectively between mono- and multi-phosphopeptides.

Iron oxide (Fe_3O_4) or magnetic nanoparticles (MNPs) [261] was used for the analysis of small molecules, such as pesticides and plant hormones, peptides [262], surfactants [263], mercury [129], glycans [126], glycolipids [127], biomolecules in cultured cells [264], carbohydrate [265], and endotoxin from urine sample [266]. Polydopamine-coated Fe_3O_4 nanoparticles (PDA@Fe_3O_4 NPs) were applied as matrix for the detection of eleven small molecule pollutants, including benzo(a)pyrene (BaP), three perfluorinated

compounds (PFCs), and seven antibiotics [267]. The ionization of these species in either positive or negative reflection mode was reported. Surface functionalized graphene-coated cobalt nanoparticles with benzylamine groups (CoC–NH_2 nanomagnets) was applied for enrichment of pentachlorophenol, bisphenol A, and PFCs [162].

Advantages and disadvantages of metal oxide nanoparticles

Metal oxides such as TiO_2 offered sensitive analysis of peptide mixture (Mix1) without any observable ion suppression [268]. TiO_2 assisted LDI-MS provided a LOD of 10 fmol for neurotensin peptide sutent, a small tyrosine kinase inhibitor, and 50 fmol for verapamil. There was no observation of ion suppression for the analysis of mixture analytes. It was reported that TiO_2 ionizes signals of 179 molecules, while a conventional matrix 2,5-dihydroxybenzoic acid (DHB) ionize only 4 molecules [133]. It was also used for imaging of endogenous low molecular weight metabolites (LMWM) in mouse brain (80–500 Da) [133]. Metal oxide such as mesoporous silica generates low energetic ions compared to the use of carbon nanotubes or graphene-assisted LDI MS [130]. Thus, it causes low fragmentation of thermal labile analytes.

Metal oxide nanoparticles including magnetic silica microspheres offered separation and can be used as a surface for LDI-MS i.e. dual functions [269]. Fe^{3+}@magnetic silica microspheres enriched phosphopeptide specifically and improve their analysis using MALDI-MS [269]. Modification of Fe_3O_4 NPs using chitosan was used for separation and detection of endotoxin from urine sample [266]. PDA@Fe_3O_4 NPs can be as a adsorbent for the separation of BaP in tap water and lake water samples using magnetic solid-phase extraction (MSPE) [267]. Au NPs coated magnetic beads was applied for amino acid analysis [270]. Magnetic graphene and carbon nanotube (graphene-CNT) was applied as matrix and adsorbent for the analysis and enrichment of small molecule compounds [271]. The surface of MNPs can be modified using several molecules including humic acids (HAs) that can be used an adsorbent of MSPE [128]. HA@MNPs offered fast separation of rhodamine B in chili oil with recoveries 73.8-81.5%, and relative standard deviations (RSDs) less than 21.3% (intraday), and 20.3% (interday) [128]. MNPs improved the sensitivity for the analysis of metal ions (> 20-100 fold) [272]. The presence of metal ions such as Fe^{3+}, and Mn^{2+} in $MnFe_2O_4$ showed highly selective enrichment for phosphopeptides because of the strong coordination interaction between metal ions (Fe^{3+}, and Mn^{2+}) and phosphate groups of phosphopeptdies [259].

The presence of many function groups on the surface of metal oxide nanoparticles can be easily modified with metal ions that offered selective interactions with small molecules. Fe_3O_4@PDA-M^{n+} modified with eight metal ions (M^{n+}), including Nb^{5+}, Ti^{4+}, Zr^{4+}, Ga^{3+}, Y^{3+}, In^{3+}, Ce^{4+}, Fe^{3+}, were applied for selective enrichment of phosphopeptides [273]. The presence of the hydroxyl and amino group of PDA provided anchoring groups of the investigated metal ions. Fe_3O_4@TCPP-DOTA-Ms, TCPP denoted tetrakis(4-carboxylphenyl) porphyrin) and DOTA for 1,4,7,10-tetraazacyclododecane *N*, *N*′, *N*″, *N*‴-tetraacetic acid, was modified with metal ions Ti^{4+}, Zr^{4+}, Fe^{3+}, Tb^{3+}, Tm^{3+}, Ho^{3+}, and applied for the analysis of α-casein tryptic digest [274]. Fe_3O_4@TCPP-DOTA-Tb-Ti showed excellent enrichment efficiency and stronger adsorption for multiple phosphorylated peptides compared to other species.

Metal oxide nanoparticles are inexpensive, and can be used as affinity probe for selective separation, enrichment, or ionization of specific analyte. They can be used efficiently to isolate phosphopeptides from standard phosphoprotein, and real samples [275].

Silicon-based assisted LDI-MS

In 1999, desorption ionization on silicon (DIOS) was reported for the first time for the analysis of small molecules [84]. Silicon-based NPs including Stöber silica NPs [276], C_{18}-SiO_2 [139], SiO_2 modified graphene [78], Fe_3O_4@SiO_2 [277], silicon nanowires (Si NWs) [68, 82], silicon nanowire arrays [278], silicon nanopost arrays (NAPA) [279, 280], Si pillar [145], silicon nanopillar arrays [144], silicon microcolumn arrays [67], silicon nanocones array [281], silicon microtips [282], silicon nanofilaments [283], silicon films [284], amorphous silicon [285], p^+ type-derived porous silicon (PSi) [140], phosphate-imprinted mesoporous silica nanoparticles (MSNs) [286], gold nanoparticles grafted onto a nanostructure silicon (Au NPs-nSi) [113], and Pd NPs-PSi [146], were applied for the analysis of small molecules (Table 3).

Silicon-based nanoparticles showed low LOD, and can be used for both positive and negative modes [68]. Silicon nanowire required 5−8 times less laser fluence for ion production than either MALDI or DIOS [287]. Silicon nanomaterials can be easily shaped into arrays, films, and nanospots which have the potential for laboratory on a chip devices. Surface of silicon nanomaterials can be tailored and that showed low degree of ion fragmentation [279]. As prepared PS (PS-H) was thermally oxidized at 300 °C (PS-OX), and then chemically grafted with cation-exchanging alkyl sulfonic acid (PS-SO_3H), and anion-exchanging propyl-octadecyl dimethylammonium chloride (PS-ODMA$^+Cl^-$) groups [140]. These chemical modification allowed the detection of only low fragmented ions (methylene blue, MB^+) and methyl orange (MO^-), respectively [140]. Silicon nanowire arrays showed high performance, and required low laser energy

[278]. The morphologies, and thicknesses of Si nanomaterials can be controlled using self-assembly of silane molecules [288]. Surface modification offered low fragmentation, and can produce spectra with no or minimal interferences peaks [288]. Silicon can be easily etched using several method including electrochemical method [146]. The porosity of Si can be easily modified with nanoparticle such as Pd which enhance the laser energy absorption due to localized surface plasmon resonance (LSPR) [146].

The surface modification of silicon-based nanomaterials may offer selective detection for species such as phosphopeptides. Ti^{4+} immobilized SiO_2 graphene-like multilayer nanosheets [141], and magnetic nanoparticles (Fe_3O_4@mSiO_2-Ti^{4+}) offered ultrasensitive enrichment of phosphopeptides [289]. They can be applied for identifying endogenous phosphopeptides in healthy human serum and saliva.

The use of porous silicon nanoparticles offered detection of small molecules without the need of extraction, or separation [276]. Hydrophobic porous silicon array offered direct analysis of methamphetamine, cocaine, and 3,4-methylenedioxy methamphetamine in oral fluids 300-times faster compared to conventional method [290]. Silica can be easily modified with ionic liquids and organic matrix CHCA without change of the chromophore group of CHCA molecule [291]. Silicon substrate can be used for selective enrichment, self-desalting, and matrix-free analysis of peptides in a single step [292].

The upper mass limit for analytes using DIOS is only restricted to small molecules below 2500 Da [143]. The nature of the porous silicon platform and the sample composition influence the performance of the technique. The reproducibility between different DIOS chips is low. However, Si pillar with suitable size offered simple sample spotting and improve the reproducibility and sensitivity for the quantitative analysis [145]. Further efforts to improve the chips reproducibility and the mass limits should be carried out.

Carbon-based nanomaterials assisted LDI-MS

Carbon nanomaterials including activated carbon [293], fullerenes, carbon nanotubes, nanodiamond, nanofibers, nanohorns [294], graphene (G) [295], graphene oxide (GO), carbon dots (C dots), N-doped graphene [155], sinapinic acid–GO [296], CuCoO–GO [161], N-doped carbon dots [297], activated carbon [147], single-walled carbon nanohorns (SWNHs) [298], and graphitic carbon nitride (g-C_3N_4) nanosheets [159], were used as surface for LDI-MS [299] (Table 4). They were applied for the analysis of small molecules including amino acids, polyamines, peptides, steroids, nucleosides, nucleotides and metallodrugs [151–153, 296, 300–308].

The first application of fullerene C_{60} as surface for LDI-MS was in 1994 [309, 310]. C_{70} fullerene was applied as a surface for the analysis of steroids [311]. Reagent hexa(sulfonbutyl)fullerene ($C_{60}[(CH_2)_4SO_3\text{-}]_6$) was used as precipitating reagent for selective detection of charged species in aqueous solutions [312]. Fullerene derivatives including dioctadecyl methanoC_{60}, C_{60}oacetic acid, and iminodiacetic acid-C_{60} [313], and C_{60}-fullerene-bound silica [314], were also reported. Fullerene derivatives were applied for several analytes including uranium [315], peptides [316], and organometallic [317].

C_{60}-fullerene silica was applied as stationary phase for solid-phase extraction (SPE) of selected flavonoids with recoveries of ~99% [314]. A study showed that fullerene–silica with a pore size of 30 nm showed better recoveries at low peptide concentrations compared to C_{18}- and C_{30}-modified silica as stationary phase [316]. Modified C_{60} using magnetic silica nanoparticles (C_{60}-f-MS) offered very fast (< 5 min) separation method for small molecules [318].

In 1995, graphite with particle size 2–150 μm was dispersed in glycerol and applied for LDI-MS for the analysis of small molecules [319, 320]. Graphite plate was used for the analysis of polypropylene glycol and polystyrene [321]. Graphite combined "Parallel Fragmentation Monitoring" (PFM) offered high-throughput quantification of citrulline with a correlation coefficient ≥ 0.997 and within- and between-day coefficient of variation (CV) of 3.1–8.7%, and 3.5–10.6%, respectively [150]. Pencil lead, is a form of graphite mixed with other components such as clay and wax, was used as a surface for the analysis of uranium in a standard materials [148]. It offered quantitative analysis for the isotope ratio analysis of actinide metals [148]. Thus, graphite assisted LDI-MS identified the presence of low micron-sized uranium oxide particles and established their distribution across a substrate surface [149].

Graphene, is an allotrope of carbon in the form of a two-dimensional, was reported as surface for the analysis of small molecules [300]. Graphene-based nanomaterials were applied for the analysis of antibiotic [161], metabolite [322], flavonoids and phenylpropanoids [323], metallodrugs [151], surfactants [78], mercury [152], peptides [296], lipids [153], nitropolycyclic aromatic hydrocarbons (nitro-PAHs) in $PM_{2.5}$ samples [154], amino acids, fatty acids, as well as nucleosides and nucleotides [324], polymers [325], and Chinese medicine herbs [305]. Graphene oxide nanoribbons (GO NRs) showed higher signals of the investigated analytes compared to conventional organic matrix [326]. The analysis of PAHs using graphene showed average recoveries of 69.2% to 119.4%, and the inter-day precisions of less than 12.3% with intra-day precisions less than 20.7% [154]. N-doped graphene improved the analysis and offered a direct monitor method of drugs in human serum [155]. Core–shell structured gold@graphitized mesoporous silica nanocomposite

(Au@GMSN) was applied for small molecules including amino acids, neutral saccharides, peptides, and traditional Chinese medicine [327]. Au@GMSN showed high ionization efficiency, offered low fragmentation, free interference spectra, and good reproducibility [327]. Other derivatives of graphene including fluorographene (FG) [328], and graphene coated porous amorphous carbon with P–O surface group and co-doped phosphorus and nitrogen (O–P, N-C/G) [329], were also reported. Graphene and their derivatives are effective adsorbents, and good surface for LDI-MS [330].

Carbon nanotube (CNT) was reported as a surface for LDI-MS for the analysis of small molecules including peptides, organic compounds, and β-cyclodextrin [76]. Dispersion of multi-wall carbon nanotubes (MWCNT) using polyaniline (PANI@MWCNTs) [331], and polydopamine (PDA@MWCNTs) [332] were reported to improve the sample homogeneity. CNT was used as film (consisting of GO-MWCNT double layer) [333], nanofibers (polyacrylonitrile-Nafion®-carbon nanotube, PAN-Nafion®-CNT) [334], or membrane [335] for the analysis of small molecules including peptides, and small drugs.

Carbon dots (C dots) were applied for a wide range of small molecules including amino acids, peptides, fatty acids, β-agonists, and neutral oligosaccharides [165]. C dots assist ionization of a target analyte in both positive and negative ion modes with relative error of 2.76-4.31% [165]. Nitrogen-doped carbon dots (N-CDs) ionize analytes such as glucose, sucrose, amino acids, nilotinib, and polyethylene glycols [166]. Carbon dots nanocomposite (Au NPs@C dots) combining chelating agent such as mefenamic acid was used for the detection of metal ions in cancer cell [167]. PAN-Nafion®-CNT was tested for the analysis of small drug molecules [188]. Data show improvement for the analysis for the small molecules. C dots such as N,S-co-doped CDs can be sprayed and applied for bisphenol S (BPS) mapping in mouse tissues [336]. N,S co-doped CDs offered quantitative analysis with very low LOD as low as the pmol level for BPS. The method can be also applied for different tissues of mouse including liver, kidney, spleen, and heart [336].

Carbon-based materials are ideal material for the analysis of small molecules using LDI-MS. They exhibit UV absorption in the wavelength range of 250-350 nm [164, 337, 338]. Thus, they can be applied for several laser types including N_2 laser (337 nm), and Nd:YAG laser (355 nm and 266 nm). Application of G-MNPs for LDI-MS offered simple separation method for small molecules [339]. Polystyrene-oxidized carbon nanotubes (PS-OCNTs) can be used as adsorbent and matrix for MALDI-MS [340]. Composite consists of MNPs, GO, and chitosan anchored Ti^{4+} offered selective enrichment of phosphopeptides from the tryptic digest of β-casein (phosphopeptides to non-phosphopeptides at a molar ratio of 1: 400). The material showed high sensitivity (0.5 fmol), large enrichment capacity (66.6 $mg \cdot g^{-1}$), and recovery 93.11% [341]. Magnetic mesoporous carbon composites was reported for selective enrichment of phosphopeptides [342]. High throughput detection of tetracycline residues in milk was achieved using G or GO as matrix [343]. Highly ordered mesoporous carbon (OMC) called CMK-8 showed the best performance for the analysis of small molecules compared to other porous materials such as CMK-3, SBA-15, and MCM-41 [344]. The material served as adsorbent and matrix for screening and identification of toxic compounds in a single drop of human whole blood [344]. Octadecyl-modified CMK-8 (C_{18}-CMK-8) provided simultaneous analysis, and simple extraction of multiple small molecules using SPE in single-drop human whole blood samples [156]. The porosity of highly OMC as well as the characteristic hydrophobicity of carbon offered simple analysis of 3402 different endogenous peptides from only 20 μL of human serum [157]. Some carbon nanomaterials such as G can be easily fabricated as substrate using 3D printed technique [345]. O–P, N-C@G can be used for dual-ion mode i.e. positive and negative-ion modes for detecting small molecules including amino acids, small peptides, saccharides, drugs, and pollutants (Fig. 5) [329]. Nanocomposite of CeO_2-carbon black enhances the detection sensitivity of drug molecules and requires no sample pretreatment or extraction [163].

Carbon nanomaterials have low water dispersion [346]. Thus, they have limitations to form homogenous spots. This requires the use of organic solvents or modification with polymers to improve the spot homogeneity. The presence of species such as oxidative debris on the surface of carbon nanomaterials such as GO depress LDI-MS efficiency [347]. Removing these species from the surface enhances the materials performance.

Quantum dots assisted LDI-MS

Quantum dots (QDs) are small semiconductor nanocrystals with particle size < 10 nm. Heavy metal based QDs including CdTe [348], HgTe [349], CdSe-ZnS [350], [71], and ZnS [72], were applied for SALDI-MS [351–353]. QDs were used for proteomics [352, 354], peptides [355], metallodrugs [351, 356], carbohydrates [357], and others [42].

QDs showed no interferences peaks at mass range below 500 *m/z* with high ionization efficiency [10, 11, 358]. QDs offered higher signals of the target analyte compared to conventional organic matrices [359]. They improved the signal-to-noise ratio, spectrum quality, and increases the number of detected peptides and the overall sequence coverage [350]. However, most of QDs, especially Cd-containing QDs are toxic [360].

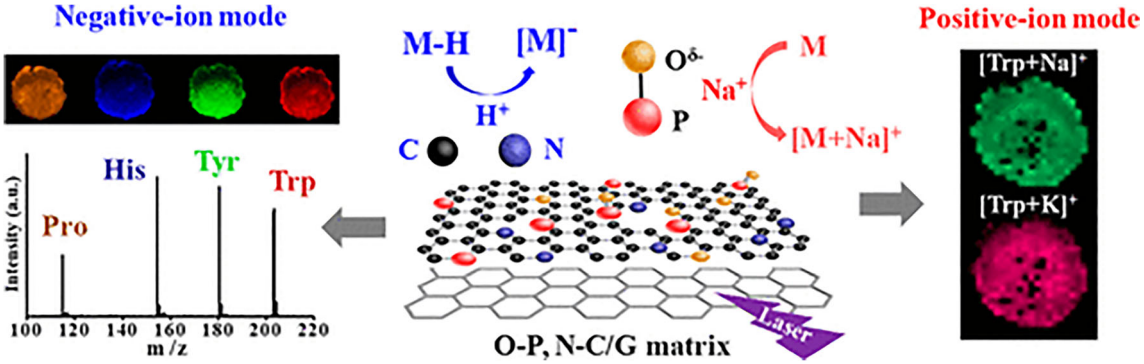

Fig. 5 Small molecules analysis for dual mode using O–P,N-C@G. Image reprinted with permission from Ref. [329]. Copyrights belong to ACS

Metal-organic frameworks (MOFs) assisted LDI-MS

Metal-organic frameworks (MOFs) are self-assembly porous material consisting of metal as connector and an organic ligand as linkers [361–371]. These combinations offer many number of MOFs (>70,000 structure in Cambridge Crystallographic Data Centre (CCDC)) [372]. However, few MOFs were reported as surface for LDI-MS [168] (Table 5). *Materials Institute Lavoisier* (MILs) MIL-101(Cr) [169], MIL-100(Fe) [177], University of Oslo (UiO) UiO-66-PDC and UiO-66-$(OH)_2$ [373], $Zn_2(bim)_4$ nanosheets [374], Fe_3O_4@SiO_2@UiO-66 core–shell magnetic microspheres [175], MIL-101(Cr)-NH_2 grafted dendrimer poly(amidoamine) (PAMAM) [375], PDA@Fe_3O_4@Zr-SO_3H [376], and Fe_3O_4-C@MIL-100 [377] (Table 5).

MOFs were applied for the analysis of monosaccharides [176], and disaccharides, peptides and starch [378], glycopeptides [379], N-glycopeptide [375], quercetin analysis [169], saccharides, amino acids, nucleosides, peptides, alkaline drugs, and natural products [373], domoic acid (DA) in shellfish samples [175], and BaP [380].

Zeolitic imidazolate frameworks (ZIFs) [371], are subclass of MOFs, coated magnetic nanocomposites (Fe_3O_4@ZIF-8) was applied as both matrix and absorbent for the separation and analysis of peptides and amino acids [171], and nitropolycyclic aromatic hydrocarbons (nitro-PAHs) [172]. ZIF-7, ZIF-8 and ZIF-90 were used as sorbent and matrix for the enrichment and analysis of bisphenols such as bisphenol A (BPA), bisphenol B (BPB), bisphenol S (BPS), bisphenol F (BPF) and bisphenol AF (BPAF) [170]. Magnetic ZIF-90 was modified with DOTA prior to immobilize enzyme trypsin (Fe_3O_4@DOTA-ZIF-90-trypsin). Fe_3O_4@DOTA-ZIF-90-trypsin showed satisfactory digestion efficiency within only 1 min with the sequence coverage (80%) that is comparable or even better than that (70%) of the traditional 12 h free trypsin digestion [381].

MOFs can be used as precursor for the synthesis of porous carbons (Table 5). Nanoporous carbon derived from MOFs MIL-53 and cCYCU-3 was reported [382]. Carbonization of MIL-101(Cr) leads to the formation of nanoporous carbon that can be used for the analysis of N-linked glycans from standard glycoprotein or complex human serum proteins [383]. The pore size of the material showed size exclusion effect and offered the analysis of N-linked glycans from standard glycoprotein or complex human serum proteins. ZrO_2 nanoporous carbons were applied for the analysis of several neurotransmitters [384].

Hierarchical porous anatase TiO_2 can be synthesized using MIL-125 (Ti) as precursor through hydrolysis and thermal decomposition [385]. The prepared material offered direct and *in situ* enrichment of phosphopeptides from undigested phosphorylated proteins. The analysis procedure is fast (40 min) and can be accomplished using a one-pot single step [385]. Fe_3O_4@SiO_2@$(Zr\text{-}Ti\text{-}PTA)_{15}$ showed also highly selective enrichment of phosphopeptides [386].

The surface of MOFs can be easily modified for separation and extraction. Polydopamine (PDA)-coated magnetic microspheres with surface modification of zirconium-based MOF (Fe_3O_4@PDA@Zr-MOF) were synthesized and applied for enrichment of phosphopeptides [387]. Polydopamine-modified hydrophilic magnetic ZIFs (Fe_3O_4@PDA@ZIF-8) were applied for the extraction of low-abundance peptides [173]. The presence of low-coordinated Zn^{2+} ions offered strong affinity towards low abundance peptides, especially those with histidine residues. Thus, the materials provided a simple and fast extraction procedure. The large surface area of the materials increases the tryptic digestion for the sequence coverage of BSA, and *human serum albumin* (HSA). The presence of free carboxylic groups in UiO-66 (denoted as UiO-66-COOH) offered a hydrophilic MOF for selective enrichment of glycopeptides from tryptic digests of standard glycoproteins and biological samples [388].

MOFs are good adsorbent due to their large surface area and pore tunability. Magnetic ZIFs nanocomposite was used to exclude large protein [173]. The materials were used for the analysis of low concentration peptide even under 200-fold dilution with BSA protein solution [173]. Fe_3O_4@MIL-100 (Fe)) [174], or magnetic graphene@MOF [389] showed selective capture of phosphopeptides. The materials offered

highly selective enrichment of phosphopeptide from the human serum (both the healthy and unhealthy) and nonfat milk [174]. Several MOFs such as UiO-66-$(OH)_2$ [373], Fe_3O_4@ZnBLD composites [390], UiO-66 incorporated poly(MAA-co-PEGDA) monolithic column [391], poly(UiO-66-NH-Met-co-PEGDA) monolithic [392], UiO-66, and UiO-67 [393], Fe_3O_4@PDA@Er(btc) [394], $[Er_2(PDA)_3(H_2O)]\cdot 2H_2O$, 1,4-phenylenediacetate (PDA) [395], Fe_3O_4@PDA@UiO-66-NH_2 [396], MIL-101(Cr) modified with urea (MIL-101(Cr)-UR_2) [397] were reported for selective enrichment of phosphopeptides. The materials were applied for standard protein digest (α-casein, β-casein and ovalbumin) as well as digested egg white proteins glycopeptides from complex biosamples. Authors recovered 14 and 4 phosphopeptides from the peptide mixture and digested egg-white, respectively [395]. MOFs have the potential to sever for solid phase microextraction (SPME) [398], immobilized metal ion affinity chromatography (IMAC), and metal oxide affinity chromatography (MOAC) [399]. Magnetic zirconium-based MOF offered rapid separation (within 5 s) using external magnetic field, high binding capacity (100 $mg\cdot g^{-1}$), good enrichment recovery (84.8%), high sensitivity (5 fmol) and good selectivity for phosphopeptides from real samples (human serum and nonfat milk) [399].

Advantages and disadvantages of MOFs

MOFs offer more than 70 000 structures [372]. Thus, they provide chemists with a rich library for the best material selection. MOFs showed background-free spectra in both positive and negative ion modes [374] with high signal-to-noise ratio [169]. They have large surface area and thus, prevent ion suppression of analyte with poor ionization efficiency. Compared to Au NPs (14 nm) and SBA-15, MIL-100(Fe) showed higher intensities [177]. MOFs such as MIL-53(Al), MIL-100(Cr), and MIL-101(Cr) offered the analysis of low-abundance peptides while simultaneously effectively excluding high-abundance proteins [400].

MOF showed sensitive, and specific enrichment of analyte such as phosphopeptides [373]. The pore size and the type of the metals can be tuned to offer selective ionization or separation of a target analytes. MOFs provided dual-metal centers; the inherent Zr—O clusters and also the immobilized Zr(IV) center [401]. They can be used as adsorbent, surface and probe for separation or extraction. Surface properties can be tuned to offer high hydrophilicity, and unique size-exclusion effect [402]. MOFs can be also used as precursor for nanocomposite with magnetic properties offering selective and efficient extraction of endogenous peptides from human serum [403]. The materials can be easily processed and hold promising future for real products [363, 404].

There are over than 70 000 MOFs in the structure database, however few MOFs were reported. The lacks of stability for several MOFs render their applications in aqueous solution difficult [405]. The costs of the material still high and further efforts to reduce their price are interested.

Covalent organic frameworks (COFs) assisted LDI-MS

Covalent organic frameworks (COFs) are organic solids in which organic building blocks are linked by covalent bonds (Table 6). COFs-based IMAC material (denoted TpPa-2-Ti^{4+}) was applied for selective enrichment of phosphorpeptides from β-casein with limit of detection 4 fmol and high selectivity (β-casein:BSA ratio 1:100) [178]. The material was applied for enrichment of phosphopeptides from non-fat milk and HeLa cells with high sensitivity and selectivity [178]. The use of COFs is in the infancy stage and requires further efforts. Fe_3O_4@COFs has applied as an adsorbent for enrichment and as a surface for SALDI-TOF-MS analysis of polycyclic aromatic hydrocarbons (PAHs) and their derivatives in PM2.5 [179]. COFs can be also used as surface for the analysis of amino acids, fatty acids, and environmental pollutants like bisphenol S (BPS) and pyrene [180].

Others substrates

Substrates such as unmodified mixed cellulose ester membrane (MCEM) [415], and disposable paper-array plate [416] were also reported. MCEM was reported as a simple, and efficient substrate LDI-MS for the detection of lead ions (Pb^{2+}) in water urine samples and drinking straws [415]. MCEM assisted LDI substrate offered LOD of 0.05 nM [415]. The method offer high tolerance at least 1000-fold relative to other metal ions for the detection of Pb^{2+} ions in aqueous solutions [415]. These new substrates are cheap and show higher sensitivity compared to conventional stainless steel plates [416].

Mechanism of laser ionization/desorption using nanoparticles

Reasonable mechanism of ionization using organic matrices or nanoparticles is under debate [1, 417]. It is hard to find single and general mechanisms that explain the ions formation for all cases. First, most of the measurements conditions aren't identical. Second, the ionization depends on several parameters including analyte properties (molecular weight, ionizability, function groups, polarity, hydrophilicity, and hydrophobicity), nanoparticles characters (size, types, surface area, capping agents, and porosity), and experimental/instrumentals conditions. Third, it is hard to characterize the ternary interactions of analyte-nanoparticles-laser.

Table 6 An overview of nanomaterial-based methods for enrichment of phosphopeptides enrichment.

Materials	Technique	LOD	Selectivity	Ref.
ZrO_2-MNPs-MPC	MOAC	1.5 fmol	1:500	[342]
$Bi_{0.15}Fe_{0.15}TiO_2$		2 nmol·L^{-1}	1:1200	[406]
Ti^{4+}-PDA-G	IMAC		1:200	[407]
ZnMMs		250 fmol	1:100	[408]
Ti^{4+}-PA-MNPs		0.8 nmol·L^{-1}	1:2000	[132]
Ti^{4+}-4μ-PEO		2 fmol	1:1000	[409]
Ti^{4+}-ATP-MNPs		3 amol	1:5000	[410]
Ti^{4+}@poly(VPA-co-EDMA)		10 fmol	1:1000	[254]
Fe_3O_4@PDA-Ti/Nb		2 fmol		[411]
Fe_3O_4@nSiO_2@mSiO_2-TiO_2–Ti^{4+}		4 pmol	1:50	[412]
MagSiO_2@SiO_2@PDA@Ti^{4+}		50 fmol	1:500	[255]
MIL-101 Cr-Urea	MOFs	0.1 nmol·L^{-1}		[397]
Fe_3O_4@PDA@Er(btc)		0.02 fmol·μL^{-1}		[394]
Fe_3O_4@MIL-100(Fe)		0.01 fmol·μL^{-1}		[174]
Fe_3O_4@PDA@Zr-MOF				[387]
Fe_3O_4@MIL-101(Fe)		0.08 fmol·μL^{-1}	1:1000	[413]
UiO-66 and UiO-67		0.1 fmol·μL^{-1}	1:200	[393]
Ti-based MOF nanosheets			1:10000	[414]
Mesoporous magnetic material	MOFs-derived NPs	0.2 fmol·μL^{-1}	1:1000	[403]

4μ-PEO, 4-armed Poly(ethylene oxide); ATP, Adenosine triphosphate; G, graphene; MPC, mesoporous carbon; PDA, Polydopamine; VPA-co-EDMA, poly(vinylphosphonic acid-co-ethylene dimethacrylate); ZMMs, Zinc immomoblized magnetic microspheres

After sample spotting, the laser ablates the target analyte and desorbs/ionize before the detection. The hot plumes produced due to the laser ablation have many species including neutral, ionized, and non-ionized species. The laser-spot (contain nanoparticles and target analyte) interaction is very complicated and difficult to be investigated due to the high vacuum. Thus, it is very hard to find suitable explanation of what is going on the hot plume. However, the ion formation using matrices could be caused due to primary [418, 419], or secondary [1] ionization process. Primary ionization process can be due to multiphoton ionization (MPI), disproportionation, thermal proton transfer [420], excited-state proton transfer (ESPT), and spallation [418, 419]. While, secondary ionization process can be due to H^+ transfer, cationization, e^- capture and H^+ transfer, e^- transfer, and ejection. A model called "Lucky Survivor" hypothesis that the analyte may ionize in the solution and retain their solution-state charge within the solid state matrix [421]. Another mechanisms postulate that the ionization is due to electronic excitation [422]. Matrix-assisted ionization (MAI) or matrix assisted ionization *vacuum* (MAIV) using only matrix, and vacuum without the need of laser energy or voltage for ionization was also reported [423]. The ionization takes place simply after exposing the spot (matrix with analyte) to the vacuum. A study showed also that hot electron transfer in LSPR plays a key role in ionizing molecules during LDI process [424].

It is very hard to find a suitable single mechanism for all nanoparticles due to several reasons [425]. Most of the proposed mechanisms are mainly investigated for organic matrices. The organic matrix absorb the laser energy prior to the self-ionization. Thus, it was proposed that the organic matrix undergo proton transfer with the target analyte. The mechanism may be suitable for nanoparticles that have absorbance match the wavelength of the laser. A few studies investigate the mechanism of NPs assisted LDI-MS [103]. However, several mechanisms including proton transfer from the capping agent [426], thermal-driven desorption [427], vaporization, or phase explosion [428], heat confinement [429], and cationization [213], were proposed. The mechanism of LDI depends on several parameters, including laser properties (wavelength, photon energy, energy density, pulse width, incident angle of the beam), nanoparticles properties (size, surface properties, capping agents), nanoparticle-analyte interactions, laser-nanostructure interactions [430], sample preparation, and additives. For instance, the use of hypophosphite as reducing agent during the synthesis of Pd NPs decreases their melting points and subsequently decreases laser fluence requirements for LDI-MS [124].

Analysis of key parameters affecting nanoparticles performance

There are several key parameters that affecting the analysis of small molecules using nanoparticles (Fig. 6). These parameters should be investigated to achieve high sensitivity and better selectivity.

Compositions of nanoparticles

The chemical composition of nanoparticles affects their performance. A comparison among metallic nanoparticles of Ag, Au, Cu and Pt showed that protonated molecules

Fig. 6 Analysis of key parameters affecting nanoparticles performance including composition, surface, concentration, thickness, additives, surface area, pore size, and MALDI-MS instrument parameters

of analytes were predominated in the mass spectra when Au and Pt nanoparticles were used [426]. Pt nanoparticles showed the highest performance due to their smaller heat conductivity and higher melting temperature [426]. Adjusting the Ag–Au ratio tunes the surface plasmonic resonance absorption and hence influences the contrast imaging of latent fingerprints (LFPs) [431].

The chemical structure of carbon-based materials offers UV absorption in the wavelength range of 250-350 nm [164, 337, 338]. Thus, they can work for the analysis of small molecules using different lasers. The absorption of MOFs can be tuned using metal clusters or organic linker with the suitable chromophores. MIL-101(Cr) showed stronger absorption in the UV region of ~272 nm than MIL101(Fe) for the same concentration [169]. Thus, MIL-101(Cr) offered stronger absorption of laser energy and energy transfer to analytes. The properties of MOFs can be tuned using metal clusters, pore structure, organic linker, and their function groups.

Oxidized carbon nanotubes showed higher solubility in water compared to non-oxidized carbon nanotubes [164]. The presence of oxygen function groups in oxidized carbon nanotubes offered high dispersion, and better performance for the analysis of small molecules. Suitable functional groups facilitate the material modification and offered tunable properties.

Particle size and morphology of nanoparticles

It is shown that the size and shape of nanocrystals influenced the way of packing carbohydrates onto plate, and thus influences homogeneity and reproducibility of mass spectrometry analysis [432]. It was reported that large GO sheets (> 0.5 μm) have high tendency toward fragmentation under LDI than that of small GO sheets (< 0.5 μm) [433]. Therefore, nanosized GO showed high performance compared to large GO [433].

Several morphology of silicon, including nanowire [278], nanopost [279], nanopillar [144], microcolumn [67], nanofilaments [283], films [284], amorphous silicon [285], p^+ type-derived PSi [140], were reported. The morphology plays a role in the materials performance. The relation of the nanoparticles morphology and their performance should be correlated for the same analyte under identical conditions.

Surface properties of nanoparticles

Surface of NPs plays a leading role in the performance for LDI-MS [348]. Laser radiation interacts first with the surface or capping agents of NPs. Surface of NPs can be tuned the materials absorbance of laser energy [348]. It can be used also for selective trap and ionization for the aromatic molecular targets due to π-π interactions [434]. **L**aser **a**blation of Au **i**n **s**olution offered chemical-free size **s**elected Au NPs (LASiS) [435]. LASiS showed very low background in the low mass region (<500 Da) compared to citrate stabilized Au NPs (citrate-Au NPs), and dihydroxyacetophenone (DHAP) [435]. It was reported that the analyte ablation from the substrate plays trivial role for SALDI efficiency compared to the chemical properties of the surface [436]. The efficiency of LDI can be enhanced via modifying surfaces of the substrates with a plasmonic hot-electron transfer effect [437]. Magnetic nanoparticle modified with gluconic acid, citric acid, lactobionic acid, or glutathione reveals that the best capping agent for glycan, and peptide is gluconic acid and citric acid, respectively [438]. Another study showed that the chemical modification of graphene (e.g., oxidation, fluorination, amination, and carboxylation) affect the analysis of chemical contaminates in both modes, negative and positive [439]. However, the materials performance depend also on the analyte and incubation time [439].

Surface-based techniques such as silicon arrays, chips, thin films, and influenced by the surface properties. Silicon-based techniques require a clean surface with certain physicochemical properties [440]. A study showed a correlation between the substrate physicochemical properties and the LDI performance [440]. Results indicated that thick nanostructure layer was effective for LDI-MS compared to thinner nanostructure. The surface cleaning using plasma etching can effectively remove the surface contamination and increased the thickness of the oxide's layer. It was reported that the presence of fluorine and hydroxyl termination in silicon nanostructure enhanced the material performance [440]. Amorphous silicon showed higher ionization efficiencies >1% compared to hydrogen-passivated amorphous silicon [285]. The surface of NPs can be tuned for laser absorption [353].

The surface of Au NPs can be modified with conventional matrix CHCA for the analysis of peptides [42, 441]. The modification of NPs surface with conventional matrix offer higher mass signals compared to the corresponding conventional CHCA matrix [442]. The surface of Au NPs can be tuned to achieve a matrix-free method [443]. The encapsulation of Au NPs into strong acidic material such as zeolite showed high ionization of amino acids regardless of their isoelectric points [110]. LSPR properties of plasmonic metallic nanoparticle is also a key parameter during the LDI process [424]. The high density of surface ligands such as smaller nucleolin-binding aptamer (AS1411) of Au NPs may enhance multivalent binding with nucleolin molecules on tumor cell membranes [197].

Chemical engineering of the nanoparticles surface is useful for applications such as microextraction and separation. The surface of Fe_3O_4@PDA-M^{n+} can be easily modified with eight metal ions, including Nb^{5+}, Ti^{4+}, Zr^{4+}, Ga^{3+}, Y^{3+}, In^{3+}, Ce^{4+}, Fe^{3+}, for selective enrichment of phosphopeptides [273]. The hydroxyl and amino group of PDA offer anchoring groups for these metals and create new functions for the synthesized materials.

Additives

Additives influence the performance of nanoparticles for LDI-MS. The presence of perfluorinated surfactants perfluorooctanesulfonic acid enhanced the signal-to-noise ratio of tryptic digests for DIOS [444]. These additives showed 3-fold improvements in the number of peptides identification. Lithium-rich metal oxide (MnO_2, NiO and Co_3O_4) ionize small molecules due to lithium adducts [247]. Conjugation nanoparticles with organic matrix improve their performance without ionization suppression for high salt concentrations spots [445]. Effect of additives (NH_4OH, NaOH, LiOH, NaCl, or trifluoroacetic acid) on the performance of magnetic nanoparticle reveals that both cation and anion have effect on LDI efficiency [438]. However, Na^+ and OH^- ions were the most effective in promoting cross-ring fragmentation, compared with NH_4^+, Li^+, or Cl^- ions [438].

Concentration of nanoparticles

Concentration of nanoparticles influences the analysis performance for LDI-MS. The analysis of carbohydrates using low concentration of organic matrix modified MNPs offer soft ionization [265]. In other hand, the high concentration increases the fragmentation for carbohydrate [265].

Thickness of thin films or coating

The analysis of small molecules using thin films, chips and substrate modified nanoparticles depends on the thickness of these thin film technologies [333]. Optimization of the thickness is critical and should be considered during analysis. There are several methods to control the thickness of films including layer-by-layer (LBL) assembly cycles [333]. The thickness of GO-MWCNT-NH_2 multilayer-coated substrates influences the analysis of small molecules as shown in Fig. 7. The optimal number of LBL is varied based on the properties of the investigated analyte. The optimum number of GO film layers for LDI-MS analysis shows dependence on the chemical structures of small molecules, and the laser energy threshold needed for LDI of small molecules on GO-MWCNT films could be lowered as the number of LBL assembled GO films increased underneath the MWCNT layer [446]. The thickness of NPs on the tissue or the investigated organs is critical for imaging. The sputtered silver coating thickness was optimized for mouse and rat tissues including brain, kidney, liver, and testis [213]. The optimized thickness for mouse brain tissue section was 23 ± 2 nm and 16 ± 2 nm for the other tissues. Optimal thickness is very important to avoid ion suppression. The LDI efficiency depends on the thickness, assembly sequence and surface roughness of the hybrid films [447].

Pore size and surface area for porous materials

Porous nanostructures offered tunable properties for high performance of separation and microextraction. The pore structure of silicon-based materials retain the small analyte and enhances LDI process [143, 285]. The porosity of silicon can be tuned using etching solution, current density, or etching time [143]. Silicon substrate with highly disordered structure and high concentration of "dangling bonds" or deep gap states showed high ion generation [285].

The pore size and surface area for fullerene–silica materials influence the performance of LDI process. Data

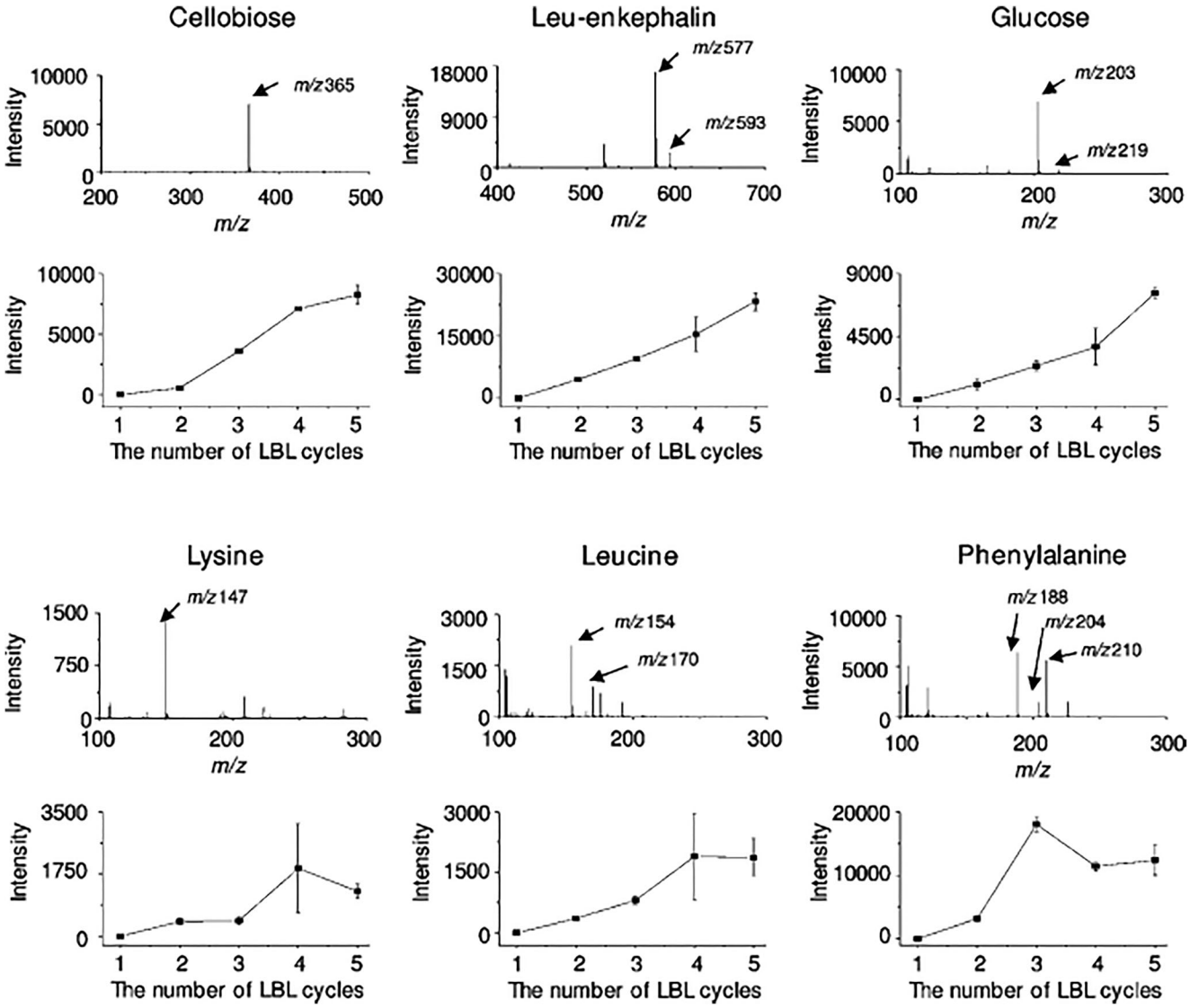

Fig. 7 Effect of the number of LBL assembly cycle of GO/MWCNT-NH_2 multilayer-coated substrates for the analysis of various small molecules, cellobiose, Leu-enkephalin, glucose, lysine, leucine and phenylalanine. Figure reprinted with permission from Ref. [333]

showed that the large pores facilitate the analytes desorption. The high surface area of fullerenes offered high efficiency for the laser energy transfer to the analytes. Thus, the material offers high sensitivity with low LOD (picomol level) [448]. The materials produced interference-free spectra.

The crystallinity of nanoparticles

The crystal orientation on silicon showed low effect on the substrate performance [143]. The crystal orientation affect the pore shape and directionality but not pore size [143]. A few studies are available in the literature focusing on the materials crystallinity and their effect on LDI efficiency.

Instrumental parameters

Instrumental parameters, including type of analyzer; time-of-flight tube (TOF) or Fourier-transform ion cyclotron resonance (FTICR) [214], length of TOF tube, laser wavelength, mode of ionization [137], affect the results of nanoparticles. The mode of ionization affect the performance of nanoparticles [438]. For instance, there is no ionization performance of magnetic nanoparticle using different capping agents and additives in negative mode [438]. In contrast, the nanoparticle showed good performance in positive mode.

Other parameters

Other parameters such as the analyte and incubation time [439], surface disorders, thermal conductivity and physically

or chemically adsorbed water [449], surface contamination [450], phase-transition properties of NPs [202], and melting properties of the nanoparticles during laser irradiation [124], affect the signal intensities of analyte ions. LDI efficiency is significantly affected by small changes in the analyte attaching to the target [451].

Conclusions and Outlooks

The use of nanoparticles for the analysis of small molecules using LDI-MS is promising. Nanoparticles offer high sensitivity and better selectivity compared to conventional organic matrices. The material sensitivity can be increased using the suitable nanoparticles and signal amplification [452]. The key parameters of nanoparticles including composition, size, porosity, surface, and crystallinity influence the material performance. Sensitive nanoparticles are varied from analyte to analyte. Thus, each nanoparticle class can be suitable for certain type of analytes.

The surface properties of nanoparticles influence the material performance. The surface modification can be tuned to achieve high selectivity for separation or extraction applications. The surface of nanoparticles can be also tuned to improve the materials absorbance for laser energy and thus the material performance.

The analysis of small molecules using nanoparticles offer free background spectra. They show no peak overlap and can ionize almost the entire analytes in a mixture without observable ion suppression. The ionization efficiency of nanoparticles is high due to their large surface area. Thus, they can be used for the poor ionization analytes via direct ionization or the formation of adducts with the investigated analyte.

The modification of nanoparticle surface with organic matrices is attractive. Organic matrices could serve as capping or stabilizing agents and at the same time as binary matrix for LDI-MS. The combination of two or more diverse kinds of inorganic materials offers a better performance because of the synergic effect of the composite. They also offer several tasks including matrix, separation, enrichment, extraction, and selective ionization.

The preparation of inorganic nanomaterials in some cases is complicated and requires expensive reagents. Further efforts for simple and cheap methods are necessary. The method should be simple and easy for further modification. Thus, they can serve as selective probe or adsorbent for separation and extraction prior to the analysis.

Analysis of small molecules using thin film or chip-based technology is simple, direct and requires no matrix. However, they lack high reproducibility. Extract efforts to raise the mass ceiling and improve the reproducibility of the porous silicon material is necessary. In general, factors affecting the reproducibility should be also investigated [453].

A few materials were used for quantification analysis using LDI-MS compared to other techniques [454, 455] (Tables 1, 2, 3, 4, 5 and 6). The high standard deviation of the signals limits the application of nanoparticles for quantification analysis. Compared to several types of nanomaterials, MOFs are promising (Tables 1, 2, 3, 4, 5 and 6). The large surface area and the presence of tunable pore size improve the signals and reduce the signal fluctuation. Thus, they offer high regression coefficient (R^2> 95%).

Nanoparticles show promising application for preconcentration of low concentration of analytes such as phosphopeptides (Table 7) [174, 397, 406–414]. The large surface area of nanoparticle offers high ionization efficiency of the target species in the presence of other interference analytes. Nanoparticles can be easily modified with magnetic nanoparticles for easy separation or preconcentration with very low LOD and high selectivity (phosphopeptides:nonphsophopeptides, Table 7).

Nanoparticles advanced LDI-MS. There are several challenges facing the applications of nanoparticles for LD-MS. However, these challenges can be circumvented. Searching of good spots is also a challenge. Thus, materials such as superhydrophobic silicon structure with hydrophilic copper particles to make His-tagged model peptide molecules is reported to capture analytes and offer simple searching method [456]. The analyte can be also confined on a surface of Si pillar [145]. This can be also achieved using very small sample spot with size smaller than the laser spots [453]. Biological activity of nanoparticles is important and has to be taken into account during applications [18, 29, 301, 308, 457–459]. Synergetic effect of nanocomposite should be also considered [460].

Compliance with ethical standards The author(s) declare that they have no competing interests.

Abbreviations *ALD,* Atomic layer deposition; *BSA,* Bovine serum albumin; *Au NPET,* cationic gold nanoparticle enhanced target; *CLs,* Cardiolipins; *CPC,* Cetyl pyridinium chloride monohydrate; *CTAB,* cetyltrimethyl ammonium chloride; *CV,* coefficient of variation; *DIOS,* Desorption ionization on silicon; *DIOM,* desorption ionization on mesoporous silicate; *DDAB,* didodecyldimethyl ammonium bromide; *ESI-MS,* Electrospray ionization mass spectrometry; *GSH,* glutathione; *GALDI-MS,* Graphite assisted LDI-MS; *MILs, Materials Institute Lavoisier*; *MALDI-MS,* Matrix assisted laser desorption ionization mass spectrometry; *ME-NIMS,* matrix-enhanced nanostructure initiator mass spectrometry; *MELDI,* material enhanced laser desorption ionization; *IMAC,* Metal affinity chromatography; *nano-PALDI,* nanoparticle assisted LDI; *NIMS,* nanostructure initiator mass spectrometry; *NALDI,* nanostructure-assisted laser desorption/ionization; *TOAB,* tetraoctylammonium bromide; *TMAOH,* tetramethyl ammonium hydroxide pentahydrate; *4-MPBA,* mercaptophenylboronic acid; *NALDI-MS,* nanowire assisted LDI-MS; *NSAIDs,* non-steroidal anti-inflammatory drugs; *PEG 200,* polyethylene glycol; *PCs,* 4- phosphatidylcholines; *Pes,* phosphatidylethanolamines; *PIs,* phosphatidylinositols; *PGs,* phosphatidylglycerols; *QA,* Quaternary ammonium; *SPALDI,* silicon nanoparticle assisted laser desorption ionization; *SDS,* sodium dodecyl sulfate; *SALDI-MS,* surface assisted laser desorption ionization mass spectrometry; *SELDI-MS,* surface enhanced LDI-MS; *TAGs,* triacylglycerols; *UiO-66,* University of Oslo

References

1. Zenobi R, Knochenmuss R (1998) Ion formation in MALDI mass spectrometry. Mass Spectrom Rev 17:337–366. https://doi.org/10.1002/(sici)1098-2787(1998)17:5<337::aid-mas2>3.0.co;2-s
2. Wu KJ, Odom RW (1998) Characterizing synthetic polymers by MALDI MS. Anal Chem 70:456A–461A. https://doi.org/10.1021/ac981910q
3. Fenselau C (1997) MALDI MS and strategies for protein analysis. Anal Chem 69:661A–665A. https://doi.org/10.1021/ac971831z
4. Karas M, Bahr U, Gießmann U (1991) Matrix-assisted laser desorption ionization mass spectrometry. Mass Spectrom Rev 10: 335–357. https://doi.org/10.1002/mas.1280100503
5. Chen Y-C, Abdelhamid HN, Wu H-F (2017) Simple and direct quantitative analysis for quinidine drug in fish tissues. Mass Spectrom Lett 8:8–13. https://doi.org/10.5478/msl.2017.8.1.8
6. Sekar R, Kailasa SK, Abdelhamid HN et al (2013) Electrospray ionization tandem mass spectrometric studies of copper and iron complexes with tobramycin. Int J Mass Spectrom 338:23–29. https://doi.org/10.1016/j.ijms.2012.12.001
7. Khan N, Abdelhamid HN, Yan J-Y, et al (2015) Detection of flutamide in pharmaceutical dosage using higher electrospray ionization mass spectrometry (ESI-MS) tandem mass coupled with Soxhlet apparatus. Anal Chem Res 3: https://doi.org/10.1016/j.ancr.2015.01.001
8. Abdelhamid HN, Wu H (2015) Soft ionization of metallo-mefenamic using electrospray ionization mass spectrometry. Mass Spectrom Lett 6:43–47. https://doi.org/10.5478/MSL.2015.6.2.43
9. Hofstadler SA, Sannes-Lowery KA (2006) Applications of ESI-MS in drug discovery: interrogation of noncovalent complexes. Nat Rev Drug Discov 5:585–595. https://doi.org/10.1038/nrd2083
10. Abdelhamid HN (2016) Ionic liquids for mass spectrometry: Matrices, separation and microextraction. TrAC Trends Anal Chem 77:122–138
11. Abdelhamid HN (2017) Organic matrices, ionic liquids, and organic matrices@nanoparticles assisted laser desorption/ionization mass spectrometry. TrAC Trends Anal Chem 89:68–98. https://doi.org/10.1016/j.trac.2017.01.012
12. H. N. Abdelhamid (2013) Applications of Nanomaterials and Organic Semiconductors for Bacteria &Biomolecules analysis/biosensing using Laser Analytical Spectroscopy. M.Sc. Thesis, National Sun-Yat Sen University
13. Abdelhamid HN (2015) Ionic liquids matrices for laser assisted desorption/Ionization mass spectrometry. Mass Spectrom Purif Tech 01:109–119. https://doi.org/10.4172/2469-9861.1000109
14. Abdelhamid HN, Gopal J, Wu HF (2013) Synthesis and application of ionic liquid matrices (ILMs) for effective pathogenic bacteria analysis in matrix assisted laser desorption/ionization (MALDI-MS). Anal Chim Acta 767:104–111
15. Abdelhamid HN, Khan MS, Wu H-F (2014) Design, characterization and applications of new ionic liquid matrices for multifunctional analysis of biomolecules: a novel strategy for pathogenic bacteria biosensing. Anal Chim Acta 823:51–60. https://doi.org/10.1016/j.aca.2014.03.026
16. Abdelhamid HN (2016) Physicochemical properties of proteomic ionic liquids matrices for MALDI-MS. J Data Min Genomics Proteomics 7:2153–0602.1000. https://doi.org/10.4172/2153-0602.1000189
17. He X, Chen Q, Zhang Y, Lin JM (2014) Recent advances in microchip-mass spectrometry for biological analysis. TrAC Trends Anal Chem 53:84–97
18. Abdelhamid HN, Wu H-F (2014) Proteomics analysis of the mode of antibacterial action of nanoparticles and their interactions with proteins. TrAC Trends Anal Chem 65:30–46
19. Kumaran S, Abdelhamid HN, Wu H-F (2017) Quantification analysis of protein and mycelium contents upon inhibition of melanin for: Aspergillus Niger: A study of matrix assisted laser desorption/ionization mass spectrometry (MALDI-MS). RSC Adv 7:30289–30294. https://doi.org/10.1039/c7ra03741d
20. He Z, Chen Q, Chen F et al (2016) Multiplexed glycan pro fi ling using MALDI-TOF mass spectrometry. Chem Sci 7:5448–5452. https://doi.org/10.1039/C6SC00215C
21. Zhang Y, Li H, Ma Y, Lin J (2014) Lipid profiling of mammalian cells with in situ matrix-assisted laser desorption ionization-mass spectrometry. Sci China Chem 57:442–446. https://doi.org/10.1007/s11426-013-4960-3
22. Santos IC, Hildenbrand ZL, Schug KA (2016) Applications of MALDI-TOF MS in environmental microbiology. Analyst 141: 2827–2837. https://doi.org/10.1039/C6AN00131A
23. Law KP, Larkin JR (2011) Recent advances in SALDI-MS techniques and their chemical and bioanalytical applications. Anal Bioanal Chem 399:2597–2622. https://doi.org/10.1007/s00216-010-4063-3
24. Calvano CD, Monopoli A, Cataldi TRI, Palmisano F (2018) MALDI matrices for low molecular weight compounds: an endless story? Anal Bioanal Chem 410:4015–4038. https://doi.org/10.1007/s00216-018-1014-x
25. Abdelhamid HN (2015) Ionic liquids for mass spectrometry: matrices, separation and microextraction. TrAC Trends Anal Chem. https://doi.org/10.1016/j.trac.2015.12.007
26. Abdelhamid HN (2015) Ionic Liquids Matrices for Laser Assisted Desorption/Ionization MassSpectrometry Mass Spectrom Purif Tech 2015: https://doi.org/10.4172/2469-9861.1000109
27. Abdelhamid HN (2016) Physicochemical Properties of Proteomic Ionic Liquids Matrices for MALDI-MS. J Data Mining Genomics Proteomics 07:1–6. https://doi.org/10.4172/2153-0602.1000189
28. Abdelhamid HN (2018) Ionic liquid-assisted laser desorption/ionization–mass spectrometry: matrices, microextraction, and separation. Methods Protoc 1:23. https://doi.org/10.3390/mps1020023
29. Dowaidar M, Abdelhamid HN, Hällbrink M et al (2017) Graphene oxide nanosheets in complex with cell penetrating peptides for oligonucleotides delivery. BBA-GEN SUBJECTS 1861: 2334–2341. https://doi.org/10.1016/j.bbagen.2017.07.002
30. Abdelhamid HN (2015) Delafossite Nanoparticle as New Functional Materials: Advances in Energy, Nanomedicine and Environmental Applications. Mater Sci Forum 832:28–53. https://doi.org/10.4028/www.scientific.net/MSF.832.28
31. Etman AS, Abdelhamid HN, Yuan Y et al (2018) Facile Water-Based Strategy for Synthesizing MoO3– x Nanosheets: Efficient Visible Light Photocatalysts for Dye Degradation. ACS Omega 3: 2193–2201. https://doi.org/10.1021/acsomega.8b00012
32. Dowaidar M, Abdelhamid HN, Hällbrink M et al (2017) Magnetic Nanoparticle Assisted Self-assembly of Cell Penetrating Peptides-Oligonucleotides Complexes for Gene Delivery. Sci Rep 7:9159. https://doi.org/10.1038/s41598-017-09803-z
33. Abdelhamid HN, Zou X (2018) Template-free and room temperature synthesis of hierarchical porous zeolitic imidazolate framework nanoparticles and their dye and CO 2 sorption. Green Chem 20:1074–1084. https://doi.org/10.1039/C7GC03805D
34. Abdelhamid HN, Kumaran S, Wu H-F (2016) One-pot synthesis of CuFeO2 nanoparticles capped with glycerol and proteomic analysis of their nanocytotoxicity against fungi. RSC Adv 6: 97629–97635. https://doi.org/10.1039/C6RA13396G
35. Iqbal MN, Abdel-Magied AF, Abdelhamid HN et al (2017) Mesoporous Ruthenium Oxide: A Heterogeneous Catalyst for Water Oxidation. ACS Sustain Chem Eng 5:9651–9656. https://doi.org/10.1021/acssuschemeng.7b02845
36. Dowaidar M, Nasser Abdelhamid H, Hällbrink M et al (2018) Chitosan enhances gene delivery of oligonucleotide complexes

with magnetic nanoparticles–cell-penetrating peptide. J Biomater Appl 33:392–401. https://doi.org/10.1177/0885328218796623
37. Abdelhamid HN, Wu H-F (2019) Nanoparticles Advanced Drug Delivery for Cancer Cells. In: Keservani RK, Sharma AK (eds) Nanoparticulate Drug Delivery Systems. pp 121–144
38. Keservani RK, Sharma AK (2019) Nanoparticulate Drug Delivery Systems. Apple Academic Press
39. Abdelhamid HN, Wu H-F (2019) Nanoparticles Advance Drug Delivery for Cancer Cells. In: Keservani RK, Sharma AK (eds) Nanoparticulate Drug Delivery Systems. Apple Academic Press, USA, pp 121–150
40. Abdelhamid HN (2019) Nanoparticles Assisted Laser Desorption/Ionization Mass Spectrometry. In: Handbook of Smart Materials in Analytical Chemistry. John Wiley & Sons, Ltd, Chichester, pp 729–755
41. Tanaka K, Waki H, Ido Y et al (1988) Protein and polymer analyses up to m/z 100,000 by laser ionization TOF-MS. Rapid Commun Mass Spectrom 2:151
42. Shi CY, Deng CH (2016) Recent advances in inorganic materials for LDI-MS analysis of small molecules. Analyst 141:2816–2826. https://doi.org/10.1039/C6AN00220J
43. Kuzema PA (2011) Small-molecule analysis by surface-assisted laser desorption/ionization mass spectrometry. J Anal Chem 66: 1227–1242. https://doi.org/10.1134/S1061934811130065
44. Zhu Z-J, Rotello VM, Vachet RW (2009) Engineered nanoparticle surfaces for improved mass spectrometric analyses. Analyst 134: 2183–2188. https://doi.org/10.1039/b910428c
45. Arakawa R, Kawasaki H (2010) Functionalized Nanoparticles and Nanostructured Surfaces for Surface-Assisted Laser Desorption/ Ionization Mass Spectrometry. Anal Sci 26:1229–1240. https://doi.org/10.2116/analsci.26.1229
46. Lu M, Yang X, Yang Y et al (2017) Nanomaterials as Assisted Matrix of Laser Desorption/Ionization Time-of-Flight Mass Spectrometry for the Analysis of Small Molecules. Nanomaterials 7:87. https://doi.org/10.3390/nano7040087
47. Kawasaki H, Akira T, Watanabe T et al (2009) Sulfonate group-modified FePtCu nanoparticles as a selective probe for LDI-MS analysis of oligopeptides from a peptide mixture and human serum proteins. Anal Bioanal Chem 395:1423–1431. https://doi.org/10.1007/s00216-009-3122-0
48. Castellana ET, Russell DH (2007) Tailoring nanoparticle surface chemistry to enhance laser desorption ionization of peptides and proteins. Nano Lett 7:3023–3025. https://doi.org/10.1021/nl071469w
49. Huang YF, Chang HT (2007) Analysis of adenosine triphosphate and glutathione through gold nanoparticles assisted laser desorption/ionization mass spectrometry. Anal Chem 79:4852–4859. https://doi.org/10.1021/ac070023x
50. Su CL, Tseng WL (2007) Gold nanoparticles as assisted matrix for determining neutral small carbohydrates through laser desorption/ ionization time-of-flight mass spectrometry. Anal Chem 79:1626–1633. https://doi.org/10.1021/ac061747w
51. McLean JA, Stumpo KA, Russel DH (2005) Size-selected (2-10 nm) gold nanoparticles for matrix assisted laser desorption ionization of peptides. J Am Chem Soc 127:5304–5305. https://doi.org/10.1021/ja043907w
52. Pilolli R, Palmisano F, Cioffi N (2012) Gold nanomaterials as a new tool for bioanalytical applications of laser desorption ionization mass spectrometry. Anal Bioanal Chem 402:601–623
53. Silina YE, Fink-straube C, Hayen H, Volmer DA (2015) Analysis of fatty acids and triacylglycerides by Pd nanoparticle-assisted laser desorption/ionization mass spectrometry. Anal Methods 7: 3701–3707. https://doi.org/10.1039/C5AY00705D
54. Kawasaki H, Yonezawa T, Watanabe T, Arakawa R (2007) Platinum nanoflowers for surface-assisted laser desorption/ ionization mass spectrometry of biomolecules. J Phys Chem C 111:16278–16283. https://doi.org/10.1021/jp075159d
55. Nayak R, Knapp DR (2007) Effects of Thin-Film Structural Parameters on Laser Desorption/Ionization from Porous Alumina. Anal Chem 79:4950–4956. https://doi.org/10.1021/ac062289u
56. Niklew M-L, Hochkirch U, Melikyan A et al (2010) Phosphopeptide Screening Using Nanocrystalline Titanium Dioxide Films as Affinity Matrix-Assisted Laser Desorption Ionization Targets in Mass Spectrometry. Anal Chem 82:1047–1053. https://doi.org/10.1021/ac902403m
57. Lee KH, Chiang CK, Lin ZH, Chang HT (2007) Determining enediol compounds in tea using surface-assisted laser desorption/ionization mass spectrometry with titanium dioxide nanoparticle matrices. Rapid Commun Mass Spectrom 21:2023–2030. https://doi.org/10.1002/rcm.3058
58. Taira S, Kitajima K, Katayanagi H et al (2009) Manganese oxide nanoparticle-assisted laser desorption/ionization mass spectrometry for medical applications. Sci Technol Adv Mater 10:034602. https://doi.org/10.1088/1468-6996/10/3/034602
59. Kang M-J, Pyun J-C, Lee J-C et al (2005) Nanowire-assisted laser desorption and ionization mass spectrometry for quantitative analysis of small molecules. Rapid Commun Mass Spectrom 19: 3166–3170. https://doi.org/10.1002/rcm.2187
60. Kailasa SK, Wu HF (2010) Multifunctional ZrO2 nanoparticles and ZrO2-SiO 2 nanorods for improved MALDI-MS analysis of cyclodextrins, peptides, and phosphoproteins. Anal Bioanal Chem 396:1115–1125. https://doi.org/10.1007/s00216-009-3330-7
61. Chen W-Y, Chen Y-C (2006) Affinity-based mass spectrometry using magnetic iron oxide particles as the matrix and concentrating probes for SALDI MS analysis of peptides and proteins. Anal Bioanal Chem 386:699–704. https://doi.org/10.1007/s00216-006-0427-0
62. Chen CT, Chen YC (2005) Fe3O4/TiO2 core/shell nanoparticles as affinity probes for the analysis of phosphopeptides using TiO2 surface-assisted laser desorption/ionization mass spectrometry. Anal Chem 77:5912–5919. https://doi.org/10.1021/ac050831t
63. Gholipour Y, Giudicessi SL, Nonami H, Erra-Balsells R (2010) Diamond, titanium dioxide, titanium silicon oxide, and barium strontium titanium oxide nanoparticles as matrixes for direct matrix-assisted laser desorption/ionization mass spectrometry analysis of carbohydrates in plant tissues. Anal Chem 82:5518–5526. https://doi.org/10.1021/ac1003129
64. Finkel NH, Prevo BG, Velev OD, He L (2005) Ordered silicon nanocavity arrays in surface-assisted desorption/ionization mass spectrometry. Anal Chem 77:1088–1095. https://doi.org/10.1021/ac048645v
65. Dupré M, Coffinier Y, Boukherroub R et al (2012) Laser desorption ionization mass spectrometry of protein tryptic digests on nanostructured silicon plates. J Proteome 75:1973–1990. https://doi.org/10.1016/j.jprot.2011.12.039
66. Piret G, Drobecq H, Coffinier Y et al (2010) Matrix-free laser desorption/ionization mass spectrometry on silicon nanowire arrays prepared by chemical etching of crystalline silicon. Langmuir 26:1354–1361. https://doi.org/10.1021/la902266x
67. Chen Y, Vertes A (2006) Adjustable fragmentation in laser desorption/ionization from laser-induced silicon microcolumn arrays. Anal Chem 78:5835–5844. https://doi.org/10.1021/ac060405n
68. Go EP, Apon JV, Luo G et al (2005) Desorption/ionization on silicon nanowires. Anal Chem 77:1641–1646. https://doi.org/10.1021/ac048460o
69. Shariatgorji M, Amini N, Ilag LL (2009) Silicon nitride nanoparticles for surface-assisted laser desorption/ionization of small molecules. J Nanopart Res 11:1509–1512. https://doi.org/10.1007/s11051-009-9601-6

70. Seino T, Sato H, Yamamoto A et al (2007) Matrix-free laser desorption/ionization-mass spectrometry using self-assembled germanium nanodots. Anal Chem 79:4827–4832. https://doi.org/10.1021/ac062216a
71. Chiang CK, Yang Z, Lin YW et al (2010) Detection of proteins and protein-ligand complexes using hgte nanostructure matrixes in surface-assisted laser desorption/ionization mass spectrometry. Anal Chem 82:4543–4550. https://doi.org/10.1021/ac100550c
72. Kailasa SK, Kiran K, Wu HF (2008) Comparison of ZnS semiconductor nanoparticles capped with various functional groups as the matrix and affinity probes for rapid analysis of cyclodextrins and proteins in surface-assisted laser desorption/ionization time-of-flight mass spectrometry. Anal Chem 80:9681–9688. https://doi.org/10.1021/ac8015664
73. Yonezawa T, Tsukamoto H, Hayashi S et al (2013) Suitability of GaP nanoparticles as a surface-assisted laser desorption/ionization mass spectroscopy inorganic matrix and their soft ionization ability. Analyst 138:995–999. https://doi.org/10.1039/c2an36738f
74. Najam-ul-Haq M, Rainer M, Huck CW et al (2008) Nanostructured Diamond-Like Carbon on Digital Versatile Disc as a Matrix-Free Target for Laser Desorption/Ionization Mass Spectrometry. Anal Chem 80:7467–7472. https://doi.org/10.1021/ac801190e
75. Coffinier Y, Szunerits S, Drobecq H et al (2012) Diamond nanowires for highly sensitive matrix-free mass spectrometry analysis of small molecules. Nanoscale 4:231–238. https://doi.org/10.1039/C1NR11274K
76. Xu S, Li Y, Zou H et al (2003) Carbon Nanotubes as Assisted Matrix for Laser Desorption/Ionization Time-of-Flight Mass Spectrometry. Anal Chem 75:6191–6195. https://doi.org/10.1021/ac0345695
77. Hu L, Xu S, Pan C et al (2005) Matrix-assisted laser desorption/ionization time-of-flight mass spectrometry with a matrix of carbon nanotubes for the analysis of low-mass compounds in environmental samples. Environ Sci Technol 39:8442–8447. https://doi.org/10.1021/es0508572
78. Nasser Abdelhamid H, Wu B-S, Wu H-F (2014) Graphene coated silica applied for high ionization matrix assisted laser desorption/ionization mass spectrometry: A novel approach for environmental and biomolecule analysis. Talanta 126:27–37. https://doi.org/10.1016/j.talanta.2014.03.016
79. Silina YE, Volmer DA (2013) Nanostructured solid substrates for efficient laser desorption/ionization mass spectrometry (LDI-MS) of low molecular weight compounds. Analyst 138:7053. https://doi.org/10.1039/c3an01120h
80. Cha S, Yeung ES (2007) Colloidal graphite-assisted laser desorption/ionization mass spectrometry and MSn of small molecules. 1. Imaging of cerebrosides directly from rat brain tissue. Anal Chem 79:2373–2385. https://doi.org/10.1021/ac062251h
81. Taira S, Sugiura Y, Moritake S et al (2008) Nanoparticle-assisted laser desorption/ionization based mass imaging with cellular resolution. Anal Chem 80:4761–4766. https://doi.org/10.1021/ac800081z
82. Wyatt MF, Ding S, Stein BK et al (2010) Analysis of various organic and organometallic compounds using nanostructure-assisted laser desorption/ionization time-of-flight mass spectrometry (NALDI-TOFMS). J Am Soc Mass Spectrom 21:1256–1259. https://doi.org/10.1016/j.jasms.2010.03.038
83. Moening TN, Brown VL, He L et al (2016) Matrix-enhanced nanostructure initiator mass spectrometry (ME-NIMS) for small molecule detection and imaging. Anal Methods 8:8234–8240. https://doi.org/10.1039/C6AY02753A
84. Wei J, Buriak JM, Siuzdak G (1999) Desorption-ionization mass spectrometry on porous silicon. Nature 399:243–246. https://doi.org/10.1038/20400
85. Northen TR, Yanes O, Northen MT et al (2007) Clathrate nanostructures for mass spectrometry. Nature 449:1033–1036. https://doi.org/10.1038/nature06195
86. Feuerstein I, Najam-ul-Haq M, Rainer M et al (2006) Material-Enhanced Laser Desorption/Ionization (MELDI)-A New Protein Profiling Tool Utilizing Specific Carrier Materials for Time of Flight Mass Spectrometric Analysis. J Am Soc Mass Spectrom 17:1203–1208. https://doi.org/10.1016/j.jasms.2006.04.032
87. Wen X, Dagan S, Wysocki VH (2007) Small-Molecule Analysis with Silicon-Nanoparticle-Assisted Laser Desorption/Ionization Mass Spectrometry. Anal Chem 79:434–444. https://doi.org/10.1021/ac061154l
88. Lee CS, Kang KK, Kim JH et al (2007) Analysis of small molecules by desorption/ionization on mesoporous silicate (DIOM)-mass spectrometry (MS). Microporous Mesoporous Mater 98:200–207. https://doi.org/10.1016/j.micromeso.2006.09.005
89. Sekuła J, Nizioł J, Rode W, Ruman T (2015) Gold nanoparticle-enhanced target (AuNPET) as universal solution for laser desorption/ionization mass spectrometry analysis and imaging of low molecular weight compounds. Anal Chim Acta 875:61–72. https://doi.org/10.1016/j.aca.2015.01.046
90. Bergman N, Shevchenko D, Bergquist J (2014) Approaches for the analysis of low molecular weight compounds with laser desorption/ionization techniques and mass spectrometry. Anal Bioanal Chem 406:49–61. https://doi.org/10.1007/s00216-013-7471-3
91. Muthu M, Gopal J, Chun S (2017) Nanopost array laser desorption ionization mass spectrometry (NAPA-LDI MS): Gathering moss? TrAC Trends Anal Chem 97:96–103. https://doi.org/10.1016/j.trac.2017.08.016
92. Abdelhamid HN (2018) Nanoparticle assisted laser desorption/ionization mass spectrometry for small molecule analytes. Microchim Acta 185:200. https://doi.org/10.1007/s00604-018-2687-8
93. Qiao L, Liu B, Girault HH (2010) Nanomaterial-assisted laser desorption ionization for mass spectrometry-based biomedical analysis. Nanomedicine (London) 5:1641–1652. https://doi.org/10.2217/nnm.10.127
94. Kailasa SK, Wu H-F (2010) Surface modified silver selinide nanoparticles as extracting probes to improve peptide/protein detection via nanoparticles-based liquid phase microextraction coupled with MALDI mass spectrometry. Talanta 83:527–534. https://doi.org/10.1016/j.talanta.2010.09.040
95. Kailasa SK, Wu HF (2015) Nanomaterial-based miniaturized extraction and preconcentration techniques coupled to matrix-assisted laser desorption/ionization mass spectrometry for assaying biomolecules. TrAC Trends Anal Chem 65:54–72
96. Kailasa SK, Wu H-F (2014) Recent developments in nanoparticle-based MALDI mass spectrometric analysis of phosphoproteomes. Microchim Acta 181:853–864. https://doi.org/10.1007/s00604-014-1191-z
97. Kailasa SK, Mehta VN, Wu H-F (2014) Recent developments of liquid-phase microextraction techniques directly combined with ESI- and MALDI-mass spectrometric techniques for organic and biomolecule assays. RSC Adv 4:16188–16205. https://doi.org/10.1039/c3ra47347c
98. Guinan T, Kirkbride P, Pigou PE et al (2015) Surface-assisted laser desorption ionization mass spectrometry techniques for application in forensics. Mass Spectrom Rev 34:627–640
99. Huang YF, Chang HT (2006) Nile red-adsorbed gold nanoparticle matrixes for determining aminothiols through surface-assisted laser desorption/ionization mass spectrometry. Anal Chem 78:1485–1493. https://doi.org/10.1021/ac0517646
100. Svatoš A (2010) Mass spectrometric imaging of small molecules. Trends Biotechnol 28:425–434

101. Walton BL, Verbeck GF (2014) Soft-landing ion mobility of silver clusters for small-molecule matrix-assisted laser desorption ionization mass spectrometry and imaging of latent fingerprints. Anal Chem 86:8114–8120. https://doi.org/10.1021/ac5010822
102. Chiang N-C, Chiang C-K, Lin Z-H et al (2009) Detection of aminothiols through surface-assisted laser desorption/ionization mass spectrometry using mixed gold nanoparticles. Rapid Commun Mass Spectrom 23:3063–3068. https://doi.org/10.1002/rcm.4221
103. Anna Picca R, Damiana Calvano C, Cioffi N, Palmisano F (2017) Mechanisms of Nanophase-Induced Desorption in LDI-MS. A Short Review Nanomaterials 7:75. https://doi.org/10.3390/nano7040075
104. Chiang C-K, Chen W-T, Chang H-T (2011) Nanoparticle-based mass spectrometry for the analysis of biomolecules. Chem Soc Rev 40:1269–1281. https://doi.org/10.1039/C0CS00050G
105. Xu L, Qi X, Li X et al (2016) Recent advances in applications of nanomaterials for sample preparation. Talanta 146:714–726
106. Wan D, Gao M, Wang Y et al (2013) A rapid and simple separation and direct detection of glutathione by gold nanoparticles and graphene-based MALDI-TOF-MS. J Sep Sci 36:629–635. https://doi.org/10.1002/jssc.201200766
107. Li W, Khan M, Li H et al (2019) Homogenous deposition of matrix–analyte cocrystals on gold-nanobowl arrays for improving MALDI-MS signal reproducibility. Chem Commun 55:2166–2169. https://doi.org/10.1039/C8CC09945F
108. Pan X-Y, Chen C-H, Chang Y-H et al (2019) Osteoporosis risk assessment using multilayered gold-nanoparticle thin film via SALDI-MS measurement. Anal Bioanal Chem 411:2793–2802. https://doi.org/10.1007/s00216-019-01759-5
109. Yao G, Zhang H, Deng C et al (2009) Facile synthesis of 4-mercaptophenylboronic acid functionalized gold nanoparticles for selective enrichment of glycopeptides. Rapid Commun Mass Spectrom 23:3493–3500. https://doi.org/10.1002/rcm.4258
110. Yang M, Fujino T (2014) Gold nanoparticles loaded on zeolite as inorganic matrix for laser desorption/ionization mass spectrometry of small molecules. Chem Phys Lett 592:160–163. https://doi.org/10.1016/j.cplett.2013.12.027
111. Marsico ALM, Creran B, Duncan B et al (2015) Inkjet-Printed Gold Nanoparticle Surfaces for the Detection of Low Molecular Weight Biomolecules by Laser Desorption/Ionization Mass Spectrometry. J Am Soc Mass Spectrom 26:1931–1937. https://doi.org/10.1007/s13361-015-1223-x
112. Huang S, Chen G, Ou R et al (2018) Ultrathin Self-Assembled Diphenylalanine Nanosheets through a Gold-Stabilized Strategy for High-Efficiency Adsorption/Desorption/Ionization. Anal Chem 90:8607–8615. https://doi.org/10.1021/acs.analchem.8b01855
113. Tsao CW, Yang ZJ (2015) High Sensitivity and High Detection Specificity of Gold-Nanoparticle-Grafted Nanostructured Silicon Mass Spectrometry for Glucose Analysis. ACS Appl Mater Interfaces 7:22630–22637. https://doi.org/10.1021/acsami.5b07395
114. Hayasaka T, Goto-Inoue N, Zaima N et al (2010) Imaging mass spectrometry with silver nanoparticles reveals the distribution of fatty acids in mouse retinal sections. J Am Soc Mass Spectrom 21:1446–1454. https://doi.org/10.1016/j.jasms.2010.04.005
115. Chu H-W, Lai C-S, Ko J-Y et al (2019) Nanoparticle-Based LDI-MS Immunoassay for the Multiple Diagnosis of Viral Infections. ACS Sensors 4:1543–1551. https://doi.org/10.1021/acssensors.9b00054
116. Wang M-T, Liu M-H, Wang CRC, Chang SY (2009) Silver-coated gold nanoparticles as concentrating probes and matrices for surface-assisted laser desorption/ionization mass spectrometric analysis of aminoglycosides. J Am Soc Mass Spectrom 20:1925–1932. https://doi.org/10.1016/j.jasms.2009.06.018
117. Nizioł J, Rode W, Zieliński Z, Ruman T (2013) Matrix-free laser desorption-ionization with silver nanoparticle-enhanced steel targets. Int J Mass Spectrom 335:22–32. https://doi.org/10.1016/j.ijms.2012.10.009
118. Jackson SN, Baldwin K, Muller L et al (2014) Imaging of lipids in rat heart by MALDI-MS with silver nanoparticles. Anal Bioanal Chem 406:1377–1386. https://doi.org/10.1007/s00216-013-7525-6
119. Castellana E, Sherrod S, Russell D (2008) Nanoparticles for Selective Laser Desorption/Ionization in Mass Spectrometry. J Assoc Lab Autom 13:330–334. https://doi.org/10.1016/j.jala.2008.08.002
120. Gamez RC, Castellana ET, Russell DH (2013) Sol-Gel-derived silver-nanoparticle-embedded thin film for mass spectrometry-based biosensing. Langmuir 29:6502–6507. https://doi.org/10.1021/la4008526
121. Zhu Q, Teng F, Wang Z, et al (2019) Superhydrophobic Glass Substrates Coated with Fluorosilane-Coated Silica Nanoparticles and Silver Nanoparticles for Surface-Assisted Laser Desorption/Ionization Mass Spectrometry. ACS Appl Nano Mater acsanm.9b00688. https://doi.org/10.1021/acsanm.9b00688
122. Sudhir P-R, Shrivas K, Zhou Z-C, Wu H-F (2008) Single drop microextraction using silver nanoparticles as electrostatic probes for peptide analysis in atmospheric pressure matrix-assisted laser desorption/ionization mass spectrometry and comparison with gold electrostatic probes and silver hydrophobic. Rapid Commun Mass Spectrom 22:3076–3086. https://doi.org/10.1002/rcm.3710
123. Hong M, Xu L, Wang F et al (2016) A direct assay of carboxyl-containing small molecules by SALDI-MS on a AgNP/rGO-based nanoporous hybrid film. Analyst 141:2712–2726. https://doi.org/10.1039/c5an02440d
124. Silina YE, Koch M, Volmer DA (2015) Influence of surface melting effects and availability of reagent ions on LDI-MS efficiency after UV laser irradiation of Pd nanostructures. J Mass Spectrom 50:578–585. https://doi.org/10.1002/jms.3564
125. Chen Y-S, Ding J, He X-M et al (2018) Synthesis of tellurium nanosheet for use in matrix assisted laser desorption/ionization time-of-flight mass spectrometry of small molecules. Microchim Acta 185:368. https://doi.org/10.1007/s00604-018-2882-7
126. Liang Q, Macher T, Xu Y et al (2014) MALDI MS in-source decay of glycans using a glutathione-capped iron oxide nanoparticle matrix. Anal Chem 86:8496–8503. https://doi.org/10.1021/ac502422a
127. Tseng M-C, Obena R, Lu Y-W et al (2010) Dihydrobenzoic Acid Modified Nanoparticle as a MALDI-TOF MS Matrix for Soft Ionization and Structure Determination of Small Molecules with Diverse Structures. J Am Soc Mass Spectrom 21:1930–1939. https://doi.org/10.1016/j.jasms.2010.08.001
128. Zhao Q, Xu J, Yin J, Feng Y-Q (2015) Humic acids as both matrix for matrix-assisted laser desorption/ionization time-of-flight mass spectrometry and adsorbent for magnetic solid phase extraction. Anal Chim Acta 889:138–146. https://doi.org/10.1016/j.aca.2015.07.040
129. Abdelhamid HN, Lin YC, Wu HF (2017) Thymine chitosan nanomagnets for specific preconcentration of mercury (II) prior to analysis using SELDI-MS. Microchim Acta 184:1517–1527. https://doi.org/10.1007/s00604-017-2083-9
130. Yang H, Su R, Wishnok JS et al (2019) Magnetic silica nanoparticles for use in matrix-assisted laser desorption ionization mass spectrometry of labile biomolecules such as oligosaccharides, amino acids, peptides and nucleosides. Microchim Acta 186:104. https://doi.org/10.1007/s00604-018-3208-5
131. Abdelhamid HN, Wu H-F (2014) Facile synthesis of nano silver ferrite (AgFeO2) modified with chitosan applied for biothiol

separation. Mater Sci Eng C 45:438–445. https://doi.org/10.1016/j.msec.2014.08.071
132. Zhang K, Hu D, Deng S et al (2019) Phytic acid functionalized Fe3O4 nanoparticles loaded with Ti(IV) ions for phosphopeptide enrichment in mass spectrometric analysis. Microchim Acta 186: 68. https://doi.org/10.1007/s00604-018-3177-8
133. Shrivas K, Hayasaka T, Sugiura Y, Setou M (2011) Method for Simultaneous Imaging of Endogenous Low Molecular Weight Metabolites in Mouse Brain Using TiO 2 Nanoparticles in Nanoparticle-Assisted Laser Desorption/Ionization-Imaging Mass Spectrometry. Anal Chem 83:7283–7289. https://doi.org/10.1021/ac201602s
134. Wang J, Li J, Wang Y et al (2016) A novel double-component MOAC honeycomb composite with pollen grains as a template for phosphoproteomics research. Talanta 154:141–149. https://doi.org/10.1016/j.talanta.2016.03.061
135. Wei XN, Wang HL (2017) Facile fabrication of hydrophilic PAA-Ti/TiO2 nanocomposite for selective enrichment and detection of phosphopeptides from complex biological samples. Anal Chim Acta 949:67–75. https://doi.org/10.1016/j.aca.2016.10.036
136. Kim J-I, Ryu S-Y, Park J-M et al (2014) Nylon nanoweb with TiO2 nanoparticles as a solid matrix for matrix-assisted laser desorption/ionization time-of-flight mass spectrometry. Rapid Commun Mass Spectrom 28:2427–2436. https://doi.org/10.1002/rcm.7036
137. Lin Z, Cai Z (2018) Negative ion laser desorption/ionization time-of-flight mass spectrometric analysis of small molecules by using nanostructured substrate as matrices. Mass Spectrom Rev 37:681–696. https://doi.org/10.1002/mas.21558
138. Kim Y-K, Wang L-S, Landis R et al (2017) A layer-by-layer assembled MoS 2 thin film as an efficient platform for laser desorption/ionization mass spectrometry analysis of small molecules. Nanoscale 9:10854–10860. https://doi.org/10.1039/C7NR02949G
139. Amin MO, Al-Hetlani E (2019) Tailoring the surface chemistry of SiO2-based monoliths to enhance the selectivity of SALDI-MS analysis of small molecules. Talanta 200:458–467. https://doi.org/10.1016/j.talanta.2019.03.078
140. Shmigol IV, Alekseev SA, Lavrynenko OY et al (2009) Chemically modified porous silicon for laser desorption/ionization mass spectrometry of ionic dyes. J Mass Spectrom 44:1234–1240. https://doi.org/10.1002/jms.1604
141. Xu D, Gao M, Deng C, Zhang X (2016) Ultrasensitive enrichment of phosphopeptides with Ti4+ immobilized SiO 2 graphene-like multilayer nanosheets. Analyst 141:3421–3427. https://doi.org/10.1039/C6AN00361C
142. Wang Q, He XM, Chen X et al (2017) Pyridoxal 5′-phosphate mediated preparation of immobilized metal affinity material for highly selective and sensitive enrichment of phosphopeptides. J Chromatogr A 1499:30–37. https://doi.org/10.1016/j.chroma.2017.03.085
143. Shen Z, Thomas JJ, Averbuj C et al (2001) Porous silicon as a versatile platform for laser desorption/ionization mass spectrometry. Anal Chem 73:612–619. https://doi.org/10.1021/ac000746f
144. Alhmoud HZ, Guinan TM, Elnathan R et al (2014) Surface-assisted laser desorption/ionization mass spectrometry using ordered silicon nanopillar arrays. Analyst 139:5999–6009. https://doi.org/10.1039/C4AN01391C
145. Zhu Q, Teng F, Wang Z et al (2019) Confining analyte droplets on visible Si pillars for improving reproducibility and sensitivity of SALDI-TOF MS. Anal Bioanal Chem 411:1135–1142. https://doi.org/10.1007/s00216-018-01565-5
146. Li X, Chen X, Tan J et al (2017) Palladium modified porous silicon as multi-functional MALDI chip for serum peptide detection. Analyst 142:586–590. https://doi.org/10.1039/C6AN02165D
147. Guild GE, Lenehan CE, Walker GS (2010) Surface-assisted laser desorption ionisation time-of-flight mass spectrometry with an activated carbon surface for the rapid detection of underivatised steroids. Int J Mass Spectrom 294:16–22. https://doi.org/10.1016/j.ijms.2010.04.001
148. Black C, Poile C, Langley J, Herniman J (2006) The use of pencil lead as a matrix and calibrant for matrix-assisted laser desorption/ionisation. Rapid Commun Mass Spectrom 20:1053–1060. https://doi.org/10.1002/rcm.2408
149. Walton SL, Mitchell DJ (2012) A novel rapid detection approach for the analysis of radionuclides in environmental samples using graphite MALDI mass spectrometry. J Radioanal Nucl Chem 296: 1113–1118. https://doi.org/10.1007/s10967-012-2176-1
150. Ng EWY, Lam HS, Ng PC, Poon TCW (2013) Quantification of citrulline by parallel fragmentation monitoring - A novel method using graphitized carbon nanoparticles and MALDI-TOF/TOF mass spectrometry. Clin Chim Acta 420:121–127. https://doi.org/10.1016/j.cca.2012.10.039
151. Abdelhamid HN, Wu H-F (2012) A method to detect metal-drug complexes and their interactions with pathogenic bacteria via graphene nanosheet assist laser desorption/ionization mass spectrometry and biosensors. Anal Chim Acta 751:94–104. https://doi.org/10.1016/j.aca.2012.09.012
152. Abdelhamid HN, Wu H-F (2014) Ultrasensitive, Rapid, and Selective Detection of Mercury Using Graphene Assisted Laser Desorption/Ionization Mass Spectrometry. J Am Soc Mass Spectrom 25:861–868. https://doi.org/10.1007/s13361-014-0825-z
153. Hua P-Y, Manikandan M, Abdelhamid HN, Wu H-F (2014) Graphene nanoflakes as an efficient ionizing matrix for MALDI-MS based lipidomics of cancer cells and cancer stem cells. J Mater Chem B 2:7334–7343
154. Ma N, Bian W, Li R et al (2015) Quantitative analysis of nitro-polycyclic aromatic hydrocarbons in PM 2.5 samples with graphene as a matrix by MALDI-TOF MS. Anal Methods 7: 3967–3971. https://doi.org/10.1039/C5AY00341E
155. Min Q, Zhang X, Chen X et al (2014) N-doped graphene: an alternative carbon-based matrix for highly efficient detection of small molecules by negative ion MALDI-TOF MS. Anal Chem 86:9122–9130. https://doi.org/10.1021/ac501943n
156. Wang J, Liang Y, Mao Y et al (2019) A selective adsorption-based separation of low-mass molecules from biological samples towards high-throughput mass spectrometry analysis in a single drop of human whole blood. Talanta 202:237–243. https://doi.org/10.1016/j.talanta.2019.05.005
157. Qin H, Gao P, Wang F et al (2011) Highly Efficient Extraction of Serum Peptides by Ordered Mesoporous Carbon. Angew Chem Int Ed 50:12218–12221. https://doi.org/10.1002/anie.201103666
158. Kuo TR, Wang DY, Chiu YC et al (2014) Layer-by-layer thin film of reduced graphene oxide and gold nanoparticles as an effective sample plate in laser-induced desorption/ionization mass spectrometry. Anal Chim Acta 809:97–103. https://doi.org/10.1016/j.aca.2013.11.050
159. Lin Z, Zheng J, Lin G et al (2015) Negative Ion Laser Desorption/Ionization Time-of-Flight Mass Spectrometric Analysis of Small Molecules Using Graphitic Carbon Nitride Nanosheet Matrix. Anal Chem 87:8005–8012. https://doi.org/10.1021/acs.analchem.5b02066
160. Sun H, Zhang Q, Zhang L et al (2017) Facile preparation of molybdenum (VI) oxide – Modified graphene oxide nanocomposite for specific enrichment of phosphopeptides. J Chromatogr A 1521:36–43. https://doi.org/10.1016/j.chroma.2017.08.029
161. Wu E, Feng K, Shi R et al (2019) Hybrid CuCoO–GO enables ultrasensitive detection of antibiotics with enhanced laser desorption/ionization at nano-interfaces. Chem Sci 10:257–267. https://doi.org/10.1039/C8SC03692F

162. Kawasaki H, Nakai K, Arakawa R et al (2012) Functionalized graphene-coated cobalt nanoparticles for highly efficient surface-assisted laser desorption/ionization mass spectrometry analysis. Anal Chem 84:9268–9275. https://doi.org/10.1021/ac302004g
163. Al-Hetlani E, Amin MO, Madkour M, Nazeer AA (2018) CeO2-CB nanocomposite as a novel SALDI substrate for enhancing the detection sensitivity of pharmaceutical drug molecules in beverage samples. Talanta 185:439–445. https://doi.org/10.1016/j.talanta.2018.03.102
164. Pan C, Xu S, Hu L et al (2005) Using oxidized carbon nanotubes as matrix for analysis of small molecules by MALDI-TOF MS. J Am Soc Mass Spectrom 16:883–892. https://doi.org/10.1016/j.jasms.2005.03.009
165. Chen S, Zheng H, Wang J et al (2013) Carbon nanodots as a matrix for the analysis of low-molecular-weight molecules in both positive- and negative-ion matrix-assisted laser desorption/ionization time-of-flight mass spectrometry and quantification of glucose and uric acid in real samples. Anal Chem 85:6646–6652. https://doi.org/10.1021/ac401601r
166. Maleki S, Lee D, Kim Y, Kim J (2019) Synthesis and application of nitrogen-doped carbon dots as a matrix in matrix-assisted laser desorption/ionization time-of-flight mass spectrometry. Int J Mass Spectrom 442:44–50. https://doi.org/10.1016/j.ijms.2019.05.004
167. Abdelhamid HN, Talib A, Wu HF (2017) One pot synthesis of gold – carbon dots nanocomposite and its application for cytosensing of metals for cancer cells. Talanta 166:357–363. https://doi.org/10.1016/j.talanta.2016.11.030
168. Yang S-S, Shi M-Y, Tao Z-R et al (2019) Recent applications of metal–organic frameworks in matrix-assisted laser desorption/ionization mass spectrometry. Anal Bioanal Chem 411:4509–4522. https://doi.org/10.1007/s00216-019-01876-1
169. Han G, Zeng Q, Jiang Z et al (2017) MIL-101(Cr) as matrix for sensitive detection of quercetin by matrix-assisted laser desorption/ionization mass spectrometry. Talanta 164:355–361. https://doi.org/10.1016/j.talanta.2016.11.044
170. Yang X, Lin Z, Yan X, Cai Z (2016) Zeolitic imidazolate framework nanocrystals for enrichment and direct detection of environmental pollutants by negative ion surface-assisted laser desorption/ionization time-of-flight mass spectrometry. RSC Adv 6:23790–23793. https://doi.org/10.1039/C6RA00877A
171. Lin Z, Bian W, Zheng J, Cai Z (2015) Magnetic metal–organic framework nanocomposites for enrichment and direct detection of small molecules by negative-ion matrix-assisted laser desorption/ionization time-of-flight mass spectrometry. Chem Commun 51:8785–8788. https://doi.org/10.1039/C5CC02495A
172. Wang H, Wang X, Bian W et al (2019) Analysis of Nitropolycyclic Aromatic Hydrocarbons in Fine Particulate Matter by Matrix-Assisted Laser Desorption/Ionization Time-of-Flight Mass Spectrometry Using Fe3O4/ZIF-8 Magnetic Nanocomposites as Matrix. J Appl Spectrosc 86:89–95. https://doi.org/10.1007/s10812-019-00786-5
173. Zhao M, Xie Y, Chen H, Deng C (2017) Efficient extraction of low-abundance peptides from digested proteins and simultaneous exclusion of large-sized proteins with novel hydrophilic magnetic zeolitic imidazolate frameworks. Talanta 167:392–397. https://doi.org/10.1016/j.talanta.2017.02.038
174. Chen Y, Xiong Z, Peng L et al (2015) Facile Preparation of Core-Shell Magnetic Metal-Organic Framework Nanoparticles for the Selective Capture of Phosphopeptides. ACS Appl Mater Interfaces 7:16338–16347. https://doi.org/10.1021/acsami.5b03335
175. Zhang W, Yan Z, Gao J et al (2015) Metal-organic framework UiO-66 modified magnetite@silica core-shell magnetic microspheres for magnetic solid-phase extraction of domoic acid from shellfish samples. J Chromatogr A 1400:10–18. https://doi.org/10.1016/j.chroma.2015.04.061
176. Chang Y-J, Yang S-S, Yu X et al (2018) Ultrahigh efficient laser desorption ionization of saccharides by Ti-based metal-organic frameworks nanosheets. Anal Chim Acta 1032:91–98. https://doi.org/10.1016/j.aca.2018.06.035
177. Shih Y-H, Chien C-H, Singco B et al (2013) Metal–organic frameworks: new matrices for surface-assisted laser desorption–ionization mass spectrometry. Chem Commun 49:4929–4930. https://doi.org/10.1039/c3cc40934a
178. Wang H, Jiao F, Gao F et al (2017) Titanium (IV) ion-modified covalent organic frameworks for specific enrichment of phosphopeptides. Talanta 166:133–140. https://doi.org/10.1016/j.talanta.2017.01.043
179. Zhang Y, Song Y, Wu J et al (2019) A magnetic covalent organic framework as an adsorbent and a new matrix for enrichment and rapid determination of PAHs and their derivatives in PM 2.5 by surface-assisted laser desorption/ionization-time of flight-mass spectrometry. Chem Commun 55:3745–3748. https://doi.org/10.1039/C9CC00384C
180. Feng D, Xia Y (2018) Covalent organic framework as efficient desorption/ionization matrix for direct detection of small molecules by laser desorption/ionization mass spectrometry. Anal Chim Acta 1014:58–63. https://doi.org/10.1016/j.aca.2018.02.017
181. Abdelhamid HN, Wu H-F (2016) Gold nanoparticles assisted laser desorption/ionization mass spectrometry and applications: from simple molecules to intact cells. Anal Bioanal Chem 408:4485–4502. https://doi.org/10.1007/s00216-016-9374-6
182. Unnikrishnan B, Chang C-Y, Chu H-W et al (2016) Functional Gold Nanoparticles Coupled with Laser Desorption Ionization Mass Spectrometry for Bioanalysis. Anal Methods 00:1–11. https://doi.org/10.1039/C6AY02378A
183. Nayak R, Knapp DR (2010) Matrix-Free LDI Mass Spectrometry Platform Using Patterned Nanostructured Gold Thin Film. Anal Chem 82:7772–7778. https://doi.org/10.1021/ac1017277
184. Lee J-W, Lee J-H, Oh H-S et al (2012) Selective Analysis of Thiol-Containing Molecules Using Nanoengineered Micro Gold Shells and LDI-TOF MS. Bull Kor Chem Soc 33:3076–3078. https://doi.org/10.5012/bkcs.2012.33.9.3076
185. Son J, Lee G, Cha S (2014) Direct Analysis of Triacylglycerols from Crude Lipid Mixtures by Gold Nanoparticle-Assisted Laser Desorption/Ionization Mass Spectrometry. J Am Soc Mass Spectrom 25:891–894. https://doi.org/10.1007/s13361-014-0844-9
186. Cioffi N, De Palo F, Calvano CD et al (2008) Core–Shell Gold Nanoparticles as Non-Conventional Matrix for the MALDI-ToF-MS Detection of Amino Acids: A Preliminary Study. Sens Lett 6:654–661. https://doi.org/10.1166/sl.2008.454
187. Pilolli R, Ditaranto N, Monopoli A et al (2014) Designing functionalized gold surfaces and nanostructures for Laser Desorption Ionisation Mass Spectrometry. Vacuum 100:78–83. https://doi.org/10.1016/j.vacuum.2013.07.032
188. Bian J, Olesik SV, Powell DH et al (2017) Surface-assisted laser desorption/ionization time-of-flight mass spectrometry of small drug molecules and high molecular weight synthetic/biological polymers using electrospun composite nanofibers. Analyst 142:1125–1132. https://doi.org/10.1039/C6AN02444K
189. Abdelhamid HN, Wu H-F (2013) Polymer dots for quantifying the total hydrophobic pathogenic lysates in a single drop. Colloids Surf B: Biointerfaces 115C:51–60
190. Chau SL, Tang HW, Ng KM (2016) Gold nanoparticles bridging infra-red spectroscopy and laser desorption/ionization mass spectrometry for direct analysis of over-the-counter drug and botanical medicines. Anal Chim Acta 919:62–69. https://doi.org/10.1016/j.aca.2016.03.023
191. Kim S, Oh H, Yeo W-S (2015) Analysis of alkanethiolates on gold with matrix-assisted laser desorption/ionization time-of-flight

mass spectrometry. J Korean Soc Appl Biol Chem 58:1–8. https://doi.org/10.1007/s13765-015-0018-x
192. Kailasa SK, Wu H-F (2012) One-pot synthesis of dopamine dithiocarbamate functionalized gold nanoparticles for quantitative analysis of small molecules and phosphopeptides in SALDI- and MALDI-MS. Analyst 137:1629. https://doi.org/10.1039/c2an16008k
193. Chiang C-K, Chiang M-C, Lin Z-H et al (2010) Nanomaterial-based surface-assisted laser desorption/ionization mass spectrometry of peptides and proteins. J Am Soc Mass Spectrom 21:1204–1207. https://doi.org/10.1016/j.jasms.2010.02.028
194. Chiang C-K, Lin Y-W, Chen W-T, Chang H-T (2010) Accurate quantitation of glutathione in cell lysates through surface-assisted laser desorption/ionization mass spectrometry using gold nanoparticles. Nanomedicine Nanotechnology, Biol Med 6:530–537. https://doi.org/10.1016/j.nano.2010.01.006
195. Unnikrishnan B, Chang C-Y, Chu H-W et al (2016) Functional gold nanoparticles coupled with laser desorption ionization mass spectrometry for bioanalysis. Anal Methods 8:8123–8133. https://doi.org/10.1039/C6AY02378A
196. Cang J, Chen L-Y, Lin Y-S, Chang H-T (2018) Detection of Metabolites in Cells through Surface-Assisted Laser Desorption/Ionization Mass Spectrometry. ACS Omega 3:17386–17391. https://doi.org/10.1021/acsomega.8b02563
197. Tseng Y-T, Harroun SG, Wu C-W et al (2017) Satellite-like Gold Nanocomposites for Targeted Mass Spectrometry Imaging of Tumor Tissues. Nanotheranostics 1:141–153. https://doi.org/10.7150/ntno.18897
198. Creran B, Yan B, Moyano DF et al (2012) Laser desorption ionization mass spectrometric imaging of mass barcoded gold nanoparticles for security applications. Chem Commun 48:4543. https://doi.org/10.1039/c2cc30499f
199. Tang H-W, Wong MY-M, Lam W et al (2011) Molecular histology analysis by matrix-assisted laser desorption/ionization imaging mass spectrometry using gold nanoparticles as matrix. Rapid Commun Mass Spectrom 25:3690–3696. https://doi.org/10.1002/rcm.5281
200. Ràfols P, Vilalta D, Torres S et al (2018) Assessing the potential of sputtered gold nanolayers in mass spectrometry imaging for metabolomics applications. PLoS One 13:e0208908. https://doi.org/10.1371/journal.pone.0208908
201. Tang H-W, Wong MY-M, Chan SL-F et al (2011) Molecular Imaging of Banknote and Questioned Document Using Solvent-Free Gold Nanoparticle-Assisted Laser Desorption/Ionization Imaging Mass Spectrometry. Anal Chem 83:453–458. https://doi.org/10.1021/ac1020485
202. Chau S-L, Tang H-W, Cheng Y-H et al (2017) Chemical Printing of Biological Tissue by Gold Nanoparticle-Assisted Laser Ablation. ACS Omega 2:6031–6038. https://doi.org/10.1021/acsomega.7b00385
203. Sekuła J, Nizioł J, Rode W, Ruman T (2015) Silver nanostructures in laser desorption/ionization mass spectrometry and mass spectrometry imaging. Analyst 140:6195–6209. https://doi.org/10.1039/C5AN00943J
204. Hua L, Chen J, Ge L, Tan SN (2007) Silver nanoparticles as matrix for laser desorption/ionization mass spectrometry of peptides. J Nanopart Res 9:1133–1138. https://doi.org/10.1007/s11051-007-9244-4
205. Hong S, Lee JS, Ryu J et al (2011) Bio-inspired strategy for on-surface synthesis of silver nanoparticles for metal/organic hybrid nanomaterials and LDI-MS substrates. Nanotechnology 22:494020. https://doi.org/10.1088/0957-4484/22/49/494020
206. Shrivas K, Wu H-F (2008) Applications of silver nanoparticles capped with different functional groups as the matrix and affinity probes in surface-assisted laser desorption/ionization time-of-flight and atmospheric pressure matrix-assisted laser desorption/ionization ion trap mas. Rapid Commun Mass Spectrom 22:2863–2872. https://doi.org/10.1002/rcm.3681
207. Chiu TC, Chang LC, Chiang CK, Chang HT (2008) Determining Estrogens Using Surface-Assisted Laser Desorption/Ionization Mass Spectrometry with Silver Nanoparticles as the Matrix. J Am Soc Mass Spectrom 19:1343–1346. https://doi.org/10.1016/j.jasms.2008.06.006
208. Sherrod SD, Diaz AJ, Russell WK et al (2008) Silver nanoparticles as selective ionization probes for analysis of olefins by mass spectrometry. Anal Chem 80:6796–6799. https://doi.org/10.1021/ac800904g
209. Muller L, Baldwin K, Barbacci DC et al (2017) Laser Desorption/Ionization Mass Spectrometric Imaging of Endogenous Lipids from Rat Brain Tissue Implanted with Silver Nanoparticles. J Am Soc Mass Spectrom 28:1716–1728. https://doi.org/10.1007/s13361-017-1665-4
210. Muller L, Kailas A, Jackson SN et al (2015) Lipid imaging within the normal rat kidney using silver nanoparticles by matrix-assisted laser desorption/ionization mass spectrometry. Kidney Int 88:186–192. https://doi.org/10.1038/ki.2015.3
211. Jun JH, Song Z, Liu Z et al (2010) High-Spatial and High-Mass Resolution Imaging of Surface Metabolites of Arabidopsis thaliana by Laser Desorption-Ionization Mass Spectrometry Using Colloidal Silver. Anal Chem 82:3255–3265. https://doi.org/10.1021/ac902990p
212. Nizioł J, Ruman T (2013) Surface-transfer mass spectrometry imaging on a monoisotopic silver nanoparticle enhanced target. Anal Chem 85:12070–12076. https://doi.org/10.1021/ac4031658
213. Dufresne M, Thomas A, Breault-Turcot J et al (2013) Silver-Assisted Laser Desorption Ionization For High Spatial Resolution Imaging Mass Spectrometry of Olefins from Thin Tissue Sections. Anal Chem 85:3318–3324. https://doi.org/10.1021/ac3037415
214. Guan M, Zhang Z, Li S et al (2018) Silver nanoparticles as matrix for MALDI FTICR MS profiling and imaging of diverse lipids in brain. Talanta 179:624–631. https://doi.org/10.1016/j.talanta.2017.11.067
215. Picca RA, Calvano CD, Lo Faro MJ et al (2016) Functionalization of silicon nanowire arrays by silver nanoparticles for the laser desorption ionization mass spectrometry analysis of vegetable oils. J Mass Spectrom 51:849–856. https://doi.org/10.1002/jms.3826
216. Yang M, Fujino T (2013) Silver nanoparticles on zeolite surface for laser desorption/ionization mass spectrometry of low molecular weight compounds. Chem Phys Lett 576:61–64. https://doi.org/10.1016/j.cplett.2013.05.030
217. Zhao Y, Deng G, Liu X et al (2016) MoS2/Ag nanohybrid: A novel matrix with synergistic effect for small molecule drugs analysis by negative-ion matrix-assisted laser desorption/ionization time-of-flight mass spectrometry. Anal Chim Acta 937:87–95. https://doi.org/10.1016/j.aca.2016.06.026
218. Kim Y-K, Kang K, Kim H et al (2019) Laser desorption/ionization mass spectrometry-based compositional analysis of Au–Ag nanoplates synthesized by galvanic replacement and their application for small molecule analysis. J Ind Eng Chem 71:318–326. https://doi.org/10.1016/j.jiec.2018.11.042
219. Shrivas K, Agrawal K, Wu H-F (2011) Application of platinum nanoparticles as affinity probe and matrix for direct analysis of small biomolecules and microwave digested proteins using matrix-assisted laser desorption/ionization mass spectrometry. Analyst 136:2852. https://doi.org/10.1039/c1an15211d
220. Ozawa T, Osaka I, Ihozaki T et al (2015) Simultaneous detection of phosphatidylcholines and glycerolipids using matrix-enhanced surface-assisted laser desorption/ionization-mass spectrometry with sputter-deposited platinum film. J Mass Spectrom 50:1264–1269. https://doi.org/10.1002/jms.3700

221. Kawasaki H, Ozawa T, Hisatomi H, Arakawa R (2012) Platinum vapor deposition surface-assisted laser desorption/ionization for imaging mass spectrometry of small molecules. Rapid Commun Mass Spectrom 26:1849–1858. https://doi.org/10.1002/rcm.6301
222. Silina YE, Meier F, Nebolsin VA et al (2014) Novel Galvanic Nanostructures of Ag and Pd for Efficient Laser Desorption/Ionization of Low Molecular Weight Compounds. J Am Soc Mass Spectrom 25:841–851. https://doi.org/10.1007/s13361-014-0853-8
223. Hansen RL, Dueñas ME, Lee YJ (2019) Sputter-Coated Metal Screening for Small Molecule Analysis and High-Spatial Resolution Imaging in Laser Desorption Ionization Mass Spectrometry. J Am Soc Mass Spectrom 30:299–308. https://doi.org/10.1007/s13361-018-2081-0
224. Schnapp A, Niehoff A-C, Koch A, Dreisewerd K (2016) Laser desorption/ionization mass spectrometry of lipids using etched silver substrates. Methods 104:194–203. https://doi.org/10.1016/j.ymeth.2016.01.014
225. Prysiazhnyi V, Dycka F, Kratochvil J et al (2019) Silver nanoparticles for solvent-free detection of small molecules and mass-to-charge calibration of laser desorption/ionization mass spectrometry. J Vac Sci Technol B 37:012906. https://doi.org/10.1116/1.5050878
226. Shastri L, Abdelhamid HN, Nawaz M, Wu H-F (2015) Synthesis, characterization and bifunctional applications of bidentate silver nanoparticle assisted single drop microextraction as a highly sensitive preconcentrating probe for protein analysis. RSC Adv 5:41595–41603. https://doi.org/10.1039/C5RA04032A
227. Gopal J, Abdelhamid HN, Huang JH, Wu HF (2016) Nondestructive detection of the freshness of fruits and vegetables using gold and silver nanoparticle mediated graphene enhanced Raman spectroscopy. Sensors Actuators B Chem 224:413–424. https://doi.org/10.1016/j.snb.2015.08.123
228. Kurita M, Arakawa R, Kawasaki H (2016) Silver nanoparticle functionalized glass fibers for combined surface-enhanced Raman scattering spectroscopy (SERS)/surface-assisted laser desorption/ionization (SALDI) mass spectrometry via plasmonic/thermal hot spots. Analyst 141:5835–5841. https://doi.org/10.1039/C6AN00511J
229. Breault-Turcot J, Chaurand P, Masson JF (2014) Unravelling non-specific adsorption of complex protein mixture on surfaces with SPR and MS. Anal Chem 86:9612–9619. https://doi.org/10.1021/ac502077b
230. Abdelhamid HN, Wu HF (2015) Reduced graphene oxide conjugate thymine as a new probe for ultrasensitive and selective fluorometric determination of mercury(II) ions. Microchim Acta 182:1609–1617. https://doi.org/10.1007/s00604-015-1461-4
231. Nitta S, Yamamoto A, Kurita M et al (2014) Gold-decorated titania nanotube arrays as dual-functional platform for surface-enhanced raman spectroscopy and surface-assisted laser desorption/ionization mass spectrometry. ACS Appl Mater Interfaces 6:8387–8395. https://doi.org/10.1021/am501291d
232. Pavlov J, Attygalle AB (2019) Gold Nanoparticles (AuNPs) as Reactive Matrix for Detection of Trace Levels of HCN in Air by Laser Desorption/Ionization Mass Spectrometry (LDI-MS). J Am Soc Mass Spectrom 30:806–813. https://doi.org/10.1007/s13361-018-02131-0
233. Sacks CD, Stumpo KA (2018) Gold nanoparticles for enhanced ionization and fragmentation of biomolecules using LDI-MS. J Mass Spectrom 53:1070–1077. https://doi.org/10.1002/jms.4282
234. Yuan M, Shan Z, Tian B et al (2005) Preparation of highly ordered mesoporous WO3-TiO2 as matrix in matrix-assisted laser desorption/ionization mass spectrometry. Microporous Mesoporous Mater 78:37–41. https://doi.org/10.1016/j.micromeso.2004.09.014
235. Chen CT, Chen YC (2004) Molecularly Imprinted TiO2-Matrix-Assisted Laser Desorption/Ionization Mass Spectrometry for Selectively Detecting ??-Cyclodextrin. Anal Chem 76:1453–1457. https://doi.org/10.1021/ac034986h
236. Kim J-I, Park J-M, Noh J-Y et al (2016) Analysis of benzylpenicillin in milk using MALDI-TOF mass spectrometry with top-down synthesized TiO2 nanowires as the solid matrix. Chemosphere 143:64–70. https://doi.org/10.1016/j.chemosphere.2015.04.002
237. Abdelhamid HN, Bhaisare ML, Wu H-F (2014) Ceria nanocubic-ultrasonication assisted dispersive liquid-liquid microextraction coupled with matrix assisted laser desorption/ionization mass spectrometry for pathogenic bacteria analysis. Talanta 120:208–217. https://doi.org/10.1016/j.talanta.2013.11.078
238. Chen CT, Chen YC (2004) Desorption/ionization mass spectrometry on nanocrystalline titania sol-gel-deposited films. Rapid Commun Mass Spectrom 18:1956–1964. https://doi.org/10.1002/rcm.1572
239. Taira S, Taguchi H, Fukuda R et al (2014) Silver Oxide Based Nanoparticle Assisted Laser Desorption/Ionization Mass Spectrometry for the Detection of Low Molecular Weight Compounds. Mass Spectrom 3:S0025–S0025. https://doi.org/10.5702/massspectrometry.S0025
240. Abdelhamid HN, Talib A, Wu H-F (2015) Facile synthesis of water soluble silver ferrite (AgFeO2) nanoparticles and their biological application as antibacterial agents. RSC Adv 5:34594–34602
241. Abdelhamid HN, Talib A, Wu H-F (2015) Correction: Facile synthesis of water soluble silver ferrite ($AgFeO_2$) nanoparticles and their biological application as antibacterial agents. RSC Adv 5:39952–39953. https://doi.org/10.1039/C5RA90041G
242. Lin Z, Zheng J, Bian W, Cai Z (2015) CuFe2O4 magnetic nanocrystal clusters as a matrix for the analysis of small molecules by negative-ion matrix-assisted laser desorption/ionization time-of-flight mass spectrometry. Analyst 140:5287–5294. https://doi.org/10.1039/C5AN00625B
243. Watanabe T, Kawasaki H, Yonezawa T, Arakawa R (2008) Surface-assisted laser desorption/ionization mass spectrometry (SALDI-MS) of low molecular weight organic compounds and synthetic polymers using zinc oxide (ZnO) nanoparticles. J Mass Spectrom 43:1063–1071. https://doi.org/10.1002/jms.1385
244. Gedda G, Abdelhamid HN, Khan MS, Wu H-F (2014) ZnO nanoparticle-modified polymethyl methacrylate-assisted dispersive liquid–liquid microextraction coupled with MALDI-MS for rapid pathogenic bacteria analysis. RSC Adv 4:45973–45983. https://doi.org/10.1039/C4RA03391D
245. Bernier MC, Wysocki VH, Dagan S (2015) Laser desorption ionization of small molecules assisted by tungsten oxide and rhenium oxide particles. J Mass Spectrom 50:891–898. https://doi.org/10.1002/jms.3597
246. López De Laorden C, Beloqui A, Yate L et al (2015) Nanostructured indium tin oxide slides for small-molecule profiling and imaging mass spectrometry of metabolites by surface-assisted laser desorption ionization ms. Anal Chem 87:431–440. https://doi.org/10.1021/ac5025864
247. Li Z, Zhang Y-W, Xin Y-L et al (2014) A lithium-rich composite metal oxide used as a SALDI-MS matrix for the determination of small biomolecules. Chem Commun 50:15397–15399. https://doi.org/10.1039/C4CC07479C
248. Xu D, Yan G, Gao M et al (2017) Selective enrichment of glycopeptides/phosphopeptides using Fe3O4@Au-B(OH)2@mTiO2 core-shell microspheres. Talanta 166:154–161. https://doi.org/10.1016/j.talanta.2017.01.030
249. Lin H, Yuan K, Deng C (2017) Preparation of a TiO2 -NH2 modified MALDI plate for on-plate simultaneous enrichment of

phosphopeptides and glycopeptides. Talanta 175:427–434. https://doi.org/10.1016/j.talanta.2017.07.078
250. Gao C, Zhen D, He N et al (2019) Two-dimensional TiO2 nanoflakes enable rapid SALDI-TOF-MS detection of toxic small molecules (dyes and their metabolites) in complex environments. Talanta 196:1–8. https://doi.org/10.1016/j.talanta.2018.11.104
251. Zhao D, He Z, Wang G et al (2016) Three-dimensional ordered titanium dioxide-zirconium dioxide film-based microfluidic device for efficient on-chip phosphopeptide enrichment. J Colloid Interface Sci 478:227–235. https://doi.org/10.1016/j.jcis.2016.05.054
252. Dai J, Wang M, Liu H (2017) Highly selective enrichment of phosphopeptides using Zr4+-immobilized Titania nanoparticles. Talanta 164:222–227. https://doi.org/10.1016/j.talanta.2016.11.058
253. Chen X, Li S, Zhang X et al (2015) Weaving a two-dimensional fishing net from titanoniobate nanosheets embedded with Fe 3 O 4 nanocrystals for highly efficient capture and isotope labeling of phosphopeptides. Nanoscale 7:5815–5825. https://doi.org/10.1039/C4NR07041K
254. Salimi K, Usta DD, Çelikbıçak Ö et al (2017) Highly selective enrichment of phosphopeptides by titanium (IV) attached monodisperse-porous poly(vinylphosphonic acid-co-ethylene dimethacrylate) microspheres. J Chromatogr A 1496:9–19. https://doi.org/10.1016/j.chroma.2017.03.052
255. Salimi K, Usta DD, Çelikbıçak Ö et al (2017) Ti(IV) carrying polydopamine-coated, monodisperse-porous SiO2 microspheres with stable magnetic properties for highly selective enrichment of phosphopeptides. Colloids Surfaces B Biointerfaces 153:280–290. https://doi.org/10.1016/j.colsurfb.2017.02.028
256. Min Q, Li S, Chen X et al (2015) Magnetite/ceria-codecorated titanoniobate nanosheet: A 2D catalytic nanoprobe for efficient enrichment and programmed dephosphorylation of phosphopeptides. ACS Appl Mater Interfaces 7:9563–9572. https://doi.org/10.1021/acsami.5b01006
257. Long X, Zhang Z, Li J et al (2017) A combination strategy using two novel cerium-based nanocomposite affinity probes for the selective enrichment of mono- and multi-phosphopeptides in mass spectrometric analysis. Chem Commun 53:4620–4623. https://doi.org/10.1039/C7CC00540G
258. Long X-Y, Zhang Z-J, Li J-Y, et al (2017) Controllable Preparation of CuFeMnO 4 Nanospheres as a Novel Multifunctional Affinity Probe for Efficient Adsorption and Selective Enrichment of Low-Abundance Peptides and Phosphopeptides. Anal Chem acs.analchem.7b02476. https://doi.org/10.1021/acs.analchem.7b02476
259. Long XY, Li JY, Sheng D, Lian HZ (2017) Spinel-type manganese ferrite (MnFe2O4) microspheres: A novel affinity probe for selective and fast enrichment of phosphopeptides. Talanta 166:36–45. https://doi.org/10.1016/j.talanta.2017.01.025
260. Zhang L, Xiong Z, Chen Y et al (2016) Soft-template synthesis of hydrophilic metallic zirconia nanoparticle-incorporated ordered mesoporous carbon composite and its application in phosphopeptide enrichment. RSC Adv 6:30014–30020. https://doi.org/10.1039/C6RA00326E
261. Abdelhamid HN (2016) Laser Assisted Synthesis, Imaging and Cancer Therapy of Magnetic Nanoparticles. Mater Focus 5:305–323. https://doi.org/10.1166/mat.2016.1336
262. Komori H, Hashizaki R, Osaka I et al (2015) Nanoparticle-assisted laser desorption/ionization using sinapic acid-modified iron oxide nanoparticles for mass spectrometry analysis. Analyst 140:8134–8137. https://doi.org/10.1039/C5AN02081F
263. Abdelhamid HN, Lin YC, Wu H-F (2017) Magnetic nanoparticle modified chitosan for surface enhanced laser desorption/ionization mass spectrometry of surfactants. RSC Adv 7:41585–41592. https://doi.org/10.1039/C7RA05982E
264. Moritake S, Taira S, Sugiura Y et al (2009) Magnetic nanoparticle-based mass spectrometry for the detection of biomolecules in cultured cells. J Nanosci Nanotechnol 9:169–176. https://doi.org/10.1166/jnn.2009.J012
265. Obena RP, Tseng M-C, Primadona I et al (2015) UV-activated multilayer nanomatrix provides one-step tunable carbohydrate structural characterization in MALDI-MS. Chem Sci 6:4790–4800. https://doi.org/10.1039/C5SC00546A
266. Gopal J, Abdelhamid HN, Hua P-Y, Wu H-F (2013) Chitosan nanomagnets for effective extraction and sensitive mass spectrometric detection of pathogenic bacterial endotoxin from human urine. J Mater Chem B 1:2463. https://doi.org/10.1039/c3tb20079e
267. Ma Y, Zhang X, Zeng T et al (2013) Polydopamine-Coated Magnetic Nanoparticles for Enrichment and Direct Detection of Small Molecule Pollutants Coupled with MALDI-TOF-MS. ACS Appl Mater Interfaces 5:1024–1030. https://doi.org/10.1021/am3027025
268. Piret G, Kim D, Drobecq H et al (2012) Surface-assisted laser desorption-ionization mass spectrometry on titanium dioxide (TiO2) nanotube layers. Analyst 137:3058–3063. https://doi.org/10.1039/c2an35207a
269. Xu X, Deng C, Gao M et al (2006) Synthesis of Magnetic Microspheres with Immobilized Metal Ions for Enrichment and Direct Determination of Phosphopeptides by Matrix-Assisted Laser Desorption Ionization Mass Spectrometry. Adv Mater 18:3289–3293. https://doi.org/10.1002/adma.200601546
270. Kim M, Park J, Noh J, et al (2018) Gold-Nanoparticle-Coated Magnetic Beads for Concentration and Ionization of Analytes for Laser Desorption/Ionization Mass Spectrometry. Rapid Commun Mass Spectrom rcm.8372. https://doi.org/10.1002/rcm.8372
271. Shi C, Meng J, Deng C (2012) Facile synthesis of magnetic graphene and carbon nanotube composites as a novel matrix and adsorbent for enrichment and detection of small molecules by MALDI-TOF MS. J Mater Chem 22:20778. https://doi.org/10.1039/c2jm34745h
272. Obena RP, Lin PC, Lu YW et al (2011) Iron oxide nanomatrix facilitating metal ionization in matrix-assisted laser desorption/ionization mass spectrometry. Anal Chem 83:9337–9343. https://doi.org/10.1021/ac2017184
273. Jiang J, Sun X, Li Y et al (2018) Facile synthesis of Fe3O4@PDA core-shell microspheres functionalized with various metal ions: A systematic comparison of commonly-used metal ions for IMAC enrichment. Talanta 178:600–607. https://doi.org/10.1016/j.talanta.2017.09.071
274. Zhai R, Tian F, Xue R et al (2016) Metal ion-immobilized magnetic nanoparticles for global enrichment and identification of phosphopeptides by mass spectrometry. RSC Adv 6:1670–1677. https://doi.org/10.1039/C5RA22006H
275. Long X, Li J, Sheng D, Lian H (2016) Low-cost iron oxide magnetic nanoclusters affinity probe for the enrichment of endogenous phosphopeptides in human saliva. RSC Adv 6:96210–96222. https://doi.org/10.1039/C6RA11125D
276. Dupré M, Cantel S, Durand JO et al (2012) Silica nanoparticles pre-spotted onto target plate for laser desorption/ionization mass spectrometry analyses of peptides. Anal Chim Acta 741:47–57. https://doi.org/10.1016/j.aca.2012.06.037
277. Bhaisare ML, Abdelhamid HN, Wu B-S, Wu H-F (2014) Rapid and direct MALDI-MS identification of pathogenic bacteria from blood using ionic liquid-modified magnetic nanoparticles (Fe3O4@SiO2). J Mater Chem B 2:4671–4683. https://doi.org/10.1039/C4TB00528G
278. Wang C, Reed JM, Ma L et al (2012) Biomimic light trapping silicon nanowire arrays for laser desorption/ionization of peptides.

J Phys Chem C 116:15415–15420. https://doi.org/10.1021/jp3034402
279. Walker BN, Stolee JA, Pickel DL et al (2010) Tailored silicon nanopost arrays for resonant nanophotonic ion production. J Phys Chem C 114:4835–4840. https://doi.org/10.1021/jp9110103
280. Korte AR, Morris NJ, Vertes A (2019) High Throughput Complementary Analysis and Quantitation of Metabolites by MALDI- and Silicon Nanopost Array-Laser Desorption/Ionization-Mass Spectrometry. Anal Chem 91:3951–3958. https://doi.org/10.1021/acs.analchem.8b05074
281. Wang Y, Zeng Z, Li J et al (2013) Biomimetic Antireflective Silicon Nanocones Array for Small Molecules Analysis. J Am Soc Mass Spectrom 24:66–73. https://doi.org/10.1007/s13361-012-0498-4
282. Gorecka-Drzazga A, Dziuban J, Drzazga W et al (2005) Desorption/ionization mass spectrometry on array of silicon microtips. J Vac Sci Technol B Microelectron Nanom Struct 23:819. https://doi.org/10.1116/1.1861046
283. Tsao CW, Kumar P, Liu J, DeVoe DL (2008) Dynamic electrowetting on nanofilament silicon for matrix-free laser desorption/ionization mass spectrometry. Anal Chem 80:2973–2981. https://doi.org/10.1021/ac7026029
284. Cuiffi JD, Hayes DJ, Fonash SJ et al (2001) Desorption-ionization mass spectrometry using deposited nanostructured silicon films. Anal Chem 73:1292–1295. https://doi.org/10.1021/ac001081k
285. Alimpiev S, Grechnikov A, Sunner J et al (2008) On the role of defects and surface chemistry for surface-assisted laser desorption ionization from silicon. J Chem Phys 128:014711. https://doi.org/10.1063/1.2802304
286. Chen Y, Li D, Bie Z et al (2016) Coupling of Phosphate-Imprinted Mesoporous Silica Nanoparticles-Based Selective Enrichment with Matrix-Assisted Laser Desorption Ionization-Time-of-Flight Mass Spectrometry for Highly Efficient Analysis of Protein Phosphorylation. Anal Chem 88:1447–1454. https://doi.org/10.1021/acs.analchem.5b04343
287. Luo G, Chen Y, Daniels H et al (2006) Internal Energy Transfer in Laser Desorption/Ionization from Silicon Nanowires. J Phys Chem B 110:13381–13386. https://doi.org/10.1021/jp0609582
288. Çelikbıçak Ö, Demirel G, Pişkin E, Salih B (2012) Small molecule analysis using laser desorption/ionization mass spectrometry on nano-coated silicon with self-assembled monolayers. Anal Chim Acta 729:54–61. https://doi.org/10.1016/j.aca.2012.04.006
289. Yao J, Sun N, Wang J et al (2017) Rapid synthesis of titanium(IV)-immobilized magnetic mesoporous silica nanoparticles for endogenous phosphopeptides enrichment. Proteomics 17:1600320. https://doi.org/10.1002/pmic.201600320
290. Guinan T, Ronci M, Kobus H, Voelcker NH (2012) Rapid detection of illicit drugs in neat saliva using desorption/ionization on porous silicon. Talanta 99:791–798. https://doi.org/10.1016/j.talanta.2012.07.029
291. Mullens CP, Anugu SR, Gorski W, Bach SBH (2011) Modified silica-containing matrices towards the MALDI-TOF-MS detection of small molecules. Int J Mass Spectrom 308:311–315. https://doi.org/10.1016/j.ijms.2011.08.004
292. Zeng Z, Wang Y, Guo X et al (2014) On-Plate Self-Desalting and Matrix-Free LDI MS Analysis of Peptides With a Surface Patterned Sample Support. J Am Soc Mass Spectrom 25:895–898. https://doi.org/10.1007/s13361-014-0845-8
293. Amini N, Shariatgorji M, Thorsén G (2009) SALDI-MS Signal enhancement using oxidized graphitized carbon black nanoparticles. J Am Soc Mass Spectrom 20:1207–1213. https://doi.org/10.1016/j.jasms.2009.02.017
294. Wang J, Liu Q, Liang Y, Jiang G (2016) Recent progress in application of carbon nanomaterials in laser desorption/ionization mass spectrometry. Anal Bioanal Chem 408:2861–2873. https://doi.org/10.1007/s00216-015-9255-4
295. Abdelhamid HN, Wu H-F (2019) Graphene and Its Derivatives as Platforms for MALDI-MS. In: Tobias Stauber (ed) HANDBOOK OF GRAPHENE 2, Volume 2: Physics, Chemistry and Biology. Scrivener Publishing
296. Abdelhamid HN, Wu H-F (2015) Synthesis of a highly dispersive sinapinic acid@graphene oxide (SA@GO) and its applications as a novel surface assisted laser desorption/ionization mass spectrometry for proteomics and pathogenic bacteria biosensing. Analyst 140:1555–1565. https://doi.org/10.1039/c4an02158d
297. Lu W, Li Y, Li R et al (2016) Facile Synthesis of N-Doped Carbon Dots as a New Matrix for Detection of Hydroxy-Polycyclic Aromatic Hydrocarbons by Negative-Ion Matrix-Assisted Laser Desorption/Ionization Time-of-Flight Mass Spectrometry. ACS Appl Mater Interfaces 8:12976–12984. https://doi.org/10.1021/acsami.6b01510
298. Ma R, Lu M, Ding L et al (2013) Surface-assisted laser desorption/ionization mass spectrometric detection of biomolecules by using functional single-walled carbon nanohorns as the matrix. Chem Eur J 19:102–108. https://doi.org/10.1002/chem.201202838
299. Zhang B-T, Zheng X, Li H-F, Lin J-M (2013) Application of carbon-based nanomaterials in sample preparation: A review. Anal Chim Acta 784:1–17. https://doi.org/10.1016/j.aca.2013.03.054
300. Dong X, Cheng J, Li J, Wang Y (2010) Graphene as a novel matrix for the analysis of small molecules by MALDI-TOF MS. Anal Chem 82:6208–6214. https://doi.org/10.1021/ac101022m
301. Abdelhamid HN, Khan MS, Wu H-F (2014) Graphene oxide as a nanocarrier for gramicidin (GOGD) for high antibacterial performance. RSC Adv 4:50035–50046. https://doi.org/10.1039/C4RA07250B
302. Tang LAL, Wang J, Loh KP (2010) Graphene-based SELDI probe with ultrahigh extraction and sensitivity for DNA oligomer. J Am Chem Soc 132:10976–10977. https://doi.org/10.1021/ja104017y
303. Zhou X, Wei Y, He Q et al (2010) Reduced graphene oxide films used as matrix of MALDI-TOF-MS for detection of octachlorodibenzo-p-dioxin. Chem Commun (Camb) 46:6974–6976. https://doi.org/10.1039/c0cc01681k
304. Zhang J, Dong X, Cheng J et al (2011) Efficient analysis of nonpolar environmental contaminants by MALDI-TOF MS with graphene as matrix. J Am Soc Mass Spectrom 22:1294–1298. https://doi.org/10.1007/s13361-011-0143-7
305. Liu Y, Liu J, Yin P et al (2011) High throughput identification of components from traditional Chinese medicine herbs by utilizing graphene or graphene oxide as MALDI-TOF-MS matrix. J Mass Spectrom 46:804–815. https://doi.org/10.1002/jms.1952
306. Abdelhamid HN, Wu H-F (2013) Multifunctional graphene magnetic nanosheet decorated with chitosan for highly sensitive detection of pathogenic bacteria. J Mater Chem B 1:3950–3961. https://doi.org/10.1039/c3tb20413h
307. Shahnawaz Khan M, Abdelhamid HN, Wu H-F (2015) Near infrared (NIR) laser mediated surface activation of graphene oxide nanoflakes for efficient antibacterial, antifungal and wound healing treatment. Colloids Surf B: Biointerfaces 127C:281–291. https://doi.org/10.1016/j.colsurfb.2014.12.049
308. Wu B-S, Abdelhamid HN, Wu H-F (2014) Synthesis and antibacterial activities of graphene decorated with stannous dioxide. RSC Adv 4:3722. https://doi.org/10.1039/c3ra43992e
309. Michalak L, Fisher KJ, Alderdice DS et al (1994) C60-assisted laser desorption-ionization mass spectrometry. Org Mass Spectrom 29:512–515. https://doi.org/10.1002/oms.1210290912
310. Hopwood FG, Michalak L, Alderdice DS et al (1994) C60-assisted laser desorption/ionization mass spectrometry in the analysis of phosphotungstic acid. Rapid Commun Mass Spectrom 8:881–885. https://doi.org/10.1002/rcm.1290081105
311. Montsko G, Vaczy A, Maasz G et al (2009) Analysis of nonderivatized steroids by matrix-assisted laser desorption/

ionization time-of-flight mass spectrometry using C70 fullerene as matrix. Anal Bioanal Chem 395:869–874. https://doi.org/10.1007/s00216-009-3018-z
312. Shiea J, Huang JP, Teng CF et al (2003) Use of a water-soluble fullerene derivative as precipitating reagent and matrix-assisted laser desorption/ionization matrix to selectively detect charged species in aqueous solutions. Anal Chem 75:3587–3595. https://doi.org/10.1021/ac020750m
313. Vallant RM, Szabo Z, Trojer L et al (2007) A new analytical material-enhanced laser desorption ionization (MELDI) based approach for the determination of low-mass serum constituents using fullerene derivatives for selective enrichment. J Proteome Res 6:44–53. https://doi.org/10.1021/pr060347m
314. Vallant RM, Szabo Z, Bachmann S et al (2007) Development and application of C60-fullerene bound silica for solid-phase extraction of biomolecules. Anal Chem 79:8144–8153. https://doi.org/10.1021/ac0712392
315. Havel J, Soto-Guerrero J (2005) Matrix assisted laser desorption ionization (MALDI) and laser desorption ionization (LDI) mass spectrometry for trace uranium determination: The use of C60-fullerene as a matrix. J Radioanal Nucl Chem 263:489–492. https://doi.org/10.1007/s10967-005-0080-7
316. Böddi K, Takátsy A, Szabó S et al (2009) Use of fullerene-, octadecyl-, and triaconthyl silica for solid phase extraction of tryptic peptides obtained from unmodified and in vitro glycated human serum albumin and fibrinogen. J Sep Sci 32:295–308. https://doi.org/10.1002/jssc.200800462
317. Deacon GB, Field LD, Fisher K et al (2014) Fullerene matrices in the MALDI-TOF mass spectroscopic characterisation of organometallic compounds. J Organomet Chem 751:482–492. https://doi.org/10.1016/j.jorganchem.2013.10.025
318. Chen H, Qi D, Deng C et al (2009) Preparation of C60-functionalized magnetic silica microspheres for the enrichment of low-concentration peptides and proteins for MALDI-TOF MS analysis. Proteomics 9:380–387. https://doi.org/10.1002/pmic.200800335
319. Sunner J, Dratz E, Chen YC (1995) Graphite surface-assisted laser desorption/ionization time-of-flight mass spectrometry of peptides and proteins from liquid solutions. Anal Chem 67:4335–4342. https://doi.org/10.1021/ac00119a021
320. Chen Y-C, Shiea J, Sunner J (1998) Thin-layer chromatography–mass spectrometry using activated carbon, surface-assisted laser desorption/ionization. J Chromatogr A 826:77–86. https://doi.org/10.1016/S0021-9673(98)00726-2
321. Kim J, Kang W (2000) Use of graphite plate for homogeneous sample preparation in matrix/surface-assisted laser desorption and ionization of polypropyleneglycol and polystyrene. Bull Kor Chem Soc 21:401–404
322. Lee G, Bae S-E, Huh S, Cha S (2015) Graphene oxide embedded sol–gel (GOSG) film as a SALDI MS substrate for robust metabolite fingerprinting. RSC Adv 5:56455–56459. https://doi.org/10.1039/C5RA11497G
323. Liu C-W, Chien M-W, Su C-Y et al (2012) Analysis of flavonoids by graphene-based surface-assisted laser desorption/ionization time-of-flight mass spectrometry. Analyst 137:5809–5816. https://doi.org/10.1039/c2an36155h
324. Lu M, Lai Y, Chen G, Cai Z (2011) Matrix interference-free method for the analysis of small molecules by using negative ion laser desorption/ionization on graphene flakes. Anal Chem 83:3161–3169. https://doi.org/10.1021/ac2002559
325. Lu M, Lai Y, Chen G, Cai Z (2011) Laser desorption/ionization on the layer of graphene nanoparticles coupled with mass spectrometry for characterization of polymers. Chem Commun 47:12807. https://doi.org/10.1039/c1cc15592j
326. Liu Q, Cheng M, Wang J, Jiang G (2015) Graphene oxide nanoribbons: Improved synthesis and application in maldi mass spectrometry. Chem A Eur J 21:5594–5599. https://doi.org/10.1002/chem.201406280
327. Xu G, Liu S, Peng J et al (2015) Facile Synthesis of Gold@Graphitized Mesoporous Silica Nanocomposite and Its Surface-Assisted Laser Desorption/Ionization for Time-of-Flight Mass Spectroscopy. ACS Appl Mater Interfaces 7:2032–2038. https://doi.org/10.1021/am507894y
328. Huang X, Liu Q, Huang X et al (2017) Fluorographene as a Mass Spectrometry Probe for High-Throughput Identification and Screening of Emerging Chemical Contaminants in Complex Samples. Anal Chem 89:1307–1314. https://doi.org/10.1021/acs.analchem.6b04167
329. Zhao H, Li Y, Wang J et al (2018) Dual-Ion-Mode MALDI MS Detection of Small Molecules with the O–P,N-Doped Carbon/Graphene Matrix. ACS Appl Mater Interfaces 10:37732–37742. https://doi.org/10.1021/acsami.8b14643
330. Ashour RM, Abdelhamid HN, Abdel-Magied AF et al (2017) Rare Earth Ions Adsorption onto Graphene Oxide Nanosheets. Solvent Extr Ion Exch 35:91–103. https://doi.org/10.1080/07366299.2017.1287509
331. Meng J, Shi C, Deng C (2011) Facile synthesis of water-soluble multi-wall carbon nanotubes and polyaniline composites and their application in detection of small metabolites by matrix assisted laser desorption/ionization mass spectrometry. Chem Commun 47:11017. https://doi.org/10.1039/c1cc14319k
332. Shi C, Deng C, Zhang X, Yang P (2013) Synthesis of Highly Water-Dispersible Polydopamine-Modified Multiwalled Carbon Nanotubes for Matrix-Assisted Laser Desorption/Ionization Mass Spectrometry Analysis. ACS Appl Mater Interfaces 5:7770–7776. https://doi.org/10.1021/am4024143
333. Kim Y-K, Min D-H (2012) Fabrication of alternating multilayer films of graphene oxide and carbon nanotube and its application in mechanistic study of laser desorption/ionization of small molecules. ACS Appl Mater Interfaces 4:2088–2095. https://doi.org/10.1021/am300054z
334. Bian J, Olesik SV (2017) Surface-assisted laser desorption/ionization time-of-flight mass spectrometry of small drug molecules and high molecular weight synthetic/biological polymers using electrospun composite nanofibers. Analyst 142:1125–1132. https://doi.org/10.1039/C6AN02444K
335. Wu Z, Khan M, Mao S et al (2018) Combination of nano-material enrichment and dead-end filtration for uniform and rapid sample preparation in matrix-assisted laser desorption/ionization mass spectrometry. Talanta 181:217–223. https://doi.org/10.1016/j.talanta.2018.01.016
336. Lin Z, Wu J, Dong Y et al (2018) Nitrogen and Sulfur Co-doped Carbon-Dot-Assisted Laser Desorption/Ionization Time-of-Flight Mass Spectrometry Imaging for Profiling Bisphenol S Distribution in Mouse Tissues. Anal Chem 90:10872–10880. https://doi.org/10.1021/acs.analchem.8b02362
337. Wu J-Y, Chen Y-C (2002) A novel approach of combining thin-layer chromatography with surface-assisted laser desorption/ionization (SALDI) time-of-flight mass spectrometry. J Mass Spectrom 37:85–90. https://doi.org/10.1002/jms.264
338. Tang HW, Ng KM, Lu W, Che CM (2009) Ion desorption efficiency and internal energy transfer in carbon-based surface-assisted laser desorption/ionization mass spectrometry: Desorption mechanism(s) and the design of SALDI substrates. Anal Chem 81:4720–4729. https://doi.org/10.1021/ac8026367
339. Shi C, Meng J, Deng C (2012) Enrichment and detection of small molecules using magnetic graphene as an adsorbent and a novel matrix of MALDI-TOF-MS. Chem Commun 48:2418. https://doi.org/10.1039/c2cc17696c
340. He XM, Zhu GT, Yin J et al (2014) Electrospun polystyrene/oxidized carbon nanotubes film as both sorbent for thin film microextraction and matrix for matrix-assisted laser desorption/

ionization time-of-flight mass spectrometry. J Chromatogr A 1351:29–36. https://doi.org/10.1016/j.chroma.2014.05.045
341. Zhao Y, Zhang L, Chu Z et al (2017) Ti 4+ -immobilized chitosan-coated magnetic graphene oxide for the highly selective enrichment of phosphopeptides. Anal Methods 9:443–449. https://doi.org/10.1039/C6AY02905A
342. Zhang L, Gan Y, Sun H et al (2017) Magnetic mesoporous carbon composites incorporating hydrophilic metallic nanoparticles for enrichment of phosphopeptides prior to their determination by MALDI-TOF mass spectrometry. Microchim Acta 184:547–555. https://doi.org/10.1007/s00604-016-2046-6
343. Liu J, Liu Y, Gao M, Zhang X (2012) High throughput detection of tetracycline residues in milk using graphene or graphene oxide as MALDI-TOF MS matrix. J Am Soc Mass Spectrom 23:1424–1427. https://doi.org/10.1007/s13361-012-0400-4
344. Huang X, Liu Q, Fu J et al (2016) Screening of Toxic Chemicals in a Single Drop of Human Whole Blood Using Ordered Mesoporous Carbon as a Mass Spectrometry Probe. Anal Chem 88:4107–4113. https://doi.org/10.1021/acs.analchem.6b00444
345. Wang D, Huang X, Li J et al (2018) 3D printing of graphene-doped target for "matrix-free" laser desorption/ionization mass spectrometry. Chem Commun 54:2723–2726. https://doi.org/10.1039/C7CC09649F
346. Hussein KH, Abdelhamid HN, Zou X, Woo H-M (2019) Ultrasonicated graphene oxide enhances bone and skin wound regeneration. Mater Sci Eng C 94:484–492. https://doi.org/10.1016/j.msec.2018.09.051
347. Hong YL, Seo TH, Jang H, Kim Y-K (2019) The effect of oxidative debris on the laser desorption/ionization efficiency of graphene oxide derivatives for mass spectrometric analysis of small molecules and synthetic polymers. Anal Sci. https://doi.org/10.2116/analsci.19P205
348. Abdelhamid HN, Chen Z-Y, Wu H-F (2017) Surface tuning laser desorption/ionization mass spectrometry (STLDI-MS) for the analysis of small molecules using quantum dots. Anal Bioanal Chem 409:4943–4950. https://doi.org/10.1007/s00216-017-0433-4
349. Chang HY, Huang MF, Hsu CL et al (2015) Analyses of functional polymer-modified nanoparticles for protein sensing by surface-assisted laser desorption/ionization mass spectrometry coupled with HgTe nanomatrices. Colloids Surf B: Biointerfaces 130:157–163. https://doi.org/10.1016/j.colsurfb.2015.04.001
350. Bailes J, Vidal L, Ivanov DA, Soloviev M (2009) Quantum dots improve peptide detection in MALDI MS in a size dependent manner. J Nanobiotechnology 7:10. https://doi.org/10.1186/1477-3155-7-10
351. Abdelhamid HN, Wu H-F (2014) Monitoring metallofulfenamic–bovine serum albumin interactions: a novel method for metallodrug analysis. RSC Adv 4:53768–53776. https://doi.org/10.1039/C4RA07638A
352. Wu HF, Gopal J, Abdelhamid HN, Hasan N (2012) Quantum dot applications endowing novelty to analytical proteomics. Proteomics 12:2949–2961. https://doi.org/10.1002/pmic.201200295
353. Chen Z-Y, Abdelhamid HN, Wu H-F (2016) Effect of surface capping of quantum dots (CdTe) on proteomics. Rapid Commun Mass Spectrom 30:1403–1412. https://doi.org/10.1002/rcm.7575
354. Ke Y, Kailasa SK, Wu H-F, Chen Z-Y (2010) High resolution detection of high mass proteins up to 80,000 Da via multifunctional CdS quantum dots in laser desorption/ionization mass spectrometry. Talanta 83:178–184. https://doi.org/10.1016/j.talanta.2010.09.003
355. Shrivas K, Kailasa SK, Wu HF (2009) Quantum dots laser desorption/ionization MS: Multifunctional CdSe quantum dots as the matrix, concentrating probes and acceleration for microwave enzymatic digestion for peptide analysis and high resolution detection of proteins in a linear MALDI-TOF MS. Proteomics 9:2656–2667. https://doi.org/10.1002/pmic.200800772
356. Abdelhamid HN, Wu H-F (2015) Synthesis and characterization of quantum dots for application in laser soft desorption/ionization mass spectrometry to detect labile metal–drug interactions and their antibacterial activity. RSC Adv 5:76107–76115. https://doi.org/10.1039/C5RA11301F
357. Bibi A, Ju H (2016) Quantum dots assisted laser desorption/ionization mass spectrometric detection of carbohydrates: qualitative and quantitative analysis. J Mass Spectrom 51:291–297. https://doi.org/10.1002/jms.3753
358. Nasser Abdelhamid H, Wu HF (2013) Furoic and mefenamic acids as new matrices for matrix assisted laser desorption/ionization-(MALDI)-mass spectrometry. Talanta 115:442–450. https://doi.org/10.1016/j.talanta.2013.05.050
359. Liu C-W, Chien M-W, Chen G-F et al (2011) Quantum Dot Enhancement of Peptide Detection by Matrix-Assisted Laser Desorption/Ionization Mass Spectrometry. Anal Chem 83:6593–6600. https://doi.org/10.1021/ac201016c
360. Abdelhamid HN, El-Bery HM, Metwally AA et al (2019) Synthesis of CdS-modified chitosan quantum dots for the drug delivery of Sesamol. Carbohydr Polym 214:90–99. https://doi.org/10.1016/j.carbpol.2019.03.024
361. Abdelhamid HN (2017) Lanthanide Metal-Organic Frameworks and Hierarchical Porous Zeolitic Imidazolate Frameworks: Synthesis, Properties, and Applications. PhD Thesis, Stockholm University, Faculty of Science,
362. Abdelhamid HN, Huang Z, El-Zohry AM et al (2017) A Fast and Scalable Approach for Synthesis of Hierarchical Porous Zeolitic Imidazolate Frameworks and One-Pot Encapsulation of Target Molecules. Inorg Chem 56:9139–9146. https://doi.org/10.1021/acs.inorgchem.7b01191
363. Valencia L, Abdelhamid HN (2019) Nanocellulose leaf-like zeolitic imidazolate framework (ZIF-L) foams for selective capture of carbon dioxide. Carbohydr Polym. https://doi.org/10.1016/j.carbpol.2019.03.011
364. Abdelhamid HN, Bermejo-Gómez A, Martín-Matute B, Zou X (2017) A water-stable lanthanide metal-organic framework for fluorimetric detection of ferric ions and tryptophan. Microchim Acta 184:3363–3371. https://doi.org/10.1007/s00604-017-2306-0
365. Yang Y, Shen K, Lin J et al (2016) A Zn-MOF constructed from electron-rich π-conjugated ligands with an interpenetrated graphene-like net as an efficient nitroaromatic sensor. RSC Adv 6:45475–45481. https://doi.org/10.1039/C6RA00524A
366. Yao Q, Bermejo Gómez A, Su J et al (2015) Series of Highly Stable Isoreticular Lanthanide Metal–Organic Frameworks with Expanding Pore Size and Tunable Luminescent Properties. Chem Mater 27:5332–5339. https://doi.org/10.1021/acs.chemmater.5b01711
367. Zou X, Yao Q, Gómez AB et al (2016) A series of highly stable isoreticular lanthanide metal-organic frameworks with tunable luminescence properties solved by rotation electron diffraction and X-ray diffraction. Acta Crystallogr Sect A Found Adv 72:s136–s136. https://doi.org/10.1107/S2053273316097977
368. Abdel-Magied AF, Abdelhamid HN, Ashour RM et al (2019) Hierarchical porous zeolitic imidazolate frameworks nanoparticles for efficient adsorption of rare-earth elements. Microporous Mesoporous Mater 278:175–184. https://doi.org/10.1016/j.micromeso.2018.11.022
369. Emam HE, Abdelhamid HN, Abdelhameed RM (2018) Self-cleaned photoluminescent viscose fabric incorporated lanthanide-organic framework (Ln-MOF). Dyes Pigments 159:491–498. https://doi.org/10.1016/j.dyepig.2018.07.026
370. Abdelhamid HN, Wilk-Kozubek M, El-Zohry AM et al (2019) Luminescence properties of a family of lanthanide metal-organic

frameworks. Microporous Mesoporous Mater 279:400–406. https://doi.org/10.1016/j.micromeso.2019.01.024
371. Abdelhamid H, El-Zohry A, Cong J et al (2019) Towards implementing hierarchical porous zeolitic imidazolate frameworks in dye-sensitized solar cells. R Soc Open Sci 6:190723. https://doi.org/10.1098/rsos.190723
372. Moghadam PZ, Li A, Wiggin SB et al (2017) Development of a Cambridge Structural Database Subset: A Collection of Metal–Organic Frameworks for Past, Present, and Future. Chem Mater 29:2618–2625. https://doi.org/10.1021/acs.chemmater.7b00441
373. Chen L, Ou J, Wang H et al (2016) Tailor-Made Stable Zr(IV)-Based Metal-Organic Frameworks for Laser Desorption/Ionization Mass Spectrometry Analysis of Small Molecules and Simultaneous Enrichment of Phosphopeptides. ACS Appl Mater Interfaces 8:20292–20300. https://doi.org/10.1021/acsami.6b06225
374. Liu H-L, Chang Y-J, Fan T, Gu Z-Y (2016) Two-dimensional metal–organic framework nanosheets as a matrix for laser desorption/ionization of small molecules and monitoring enzymatic reactions at high salt concentrations. Chem Commun 52:12984–12987. https://doi.org/10.1039/C6CC07371A
375. Wang Y, Wang J, Gao M, Zhang X (2017) Functional dual hydrophilic dendrimer-modified metal-organic framework for the selective enrichment of N-glycopeptides. Proteomics 17:1700005. https://doi.org/10.1002/pmic.201700005
376. Xie Y, Deng C, Li Y (2017) Designed synthesis of ultra-hydrophilic sulfo-functionalized metal-organic frameworks with a magnetic core for highly efficient enrichment of the N-linked glycopeptides. J Chromatogr A 1508:1–6
377. Wei JP, Wang H, Luo T et al (2017) Enrichment of serum biomarkers by magnetic metal-organic framework composites. Anal Bioanal Chem 409:1895–1904. https://doi.org/10.1007/s00216-016-0136-2
378. Fu C-P, Lirio S, Liu W-L et al (2015) A novel type of matrix for surface-assisted laser desorption–ionization mass spectrometric detection of biomolecules using metal-organic frameworks. Anal Chim Acta 888:103–109. https://doi.org/10.1016/j.aca.2015.07.029
379. Zhang Y-W, Li Z, Zhao Q et al (2014) A facilely synthesized amino-functionalized metal–organic framework for highly specific and efficient enrichment of glycopeptides. Chem Commun 50:11504–11506. https://doi.org/10.1039/C4CC05179C
380. Wang J, Wang Y, Guo X et al (2018) Matrix assisted laser desorption/ionization time-of-flight mass spectrometric determination of benzo[a]pyrene using a MIL-101(Fe) matrix. Microchim Acta 185:175. https://doi.org/10.1007/s00604-017-2627-z
381. Zhai R, Yuan Y, Jiao F et al (2017) Facile synthesis of magnetic metal organic frameworks for highly efficient proteolytic digestion used in mass spectrometry-based proteomics. Anal Chim Acta 994:19–28. https://doi.org/10.1016/j.aca.2017.08.048
382. Shih YH, Fu CP, Liu WL et al (2016) Nanoporous Carbons Derived from Metal-Organic Frameworks as Novel Matrices for Surface-Assisted Laser Desorption/Ionization Mass Spectrometry. Small 12:2057–2066. https://doi.org/10.1002/smll.201502817
383. Wang Y, Wang J, Gao M, Zhang X (2017) A novel carbon material with nanopores prepared using a metal–organic framework as precursor for highly selective enrichment of N-linked glycans. Anal Bioanal Chem 409:431–438. https://doi.org/10.1007/s00216-016-9796-1
384. Huang J-C, Shih Y-H, Lirio S et al (2019) A simple approach to achieve a metastable metal oxide derived from carbonized metal–organic gels. Chem Commun 55:4475–4478. https://doi.org/10.1039/C9CC00240E
385. Zhao M, Chen T, Deng C (2016) Porous anatase TiO2 derived from a titanium metal–organic framework as a multifunctional phospho-oriented nanoreactor integrating accelerated digestion of proteins and in situ enrichment. RSC Adv 6:51670–51674. https://doi.org/10.1039/C6RA03837A
386. Xiao R, Pan Y, Li J et al (2019) Layer-by-layer assembled magnetic bimetallic metal-organic framework composite for global phosphopeptide enrichment. J Chromatogr A 1601:45–52. https://doi.org/10.1016/j.chroma.2019.05.010
387. Zhao M, Deng C, Zhang X (2014) The design and synthesis of a hydrophilic core–shell–shell structured magnetic metal–organic framework as a novel immobilized metal ion affinity platform for phosphoproteome research. Chem Commun 50:6228–6231. https://doi.org/10.1039/c4cc01038h
388. Liu Q, Xie Y, Deng C, Li Y (2017) One-step synthesis of carboxyl-functionalized metal-organic framework with binary ligands for highly selective enrichment of N-linked glycopeptides. Talanta 175:477–482. https://doi.org/10.1016/j.talanta.2017.07.067
389. Zhao M, Zhang X, Deng C (2015) Facile synthesis of hydrophilic magnetic graphene@metal-organic framework for highly selective enrichment of phosphopeptides. RSC Adv 5:35361–35364. https://doi.org/10.1039/C5RA03464G
390. Qi X, Chang C, Xu X et al (2016) Magnetization of 3-dimentional homochiral metal-organic frameworks for efficient and highly selective capture of phosphopeptides. J Chromatogr A 1468:49–54. https://doi.org/10.1016/j.chroma.2016.09.046
391. Li D, Bie Z (2017) Metal–organic framework incorporated monolithic capillary for selective enrichment of phosphopeptides. RSC Adv 7:15894–15902. https://doi.org/10.1039/C7RA00263G
392. Li D, Yin D, Chen Y, Liu Z (2017) Coupling of metal-organic frameworks-containing monolithic capillary-based selective enrichment with matrix-assisted laser desorption ionization-time-of-flight mass spectrometry for efficient analysis of protein phosphorylation. J Chromatogr A 1498:56–63. https://doi.org/10.1016/j.chroma.2016.10.054
393. Zhu X, Gu J, Yang J et al (2015) Zr-based metal–organic frameworks for specific and size-selective enrichment of phosphopeptides with simultaneous exclusion of proteins. J Mater Chem B 3:4242–4248. https://doi.org/10.1039/C5TB00113G
394. Xie Y, Deng C (2016) Highly efficient enrichment of phosphopeptides by a magnetic lanthanide metal-organic framework. Talanta 159:1–6. https://doi.org/10.1016/j.talanta.2016.05.075
395. Messner CB, Mirza MR, Rainer M et al (2013) Selective enrichment of phosphopeptides by a metal–organic framework. Anal Methods 5:2379–2383. https://doi.org/10.1039/c3ay40308d
396. Xie Y, Deng C (2017) Designed synthesis of a “One for Two” hydrophilic magnetic amino-functionalized metal-organic framework for highly efficient enrichment of glycopeptides and phosphopeptides. Sci Rep 7:1162. https://doi.org/10.1038/s41598-017-01341-y
397. Yang X, Xia Y (2016) Urea-modified metal-organic framework of type MIL-101(Cr) for the preconcentration of phosphorylated peptides. Microchim Acta 183:2235–2240. https://doi.org/10.1007/s00604-016-1860-1
398. Rocío-Bautista P, Pacheco-Fernández I, Pasán J, Pino V (2016) Are metal-organic frameworks able to provide a new generation of solid-phase microextraction coatings? – A review. Anal Chim Acta 939:26–41
399. Zhou J, Liang Y, He X et al (2017) Dual-Functionalized Magnetic Metal–Organic Framework for Highly Specific Enrichment of Phosphopeptides. ACS Sustain Chem Eng 5:11413–11421. https://doi.org/10.1021/acssuschemeng.7b02521
400. Gu Z-Y, Chen Y-J, Jiang J-Q, Yan X-P (2011) Metal–organic frameworks for efficient enrichment of peptides with simultaneous exclusion of proteins from complex biological samples. Chem Commun 47:4787. https://doi.org/10.1039/c1cc10579e

401. Peng J, Zhang H, Li X et al (2016) Dual-Metal Centered Zirconium-Organic Framework: A Metal-Affinity Probe for Highly Specific Interaction with Phosphopeptides. ACS Appl Mater Interfaces 8:35012–35020. https://doi.org/10.1021/acsami.6b12630
402. Ma W, Xu S, Ai W et al (2019) A flexible and multifunctional metal–organic framework as a matrix for analysis of small molecules using laser desorption/ionization mass spectrometry. Chem Commun 55:6898–6901. https://doi.org/10.1039/C9CC02611H
403. Zhao Y, Zhang Q, Zhang L, Zhang W (2019) Preparation of mesoporous carbon material derived from Metal-Organic Frameworks and its application in selective capture of endogenous peptides from human serum. Talanta 200:443–449. https://doi.org/10.1016/j.talanta.2019.02.097
404. Sultan S, Abdelhamid HN, Zou X, Mathew AP (2018) CelloMOF: Nanocellulose Enabled 3D Printing of Metal-Organic Frameworks. Adv Funct Mater 1805372. https://doi.org/10.1002/adfm.201805372
405. Abdelhamid HN (2019) Surfactant assisted synthesis of hierarchical porous metal-organic frameworks nanosheets. Nanotechnology. https://doi.org/10.1088/1361-6528/ab30f6
406. Zhen D, Gao C, Zhu B et al (2018) Preparation of Bi 0.15 Fe 0.15 TiO 2 Nanocomposites for the Highly Selective Enrichment of Phosphopeptides. Anal Chem 90:12414–12421. https://doi.org/10.1021/acs.analchem.8b00606
407. Tan S, Wang J, Han Q et al (2018) A porous graphene sorbent coated with titanium(IV)-functionalized polydopamine for selective lab-in-syringe extraction of phosphoproteins and phosphopeptides. Microchim Acta 185:316. https://doi.org/10.1007/s00604-018-2846-y
408. BAE SW, Il KIMJ, CHOI I et al (2017) Zinc Ion-immobilized Magnetic Microspheres for Enrichment and Identification of Multi-phosphorylated Peptides by Mass Spectrometry. Anal Sci 33:1381–1386. https://doi.org/10.2116/analsci.33.1381
409. Huang Y-L, Wang J, Jiang Y-H et al (2019) Development of amphiphile 4-armed PEO-based Ti4+ complex for highly selective enrichment of phosphopeptides. Talanta. https://doi.org/10.1016/j.talanta.2019.06.008
410. Zhang L, Zhao Q, Liang Z et al (2012) Synthesis of adenosine functionalized metal immobilized magnetic nanoparticles for highly selective and sensitive enrichment of phosphopeptides. Chem Commun 48:6274. https://doi.org/10.1039/c2cc31641b
411. Jiang J, Sun X, She X et al (2018) Magnetic microspheres modified with Ti(IV) and Nb(V) for enrichment of phosphopeptides. Microchim Acta 185:309. https://doi.org/10.1007/s00604-018-2837-z
412. Yang D-S, Ding X-Y, Min H-P et al (2017) Design and synthesis of an immobilized metal affinity chromatography and metal oxide affinity chromatography hybrid material for improved phosphopeptide enrichment. J Chromatogr A 1505:56–62. https://doi.org/10.1016/j.chroma.2017.05.025
413. Han G, Zeng Q, Jiang Z et al (2017) Simple preparation of magnetic metal-organic frameworks composite as a "bait" for phosphoproteome research. Talanta 171:283–290. https://doi.org/10.1016/j.talanta.2017.03.106
414. Yang S-S, Chang Y-J, Zhang H et al (2018) Enrichment of Phosphorylated Peptides with Metal–Organic Framework Nanosheets for Serum Profiling of Diabetes and Phosphoproteomics Analysis. Anal Chem 90:13796–13805. https://doi.org/10.1021/acs.analchem.8b04417
415. Wu HY, Unnikrishnan B, Huang CC (2014) Membrane-based detection of lead ions in seawater, urine and drinking straws through laser desorption/ionization. Sensors Actuators B Chem 203:880–886. https://doi.org/10.1016/j.snb.2014.06.140
416. Ren H, Chen W, Wang H et al (2019) Quantitative analysis of free fatty acids in gout by disposable paper-array plate based MALDI MS. Anal Biochem 579:38–43. https://doi.org/10.1016/j.ab.2019.05.013
417. Knochenmuss R (2013) MALDI and Related Methods: A Solved Problem or Still a Mystery? Mass Spectrom (Tokyo, Japan) 2: S0006. https://doi.org/10.5702/massspectrometry.S0006
418. Lu I-C, Lee C, Lee Y-T, Ni C-K (2015) Ionization Mechanism of Matrix-Assisted Laser Desorption/Ionization. Annu Rev Anal Chem 8:21–39. https://doi.org/10.1146/annurev-anchem-071114-040315
419. Chu KY, Lee S, Tsai M-T et al (2014) Thermal Proton Transfer Reactions in Ultraviolet Matrix-Assisted Laser Desorption/Ionization. J Am Soc Mass Spectrom 25:310–318. https://doi.org/10.1007/s13361-013-0792-9
420. Bae YJ, Kim MS (2015) A Thermal Mechanism of Ion Formation in MALDI. Annu Rev Anal Chem 8:41–60. https://doi.org/10.1146/annurev-anchem-081413-024102
421. Karas M, Glückmann M, Schäfer J (2000) Ionization in matrix-assisted laser desorption/ionization: singly charged molecular ions are the lucky survivors. J Mass Spectrom 35:1–12. https://doi.org/10.1002/(SICI)1096-9888(200001)35:1<1::AID-JMS904>3.0.CO;2-0
422. Niu S, Zhang W, Chait BT (1998) Direct comparison of infrared and ultraviolet wavelength matrix-assisted laser desorption/ionization mass spectrometry of proteins. J Am Soc Mass Spectrom 9:1–7. https://doi.org/10.1016/S1044-0305(97)00236-5
423. Trimpin S, Inutan ED (2013) Matrix Assisted Ionization in Vacuum, a Sensitive and Widely Applicable Ionization Method for Mass Spectrometry. J Am Soc Mass Spectrom 24:722–732. https://doi.org/10.1007/s13361-012-0571-z
424. Li Y, Cao X, Zhan L et al (2018) Hot electron transfer promotes ion production in plasmonic metal nanostructure assisted laser desorption ionization mass spectrometry. Chem Commun 54:10905–10908. https://doi.org/10.1039/C8CC05793A
425. Knochenmuss R (2014) MALDI mechanisms: wavelength and matrix dependence of the coupled photophysical and chemical dynamics model. Analyst 139:147–156. https://doi.org/10.1039/C3AN01446K
426. Yonezawa T, Kawasaki H, Tarui A et al (2009) Detailed Investigation on the Possibility of Nanoparticles of Various Metal Elements for Surface-Assisted Laser Desorption/Ionization Mass Spectrometry. Anal Sci 25:339–346. https://doi.org/10.2116/analsci.25.339
427. Ng K-M, Chau S-L, Tang H-W et al (2015) Ion-Desorption Efficiency and Internal-Energy Transfer in Surface-Assisted Laser Desorption/Ionization: More Implication(s) for the Thermal-Driven and Phase-Transition-Driven Desorption Process. J Phys Chem C 119:23708–23720. https://doi.org/10.1021/acs.jpcc.5b05957
428. Lai SK-M, Tang H-W, Lau K-C, Ng K-M (2016) Nanosecond UV Laser Ablation of Gold Nanoparticles: Enhancement of Ion Desorption by Thermal-Driven Desorption, Vaporization, or Phase Explosion. J Phys Chem C 120:20368–20377. https://doi.org/10.1021/acs.jpcc.6b06261
429. Kurita M, Arakawa R, Kawasaki H (2016) Silver nanoparticle functionalized glass fibers for combined surface-enhanced Raman scattering spectroscopy (SERS)/surface-assisted laser desorption/ionization (SALDI) mass spectrometry via plasmonic/thermal hot spots. Analyst 111:3669–3712. https://doi.org/10.1039/C6AN00511J
430. Stolee JA, Walker BN, Zorba V et al (2012) Laser–nanostructure interactions for ion production. Phys Chem Chem Phys 14:8453. https://doi.org/10.1039/c2cp00038e
431. Cheng YH, Zhang Y, Chau SL et al (2016) Enhancement of Image Contrast, Stability, and SALDI-MS Detection Sensitivity for Latent Fingerprint Analysis by Tuning the Composition of

Silver-Gold Nanoalloys. ACS Appl Mater Interfaces 8:29668–29675. https://doi.org/10.1021/acsami.6b09668
432. Popović I, Milovanović D, Miletić J et al (2016) Dependence of the quality of SALDI TOF MS analysis on the TiO2 nanocrystals' size and shape. Opt Quant Electron 48:1–6. https://doi.org/10.1007/s11082-016-0413-5
433. Kim YK, Min DH (2015) The structural influence of graphene oxide on its fragmentation during laser desorption/ionization mass spectrometry for efficient small-molecule analysis. Chem Eur J 21:7217–7223. https://doi.org/10.1002/chem.201404067
434. Taira S, Sahashi Y, Shimma S et al (2011) Nanotrap and mass analysis of aromatic molecules by phenyl group-modified nanoparticle. Anal Chem 83:1370–1374. https://doi.org/10.1021/ac102741g
435. Amendola V, Litti L, Meneghetti M (2013) LDI-MS assisted by chemical-free gold nanoparticles: Enhanced sensitivity and reduced background in the low-mass region. Anal Chem 85:11747–11754. https://doi.org/10.1021/ac401662r
436. Silina YE, Koch M, Volmer DA (2015) Impact of analyte ablation and surface acidity of Pd nanoparticles on efficiency of surface-assisted laser desorption/ionization-mass spectrometry. Int J Mass Spectrom 387:3701–3707. https://doi.org/10.1016/j.ijms.2015.06.009
437. Li Y, Luo P, Cao X et al (2019) Enhancing surface-assisted laser desorption ionization mass spectrometry performance by integrating plasmonic hot-electron transfer effect through surface modification. Chem Commun 55:5769–5772. https://doi.org/10.1039/C9CC02541C
438. Antone AJ, Liang Q, Sherwood JA et al (2019) Surface Effects of Iron Oxide Nanoparticles on the MALDI In-Source Decay Analysis of Glycans and Peptides. ACS Appl Nano Mater acsanm.9b00988. https://doi.org/10.1021/acsanm.9b00988
439. Huang X, Liu Q, Jiang G (2019) Tuning the performance of graphene as a dual-ion-mode MALDI matrix by chemical functionalization and sample incubation. Talanta 199:532–540. https://doi.org/10.1016/j.talanta.2019.03.010
440. Law KP (2010) Surface-assisted laser desorption/ionization mass spectrometry on nanostructured silicon substrates prepared by iodine-assisted etching. Int J Mass Spectrom 290:47–59. https://doi.org/10.1016/j.ijms.2009.12.003
441. Duan J, Linman MJ, Chen C-Y, Cheng QJ (2009) CHCA-modified Au nanoparticles for laser desorption ionization mass spectrometric analysis of peptides. J Am Soc Mass Spectrom 20:1530–1539. https://doi.org/10.1016/j.jasms.2009.04.009
442. Kolářová L, Kučera L, Vaňhara P et al (2015) Use of flower-like gold nanoparticles in time-of-flight mass spectrometry. Rapid Commun Mass Spectrom 29:1585–1595. https://doi.org/10.1002/rcm.7265
443. Tarui A, Kawasaki H, Taiko T et al (2009) Gold-nanoparticle-supported silicon plate with polymer micelles for surface-assisted laser desorption/ionization mass spectrometry of peptides. J Nanosci Nanotechnol 9:159–164. https://doi.org/10.1166/jnn.2009.J046
444. Nordström A, Apon JV, Uritboonthai W et al (2006) Surfactant-enhanced desorption/ionization on silicon mass spectrometry. Anal Chem 78:272–278. https://doi.org/10.1021/ac051398q
445. Marsico ALM, Duncan B, Landis RF et al (2017) Enhanced Laser Desorption/Ionization Mass Spectrometric Detection of Biomolecules Using Gold Nanoparticles, Matrix, and the Coffee Ring Effect. Anal Chem 89:3009–3014. https://doi.org/10.1021/acs.analchem.6b04538
446. Kim Y-K, Min D-H (2014) Mechanistic Study of Laser Desorption/Ionization of Small Molecules on Graphene Oxide Multilayer Films. Langmuir 30:12675–12683. https://doi.org/10.1021/la5027653
447. Kim Y-K, Na H-K, Kwack S-J et al (2011) Synergistic Effect of Graphene Oxide/MWCNT Films in Laser Desorption/Ionization Mass Spectrometry of Small Molecules and Tissue Imaging. ACS Nano 5:4550–4561. https://doi.org/10.1021/nn200245v
448. Szabo Z, Vallant RM, Takátsy A et al (2010) Laser desorption/ionization mass spectrometric analysis of small molecules using fullerene-derivatized silica as energy-absorbing material. J Mass Spectrom 45:545–552. https://doi.org/10.1002/jms.1740
449. Silina YE, Koch M, Volmer DA (2014) The role of physical and chemical properties of Pd nanostructured materials immobilized on inorganic carriers on ion formation in atmospheric pressure laser desorption/ionization mass spectrometry. J Mass Spectrom 49:468–480. https://doi.org/10.1002/jms.3362
450. Colaianni L, Kung SC, Taggart DK et al (2014) Reduction of spectral interferences using ultraclean gold nanowire arrays in the LDI-MS analysis of a model peptide ABC Highlights: Authored by Rising Stars and Top Experts. Anal Bioanal Chem 406:4571–4583. https://doi.org/10.1007/s00216-014-7876-7
451. Silina YE, Herbeck-Engel P, Koch M (2017) A study of enhanced ion formation from metal-semiconductor complexes in atmospheric pressure laser desorption/ionization mass spectrometry. J Mass Spectrom 52:43–53. https://doi.org/10.1002/jms.3898
452. Chu H-W, Unnikrishnan B, Anand A et al (2018) Nanoparticle-based laser desorption/ionization mass spectrometric analysis of drugs and metabolites. J Food Drug Anal 26:1215–1228. https://doi.org/10.1016/j.jfda.2018.07.001
453. Teng F, Zhu Q, Wang Y et al (2018) Enhancing reproducibility of SALDI MS detection by concentrating analytes within laser spot. Talanta 179:583–587. https://doi.org/10.1016/j.talanta.2017.11.056
454. Abdelhamid HN, Wu H-F (2018) Selective biosensing of Staphylococcus aureus using chitosan quantum dots. Spectrochim Acta A Mol Biomol Spectrosc 188. https://doi.org/10.1016/j.saa.2017.06.047
455. Abdelhamid HN, Wu H-F (2015) Synthesis and multifunctional applications of quantum nanobeads for label-free and selective metal chemosensing. RSC Adv 5:50494–50504. https://doi.org/10.1039/C5RA07069D
456. Coffinier Y, Kurylo I, Drobecq H et al (2014) Decoration of silicon nanostructures with copper particles for simultaneous selective capture and mass spectrometry detection of His-tagged model peptide. Analyst 139:5155–5163. https://doi.org/10.1039/C4AN01056F
457. Manikandan M, Nasser Abdelhamid H, Talib A, Wu H-F (2014) Facile synthesis of gold nanohexagons on graphene templates in Raman spectroscopy for biosensing cancer and cancer stem cells. Biosens Bioelectron 55:180–186. https://doi.org/10.1016/j.bios.2013.11.037
458. Abdelhamid HN, Wu H-F (2013) Probing the interactions of chitosan capped CdS quantum dots with pathogenic bacteria and their biosensing application. J Mater Chem B 1:6094–6106. https://doi.org/10.1039/c3tb21020k
459. Abdelhamid HN (2016) Nanoparticles as Pharmaceutical Agents. MJ Anes 1:003–003
460. Kim M-J, Yun TG, Noh J-Y et al (2019) Synergistic Effect of the Heterostructure of Au Nanoislands on TiO2 Nanowires for Efficient Ionization in Laser Desorption/Ionization Mass Spectrometry. ACS Appl Mater Interfaces 11:20509–20520. https://doi.org/10.1021/acsami.9b03386